CERTIFICATE FROM THE SUPERVISORS

This is to certify that the thesis entitled **"Investigation of low lying energy levels of internal motion in Bio-molecules and their complexes by Mid & Far FTIR Spectroscopy"** submitted by Sri **Arup Dutta** who got his name registered on 18 / 05 / 2012 for the award of **Ph.D. (Science) degree** of **Jadavpur University**, is absolutely based upon his own work under the supervision of Dr. Aloke Kr. Sarkar and Prof. Sujata Tarafdar and that neither this thesis nor any part of its has been submitted for either any degree / diploma or any other academic award anywhere before.

1. Aloke Kumar Sarkar 10/05/2018

Dr. Aloke Kumar Sarkar
Associate Professor (Retd.), Department of Physics
Bijoy Krishna Girls' College
5/3, M.G. Road, Howrah-711 101

Dr. Aloke Kumar Sarkar
Ex Associate Professor Physics
Bijoy Krishna Girls' College
Howrah – 711101

S. Tarafder 10.05.2018

Ex Professor
Department of Physics
Jadavpur University
Kolkata – 700 032

2. .....

Prof. Sujata Tarafdar
Professor, Department of Physics
Jadavpur University
Kolkata-700 032

(Signature of the Supervisors & date with official seal)

Investigation of low lying energy levels of internal motion in Bio-molecules and their complexes by Mid & Far FTIR Spectroscopy

THESIS SUBMITTED FOR THE DEGREE OF
DOCTOR OF PHILOSOPHY (SCIENCE)
OF

JADAVPUR UNIVERSITY

By

Arup Dutta

BIJOY KRISHNA GIRLS' COLLEGE
HOWRAH 711101
WEST BENGAL, INDIA

2018

ACKNOWLEDGEMENTS

I would like to express my sincere gratitude to University Grants Commission, New Delhi, India for fellowship as a Project Fellow [MRP No F.35-7/2008(SR)].

My respected supervisors, Dr. Aloke Kr. Sarkar, Associate Professor (Retd.), Department of Physics, Bijoy Krishna Girls' College, Howrah and Prof. Sujata Tarafdar, Professor, Dept. of Physics, Jadavpur University, Kolkata, guided me by their constructive suggestion and encouragement and spearheaded the research activity by their constant directive.

My colleagues, Mr Sourav Sundar Pradhan, Mr Partha Krishna Ghosh, Mr. Arnab Ganguly, Mr. Somnath Paul, Ms. Ananya Banerjee, Ms Moumita Barman and Ms. Aditi Sarkar have extended their co-operation and technical assistance in an uncounted number of ways.

I wish to thank Department of Physics, B.K. Girls' College where I completed this work and I acknowledge the cooperation of the departmental members at various stages.

I also wish to extend my acknowledgement to my relatives and friends who shared different moments at different situations.

Finally I want to give thank my loving parents and my wife Deblina whose continuous support, encouragement and love through all my life helped me to concentrate in study and research work.

Preface

The basic building block of life and bio-materials are the bio-molecules. Knowledge of the structure and function of bio-molecules is essential for biology, biochemistry, biophysics, medicine, material science and pharmacology and it even has interdisciplinary technological implications. Bio-molecules show some beautiful characteristics that cannot be found in simpler systems. In this complex field the situation is not so clear, but the goal is to describe the physics of biological systems, to develop physical models, and possibly even find new technique that characterize biological entities.

Molecules may undergo several types of motion. - translational motion, rotational motion about its internal axes, and the vibrational motion. Each molecular vibrational motion occurs with a frequency characteristic of the molecule and of the particular vibration. The energy of a vibration is measured by its amplitude (the distance moved by the atoms during the vibration), so the higher the vibrational energy, the larger the amplitude of the motion. According to quantum mechanics, only certain vibrational energies are allowed to the molecule (this is also true of rotational and translational energies), so only certain amplitudes are allowed. Associated with each vibrational motion of the molecule is a series of energy levels (or vibrational energy states). In undergoing the transition, the molecule gains vibrational energy, and the amplitude of the vibration increases. The frequency of light required to cause a transition for a particular vibration is equal to the frequency of the vibration, so we may measure the vibrational frequencies by measuring the frequencies of light absorbed by the molecule.

For a complex molecule study of IR Spectrum is not just a routine work. The over analysis of the IR spectrum from FTIR analysis may provide many new information about biomolecules and their molecular function. A normal molecule under external stimulation, under complex formation and under defect introduction will exhibit a different vibrational characteristic and a complete analysis of it following theoretical analysis will suppose to provide a molecular signature for the bio-molecules. The understanding of structure, dynamics and function of a bio-molecule is one of the most challenging area in the biological Physics. The IR spectroscopy is supposed to be a powerful tool.

In this project the overall results obtained from various specimens are compiled in the form of a database to develop a characterization technique of bio-molecule. The proposed technique is believed to provide a quantum energy map for the low lying states.

The most of the works presented in the thesis are experimental in nature. The experimental results presented in this thesis are checked carefully and the experimental errors from the instrument concern did not affect the observed physical properties. At each and every stage the accuracy of both instrument and experimental condition are checked.

ABSTRACT

The work presented in this thesis aiming to the title of it. Biomolecules are molecules that occur naturally in living organisms. The basic building block of life and bio-materials are the bio-molecules. The study of bio-molecules is similar to that of atoms, molecules, and solids. The understanding of mentioned simpler systems may help in investigations of the more complex bio-molecules. Some features are alike in these quantum-mechanical systems; ideas and concepts from molecular and condensed matter physics can thus be taken over directly. Progress in physics has often followed a path in which three areas are essential namely, structure, energy levels, and dynamics. (Structural analysis techniques have progressed and the latest breakthroughs due to Infra red (IR) which allow numerous structure-function studies, particularly the quantitative identification of the atomic assembly of large bio-molecules and the determination of the microstructure of biological tissue in dynamic situations.). Since the subject is vast only overview of the mentioned aspects are given.

The molecular spectroscopy is one of the important investigation tool used in this research however a brief discussion of its methodology is heighted here. When the intensity of the IR source is the extremely bright light provided by a synchrotron or with FTIR spectrophotometer with high signal to noise ratio, it is possible to obtain an excellent IR spectrum. The technique may be comparable to non-destructive testing in Physical/ Material Science/Life Science. In this research scheme the following studies are carried out (i) Investigation and extraction of internal motion from IR spectrum of bio-molecules/ biomaterials, (ii) Development of understanding on internal motion of complex system, (iii) Observation of the functional behavior of bio-molecules from the variation of IR spectrum and dielectric Spectrum with variation of (a) external factor (b) environmental variation (c) introduction of defects. (iv) Preparation of a comprehensive analysis on internal motion and relaxation mechanism of biomolecules as complex system. (v) Development of an over dynamical characterization and quantum energy level map of bio-molecules are performed.

The analysis of the results obtained involve type of absorption spectroscopy depending upon the frequency range of the electromagnetic radiation absorbed Microwave spectroscopy involves a transition from one molecular rotational energy level to another. Molecules may undergo several types of motion. - translational motion, rotational motion about its internal axes, and the vibrational motion. The absorption in the far infrared

corresponds to transitions from an initial state to a low energy final excited state. For isolated molecules, this excitation corresponds to rotational transitions, vibrational excitations of large molecules or roto-vibrational transitions. Their measurements at high resolution provide a better description and understanding of species or chemical reaction.

During this research program few standard bio-molecular system (whose structural and chemical characterization are available or Computer Molecular Dynamical Simulation data may developed or available) are investigated in details and compared with appropriate CMD results. In this research work an adequate analysis of the spectroscopic (FTIR) results are undertaken. The bio-molecular functions of the same system under external factors (temperature, hydration, etc) are investigated in details. Following the results a range of bio-molecular system (e.g. Acacia Arabica, Gum Agar, Manitol Sugar, human hair etc.) are investigated and analyzed. In the last part of this research program some of the mentioned bio-molecule are investigated and analyzed from quantum theoretical simulation. This research project likes to devise a technique for characterization of bio-molecules and more about this subject. The said characterization is expected to be an important outcome from the results of the study of Mid-Far IR (FTIR) of native and modified bio-molecules. The characteristics differences in vibrational/ rotational spectra of modified bio-molecules over the corresponding pure one will provide a possible roadway to characterize defect bio-molecules. The outcome of this research is good, concise and believed to provide a quantum energy map for the low lying states.

List of publications

1) **“FTIR Investigation of Structural Change in Bio-molecule”** by Arup Dutta and A. Sarkar, *Advances in Applied Science Research, 2011, 2 (1): 125-128.*

2) **“FTIR Investigation of Structural Change Due to Radiation Damage in Biomolecule”** by Arup Dutta and A. Sarkar, *Asian Journal of Chemistry; Vol. 23, No. 12 (2011), 5584-5586.*

3) **“Structural distinction between black and grey human hair: A FTIR Investigation”** by Arup Dutta and A. Sarkar, *Proceeding of International Conference on Recent Trends in Applied Physics and Material Science 2013, AIP Conf. Proc. 1536, 1250-1251 (2013).*

4) **“Vibrational Spectrum of Gum Agar in Pure and D_2O Exchange state by FTIR Analysis”** by Arup Dutta and A. Sarkar, *Proceedings of AMRP-2013, International Journal Of Engineering Research and Technology (IJERT).*

5) **“FTIR Investigation of Rotational Spectra and Structural Change due to Deuterium Exchange in Bio-Molecule”** by Arup Dutta and Aloke Kumar Sarkar, *Journal of Biomimetics, Biomaterials and Biomedical Engineering; Vol. 26, pp 73-83.*

6) **“Dynamic Light Scattering on Jatropha Latex”** by Arup Dutta, S.S.Pradhan and A. Sarkar, (c*ommunicated).*

CONTENTS

LIST OF TABLES

LIST OF FIGURES

Chapter 1

Introduction

1.1 Biomolecules and Biomaterials :

Biomolecule is a term belonging to a class of organic compounds found in living organisms. The study of structure and function of biomolecules is most fundamental aspect in biological-physics. The four major biomolecules are carbohydrates, lipids, proteins and nucleic acids.

The structure and properties of a biomaterial are dependent on the chemical and physical nature of the components present and their relative amounts. An understanding of the exact role played by a tissue and its interrelationship with the function of the entire living organism is essential if biomaterials are to be used intelligently [1]. Biology studies life in its variety and complexity. It describes how organisms go about getting food, communicating, sensing the environment, and reproducing. On the other hand, material physics looks for mathematical laws of nature and makes detailed predictions about the forces that drive idealized systems. Spanning the distance between the complexity of life and the simplicity of physical laws is the challenge of biophysics. Looking for the patterns in life and analyzing them with math and physics is a powerful way to gain insights. This knowledge can then be translated into the design and understanding of materials based on biological components or principles.

Biomaterial is a natural material used to make devices to replace a part of a living system or to function in intimate contact with living tissue. As the number of available such materials increases, it becomes more and more important to be protected from unsuitable products or materials, which haven't been thoroughly evaluated [2,3]. Most manufacturers of materials operate an extensive quality assurance program and materials are thoroughly tested before being released to the general practitioner. Many standard specification tests of both national and international standards organizations (ISO) are now available, which effectively maintain quality levels. Such specifications normally give details for the testing of certain products, the method of calculating the results and the minimum permissible result, which is acceptable. Laboratory investigation, some of which

are used in standard specification, can be used to indicate the suitability of certain materials. It is important that methods used to evaluate materials in laboratory give results, which can be correlated with clinical experience. Although laboratory investigation can provide many important and useful data on materials, the ultimate test is the controlled clinical trial and verdict of practitioners after a period of use in general practice. Many materials produce good results in the laboratory, only to be found lacking when subjected to clinical use. The majority of manufacturers carry out extensive clinical trials of new materials, normally in cooperation with a university or hospital department, prior to releasing a product for use by general practitioners.

The most common classes of materials used as biomedical materials are polymers, metals, and ceramics. These three classes are used singly and in combination to form most of the implantation devices available today.

1.1.1 Carbohydrates:

Carbohydrates form a very large group of naturally occurring organic compounds which play a vital role in daily life. They are produced in plants by the process of photosynthesis. The most common carbohydrates are glucose, fructose, sucrose, starch, cellulose etc. Chemically, the carbohydrates may be defined as polyhydroxy aldehydes or ketones. Carbohydrates are classified into three groups depending upon their behaviour on hydrolysis. In the following a brief description on carbohydrates is introduced and details may be found in standard literatures [4-8].

(i) Monosaccharides: A polyhydroxy aldehyde or ketone which cannot be hydrolysed further to a smaller molecule containing these functional groups, is known as a monosaccharide. About 20 monosaccharides occur in nature and glucose is the most common amongst them.

(ii) Disacccharides: Carbohydrates which give two monosaccharide molecules by hydrolysis are called disaccharides e.g. sucrose, maltose, lactose etc.

(iii) Polysaccharides: Carbohydrates which yield a large number of monosaccharide units by hydrolysis e.g. starch, glycogen, cellulose etc.

Disaccharides are formed by the condensation of two monosaccharide molecules. These monosaccharides join together by the loss of a water molecule between one hydroxyl group on each monosaccharide. Such a linkage, which joins the monosaccharide units together, is called glycoside linkage. Sucrose (the common sugar) consists of one molecule of glucose and one molecule of fructose joined together. Lactose (or milk sugar) is found in milk and contains one molecule of glucose and one molecule of galactose. If a large number of monosaccharide units are joined together, we get polysaccharides. These are the most common carbohydrates found in nature. They have mainly one of the following two functions- either as food materials or as structural materials. Starch is the main food storage polysaccharide of plants. It is a polymer of α-glucose and consists of two types of chains- known as amylose and amylopectin. Cellulose is a natural polysaccharide which is the main component of wood and other plant materials. It consists of long chain of β-D-glucose molecules.

1.1.2 Lipids:

The lipids include a large number of biomolecules of different types. In general, those constituents of the cell which are insoluble in water and soluble in organic solvents of low polarity (such as chloroform, ether, benzene etc.) are termed as lipids. Lipids perform a variety of biological functions. Lipids are classified into three broad categories on the basis of their molecular structure and the hydrolysis products.

(i) Simple Lipids: Those lipids which are esters and yield fatty acids and alcohols upon hydrolysis are called simple lipids. They include oils, fats and waxes. They are subdivided into two groups, depending on the nature of the alcohol component. Fats and oils are triglycerides, i.e. they are the esters of glycerol with three molecules of long chain fatty acids. Variations in the properties of fats and oils are due to the presence of different acids. These long chain acids may vary in the number of carbon atoms (between C_{12} to C_{26}) and may or may not contain double bonds. On hydrolysis of a triglyceride molecule, one molecule of glycerol and three molecules of higher fatty acids are obtained.

By definition, a fat is that triglyceride which is solid or semisolid at room temperature and an oil is the one that is liquid at room temperature. Saturated fatty acids

form higher melting triglycerides than unsaturated fatty acids. The saturated triglycerides tend to be solid fats, while the unsaturated triglycerides tend to be oils. The double bonds in an unsaturated triglyceride are easily hydrogenated to give a saturated product, and in this way an oil may be converted into a fat. Hydrogenation is used in the manufacture of vanaspati ghee from oils. Fats and oils are found in both plants and animals. Our body can produce fats from carbohydrates. This is one method that the body has for storing the energy from unused carbohydrates. The vegetable oils are found primarily in the seeds of plants.

The second type of simple lipids is waxes. They are the esters of fatty acids with long chain monohydroxy alcohols 26 to 34 carbons atoms. Waxes are wide-spread in nature and occur usually as mixtures. They form a protective coating on the surfaces of animals and plants. Some insects also secrete waxes. The main constitutent of bees wax obtained from the honey comb of bees is myricyl palmitate.

(ii) Compound Lipids: Compound lipids are esters of fatty acids and alcohol with additional compounds like phosphoric acid, sugars, proteins etc. Compound lipids by hydrolysis yield some other substances in addition to an alcohol and fatty acids. The first type of such lipids is called phospholipids, because they are the triglycerides in which two molecules of fatty acids and one molecule of phosphoric acid are present. Glycolipids contain a sugar molecule in addition to fatty acid attached to an alcohol.

(iii) Derived Lipids: Compounds which are formed from oils, fats etc. during metabolism. They include steroids and some fat soluble vitamins. Steroids are another class of lipids which are formed in our body during metabolism. These are the compounds with a distinctive ring system that provides the structural backbone for many of our hormones. Steroids do not contain ester groups and hence cannot be hydrolysed. Cholesterol is one of the most widely distributed steroids in animal and human tissues. Another important group of derived lipids is that of fat-soluble vitamins. This includes vitamins A, D, E and K, whose deficiency causes different diseases.

Fats are main food storage compounds and serve as reservoir of energy. Presence of oils or fats is essential for the efficient absorption of fat soluble vitamins A, D, E and K. Subcutaneous fats serve as biological insulator against excessive heat loss. Phospholipids

are the essential components of cell membrane. Steroids control many biological activities in living organisms. Some enzymes require lipid molecules for maximum action. Details description about lipids may found in some other materials [9-12].

1.1.3 Proteins:

Proteins are the most abundant macromolecules in living cells. These are high molecular mass complex amino acids. Proteins are most essential class of biomolecules because they play the most important role in all biological processes. A living system contains thousands of different proteins for its various functions. Our every day food like pulses, eggs, meat and milk are rich sources of proteins and are must for a balanced diet.

Proteins are classified on the basis of their chemical composition, shape and solubility into two major categories.

(i) Simple proteins: Simple proteins are those which, by hydrolysis, give only amino acids. According to their solubility, the simple proteins are further divided into two major groups fibrous and globular proteins.

(a) Fibrous Proteins: These are water insoluble animal proteins eg. elastins (protein of arteries and elastic tissues). Molecules of fibrous proteins are generally long and thread like. Measured in terms of their total mass, the largest class is the structural one. Structural proteins are fibrous proteins. The most familiar of the fibrous proteins are the keratins, which form the protective covering of all land vertebrates: skin, fur, hair, wool, claws, nails, hooves, horns, scales, beaks and feathers. Equally widespread, if less visible, are the actin and myosin proteins of muscle tissue. Another group of fibrous structural proteins are the silks and insect fibers. In addition, there are the collagens of tendons and hides, which form connective ligaments within the body and give extra support to the skin where needed. Structural proteins are the most abundant class of proteins in nature. Collagen is recognized as the most abundant mammalian protein. Structural proteins such as collagen, fibronectin and laminin are utilized in cell culture applications as attachment factors [13].

(b) Globular Proteins: These proteins are generally soluble in water, acids, bases or alcohol. Some examples of globular proteins are albumin of eggs, globulin (present in serum), and haemoglobin. Molecules of globular proteins are folded into compact units which are spherical in shape.

(ii) Conjugated proteins: Conjugated proteins are complex proteins which by hydrolysis yield not only amino acids but also other organic or inorganic components. The non-amino acid portion of a conjugated protein is called prosthetic group. Unlike simple proteins, conjugated proteins are classified on the basis of the chemical nature of their prosthetic groups [15].

1.1.4 Nucleic acids:

The study of the chemistry of heredity is one of the most fascinating field of research today. It was recognized in the 19th century that the nucleus of a living cell contains particles responsible for heredity, which were called chromosomes. In more recent years, it has been discovered that chromosomes are composed of nucleic acids. These are named so because they come from the nucleus of the cell and are acidic in nature. Two types of nucleic acids exist which are called DNA (deoxyribonucleic acid) and RNA (ribonucleic acid).They differ in their chemical composition as well as in functions [16].

Like all natural molecules, nucleic acids are linear polymeric molecules. They are chain like polymers of thousands of nucleotide units; hence they are also called polynucleotides. A nucleotide consists of three subunits: a nitrogen containing heterocyclic aromatic compound (called base), a pentose sugar and a molecule of phosphoric acid [17].

An important function of nucleic acids is the protein synthesis. The specific sequence of bases in DNA represents coded information for the manufacture of specific proteins. In the process, the information from DNA is transmitted to another nucleic acid called messenger RNA, which leaves the nucleus and goes to the cytoplasm of the cell. Messenger RNA acts as template for the incorporation of amino acids in the proper sequence in protein. The amino acids are brought to the messenger RNA in the cell, by transfer RNA. Where they form peptide bonds. In short it can be said that DNA contains

the coded message for protein synthesis whereas RNA actually carries out the synthesis of protein.

1.2 Molecular Spectroscopy:

Molecular spectroscopy refers to the field of looking at molecules using electromagnetic radiation. This technique is used both to detect and to manipulate and understand molecules. The information obtained from molecular spectroscopy relates to the energy levels and the shapes and charge densities of molecules. There are a few generic concepts and principles for all spectroscopy that are listed below:

(i) The energy of a molecule can be thought of as consist of different contributions: Rotational Energy, Vibrational Energy and Electronic Energy. The energy spacing between rotational levels is smaller than that between vibrational levels which is smaller than that between Electronic levels.

(ii) The Electromagnetic spectrum can be thought of as divided into different regions based on the wavelength/frequency/energy of the light source used. The table below lists these energies and the transitions that are probed by these energies.

Type of radiation	**Frequency(Hz)**	**Motions probed**
Microwave	10^{9}-10^{13}	Rotations
Infrared	10^{13}-10^{14}	Vibrations
Visible and Ultraviolet(UV-Vis)	$10^{14} - 10^{16}$	Electronic Transitions

Table 1. Different regions based on the frequency of the light source.

(iii) When light of a certain wavelength falls on a molecule, then the molecule will absorb light and go to an excited state such that the difference in energy between the ground state and the excited state is hc/λ, where λ is the wavelength of the light used. Alternatively, the molecule may emit electromagnetic radiation a particular wavelength by transition the higher energy state to the lower energy state. The condition used to predict the wavelength of absorption of light is

$$\frac{hc}{\lambda} = \Delta E = hc\bar{\nu} = h\nu$$

(iv) In addition to the energy and frequency criterion, there are some other conditions that are necessary in order for light to be absorbed. These refer to the symmetry of the molecule and the wave functions involved. They are referred to as selection rules. There are two kinds of selection rules - general selection rules and specific selection rules for each type of transition. These rules can be developed using quantum mechanics supplemented with the quantum mechanical theory of interaction of radiation with matter.

(v) The absorption spectrum refers to the absorption of electromagnetic radiation of definite energies/wavelengths/frequencies/wave numbers. A tunable light source which impinges on the sample and the transmitted/ scattered light is collected by a detector. The output is described as spectral lines. Typically, wavelength or wave number of the electromagnetic radiation vs. the intensity of absorbed/transmitted/scattered electromagnetic radiation is plotted. Based on this graph, one can identify specific wavelengths at which electromagnetic radiation is absorbed. This gives information about the energy spacings and can be used to characterize the molecule. The other properties of the spectrum like the line-width and the line intensity can give useful information.

1.2.1 Rotational/Microwave Spectroscopy:

The rotational motion of the diatomic molecule can be modeled as a rigid rotor with energy levels given by

$$E_J = \frac{\hbar^2}{2I} J(J+1) \quad where\ J = 0, 1, 2, \ldots$$

The letter *J* is used for molecules. Similarly, the quantum number M_J is used to denote the quantization of the Z-component of angular momentum. The moment of inertia of a diatomic molecule about its center of mass is given as $I = \mu r^2$ where μ is the reduced mass and *r* is the bond length of the molecule. The energy expression is expressed as

$$E_J = hcBJ(J+1) \quad where \quad B = \frac{\hbar}{4\pi cI}$$

The quantity *B* is referred to as the rotational constant of the molecule. It has units of inverse length and is typically expressed in cm^{-1}. For a transition from one state to another, the wave number of the electromagnetic radiation absorbed is proportional to *B*. The specific selection rules for rotational transitions are given below

$$\Delta J = \pm 1\,, \quad \Delta M_J = 0, \pm 1$$

The plus sign in ΔJ corresponds to absorption and the minus sign to emission of light [18,19]. Typically, a rotational absorption spectrum consists of a number of lines at different wave numbers corresponding to different transitions. The transitions from *J* to *J + 1* are characterized by an energy difference given by

$$E_{J+1} - E_J = 2hcBJ$$

and the corresponding wave number is *2BJ*. Thus the lines are observed at *2B, 4B, 6B, … .* Typical values of *B* are from 0.1-10 cm^{-1}.

The origin of spectral lines in molecular spectroscopy is the absorption, emission, and scattering of photon when the energy of a molecule changes. In molecules, there are energy states corresponding to nuclei vibrations and rotations. In consequence, the molecular spectra are more complex than atomic spectra and contain information on the molecular structure and the bond strength. They also provide a way of determining a variety of molecular properties, like dipole and quadrupole moments and the quantum numbers characterizing all molecular degrees of freedom. The molecular spectroscopy is also important for astrophysics and environmental science, for investigation of chemical composition, biological function and in many other areas of science and technology which

needs detailed investigation of properties of microscopic atomic and molecular objects. In the following Born-Oppenheimer approximation the energy of a molecule can be presented as sum of electronic energy E_{el}, vibrational energy E_{vib} and rotational energy E_{rot} energy [20].

$$E = E_{el} + E_{vib} + E_{rot} \quad \text{(i)}$$

Usually, transitions within the rotation energy levels manifold belong to the far infrared and microwave spectral region, transitions within the vibrational energy levels manifold belong to the infrared spectral region, and the transitions between the electronic energy levels belong to the visible, or ultraviolet spectral region. In general, the vibrational transitions result in changes in the rotational mode and the electronic transitions result in changes in the rotational and vibrational modes as well [21].

1.3 Experimental Techniques of molecular spectroscopy:

Progress in physics has often followed a path in which three areas are essential namely, structure, energy levels, and dynamics. (Structural analysis techniques have progressed and the latest breakthroughs due to Infra red (IR) which allow numerous structure-dynamics studies, particularly the quantitative identification of the atomic assembly of large bio-molecules and the determination of the microstructure of biological tissue in dynamic situations.) Due to the inherent complexity bio-molecules, (the size, structure and variety of molecules), it might be anticipated that biological samples would not be a good candidates for IR analysis.

However, when the intensity of the IR source is the extremely bright light provided by a synchrotron or with FTIR spectrophotometer with high signal to noise ratio , it is possible to obtain an excellent IR spectrum. The technique may be comparable to non-destructive testing in Physical/ Material Science/Life Science. The objectives of this research are (i) Investigation and extraction of internal motion from IR spectrum of bio-molecules/ biomaterials. (ii)To develop understanding on internal motion of complex system.(iii)To study the functional behavior of biomolecules from the variation of IR spectrum and dielectric Spectrum with variation of (a) external factor (b) environmental

variation (c) introduction of defects. (iv) preparation of a comprehensive analysis on internal motion and relaxation mechanism of biomolecules as complex system. (v) Development of an over dynamical characterization and quantum energy level map of bio-molecules under the purview of this project.

1.3.1 Fourier transform infrared spectroscopy:

Fourier transform infrared spectroscopy (FTIR) is a technique which is used to obtain an infrared spectrum of absorption, emission, photoconductivity or Raman scattering of a solid, liquid or gas. An FTIR spectrometer simultaneously collects spectral data in a wide spectral range. This confers a significant advantage over a dispersive spectrometer which measures intensity over a narrow range of wavelengths at a time. FTIR has made dispersive infrared spectrometers all but obsolete (except sometimes in the near infrared), opening up new applications of infrared spectroscopy. The term Fourier transform infrared spectroscopy originates from the fact that a Fourier transform (a mathematical process) is required to convert the raw data into the actual spectrum [22].

1.3.2 Conceptual introduction:

The goal of any absorption spectroscopy (FTIR, ultravioletvisible ("UV-Vis") spectroscopy, etc.) is to measure how well a sample absorbs light at each wavelength. The most straightforward way to do this, the "dispersive spectroscopy" technique, is to shine a monochromatic light beam at a sample, measure how much of the light is absorbed, and repeat for each different wavelength. (This is how UV-Vis spectrometers work, for example.) Fourier transform spectroscopy is a less intuitive way to obtain the same information. Rather than shining a monochromatic beam of light at the sample, this technique shines a beam containing many frequencies of light at once, and measures how much of that beam is absorbed by the sample. Next, the beam is modified to contain a different combination of frequencies, giving a second data point. This process is repeated many times. Afterwards, a computer takes all these data and works backwards to infer what the absorption is at each wavelength. The beam described above is generated by starting with a broadband light source that contains the full spectrum of wavelengths to be measured. The light shines into a Michelson interferometer having a certain configuration of mirrors, one of which is moved by a motor. As this mirror moves, each wavelength of

light in the beam is periodically blocked, transmitted, blocked, transmitted, by the interferometer, due to wave interference. Different wavelengths are modulated at different rates, so that at each moment, the beam coming out of the interferometer has a different spectrum. As mentioned, computer processing is required to turn the raw data (light absorption for each mirror position) into the desired result (light absorption for each wavelength). The processing required turns out to be a common algorithm called the Fourier transform (hence the name, "Fourier transform spectroscopy"). The raw data is sometimes called an "interferogram" [23,24].

1.3.3 Developmental background:

The first low-cost spectrophotometer capable of recording an infrared spectrum was the Perkin-Elmer Infracord produced in 1957. This instrument covered the wavelength range from 2.5 μm to 15 μm (wave number range 4000 cm^{-1} to 660 cm^{-1}). The lower wavelength limit was chosen to encompass the highest known vibration frequency due to a fundamental molecular vibration. The upper limit was imposed by the fact that the dispersing element was a prism made from a single crystal of rock-salt (sodium chloride) which becomes opaque at wavelengths longer than about 15 μm; this spectral region became known as the rock-salt region. Later instruments used potassium bromide prisms to extend the range to 25 μm (400 cm^{-1}) and caesium iodide 50 μm (200 cm^{-1}). The region beyond 50 μm (200 cm^{-1}) became known as the far-infrared region; at very long wavelengths it merges into the microwave region. Measurements in the far infrared needed the development of accurately ruled diffraction gratings to replace the prisms as dispersing elements since salt crystals are opaque in thisn region. More sensitive detectors than the bolometer were required because of the low energy of the radiation. One such was the Golay detector. An additional issue is the need to exclude atmospheric water vapour because water vapour has an intense pure rotational spectrum in this region. Far-infrared spectrophotometers were cumbersome, slow and expensive. The advantages of the Michelson interferometer were well-known, but considerable technical difficulties had to be overcome before a commercial instrument could be built. Also an electronic computer was needed to perform the required Fourier transform and this only became practicable with the advent of mini-computers, such as the PDP-8 which became available

in 1965. Digilab pioneered the world's first commercial FTIR spectrometer (Model FTS-14) in 1969 (Digilab FTIRs are now a part of Agilent technologies's molecular product line after it acquired spectroscopy business from Varian) [23, 24].

1.3.4 Michelson interferometer:

In a Michelson interferometer adapted for FTIR, light from the polychromatic infrared source, approximately a black-body radiator, is collimated and directed to a beam splitter. Ideally 50% of the light is refracted towards the fixed mirror and 50% is transmitted towards the moving mirror. Light is reflected from the two mirrors back to the beam splitter and (ideally) 50% of the original light passes into the sample compartment. There, the light is focused on the sample. On leaving the sample compartment the light is refocused on to the detector. The difference in optical path length between the two arms of the interferometer is known as retardation. An interferogram is obtained by varying the retardation and recording the signal from the detector for various values of the retardation. The form of the interferogram when no sample is present depends on factors such as the variation of source intensity and splitter efficiency with wavelength. This results in a maximum at zero retardation, when there is constructive interference at all wavelengths, followed by series of "wiggles". The position of zero retardation is determined accurately by finding the point of maximum intensity in the interferogram. When a sample is present the background interferogram is modulated by the presence of absorption bands in the sample. There are two principal advantages for an FT spectrometer compared to a scanning (dispersive) spectrometer. The multiplex or Fellgett's advantage. This arises from the fact that information from all wavelengths is collected simultaneously. It results in a higher Signal-to-noise ratio for a given scan-time or a shorter scan-time for a given resolution. The throughput or Jacquinot's advantage. This results from the fact that, in a dispersive instrument, the monochromator has entrance and exit slits which restricts the amount of light that passes through it. The interferometer throughput is determined only by the diameter of the collimated beam coming from the source. Other minor advantages include less sensitivity to stray light, and "Connes' advantage" (better wavelength accuracy), while a disadvantage is that FTIR cannot use the advanced electronic filtering techniques that often makes its signal-to-noise ratio inferior to that of dispersive measurements [25, 26].

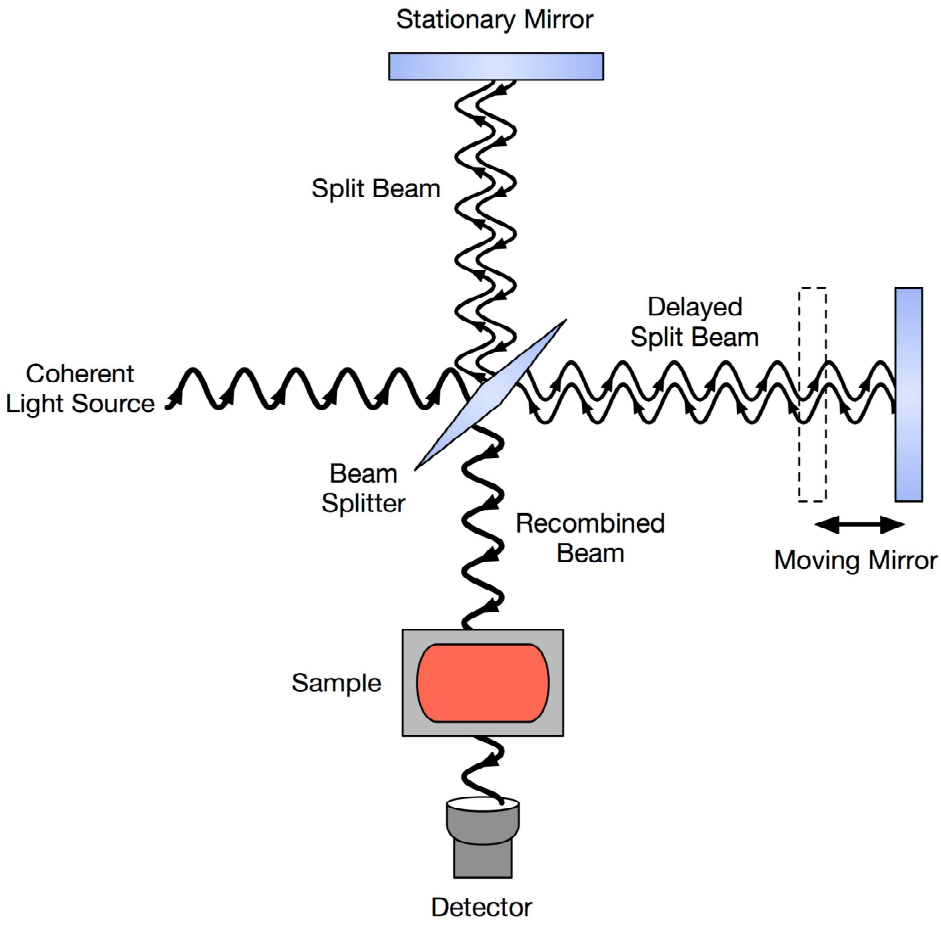

1.3.5 Beam splitter:

The beam-splitter cannot be made of a common glass, as it is opaque to infrared radiation of wavelengths longer than about 2.5μm. A thin film, usually of a plastic material, is used instead. However, as a material has limited range of optical transmittance, several beam-splitters are used interchangeably to cover a wide spectral range [27].

1.3.6 Fourier transform:

The interferogram in practice consists of a set of intensities measured for discrete values of retardation. The differences between successive retardation values are constant. Thus, a discrete Fourier transform is needed. The fast Fourier transform (FFT) algorithm is used.

1.3.7 Far-infrared FTIR:

The first FTIR spectrometers were developed for far-infrared range. The reason for this has to do with the mechanical tolerance needed for good optical performance, which is related to the wavelength of the light being used. For the relatively long wavelengths of the far infrared (~10 μm), tolerances are adequate, whereas for the rock-salt region tolerances have to be better than 1μm. A typical instrument was the cube interferometer developed at the NPL and marketed by Grubb Parsons. It used a stepper motor to drive the moving mirror, recording the detector response after each step was completed [28].

1.3.8 Mid-infrared FTIR:

With the advent of cheap microcomputers it became possible to have a computer dedicated to controlling the spectrometer, collecting the data, doing the Fourier transform and presenting the spectrum. This provided the impetus for the development of FTIR spectrometers for the rock-salt region. The problems of manufacturing ultra-high precision optical and mechanical components had to be solved. A wide range of instruments are now available commercially. Although instrument design has become more sophisticated, the basic principles remain the same. Nowadays, the moving mirror of the interferometer moves at a constant velocity, and sampling of the interferogram is triggered by finding zero-crossings in the fringes of a secondary interferometer lit by a helium-neon laser. This confers high wavenumber accuracy on the resulting infrared spectrum and avoids wavenumber calibration errors.

1.3.9 Near-infrared FTIR:

The near-infrared region spans the wavelength range between the rock-salt region and the start of the visible region at about 750 nm. Overtones of fundamental vibrations can be observed in this region. It is used mainly in industrial applications such as process control and chemical imaging.

1.3.10 A typical Interferrogram and its analysis:

Most interferometers employ a beamsplitter which takes the incoming infrared beam and divides it into two optical beams. One beam reflects off of a flat mirror which is

fixed in place. The other beam reflects off of a flat mirror which is on a mechanism which allows this mirror to move a very short distance (typically a few millimeters) away from the beamsplitter. The two beams reflect off of their respective mirrors and are recombined when they meet back at the beamsplitter. Because the path that one beam travels is a fixed length and the other is constantly changing as its mirror moves, the signal which exits the interferometer is the result of these two beams “interfering” with each other. The resulting signal is called an interferogram which has the unique property that every data point (a function of the moving mirror position) which makes up the signal has information about every infrared frequency which comes from the source.

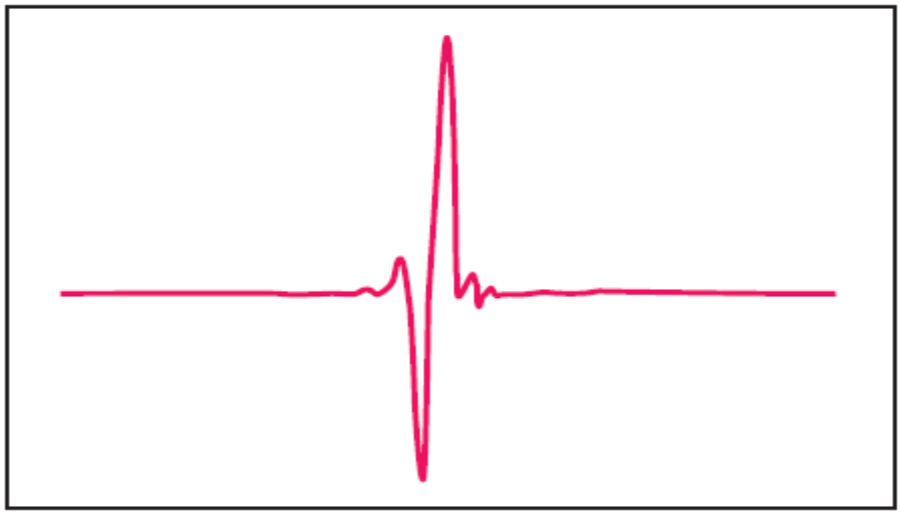

This means that as the interferogram is measured, all frequencies are being measured simultaneously. Thus, the use of the interferometer results in extremely fast measurements. Because the analyst requires a frequency spectrum (a plot of the intensity at each individual frequency) in order to make an identification, the measured interferogram signal can not be interpreted directly. A means of “decoding” the individual frequencies is required. This can be accomplished via a well-known mathematical technique called the Fourier transformation. This transformation is performed by the computer which then presents the user with the desired spectral information for analysis.

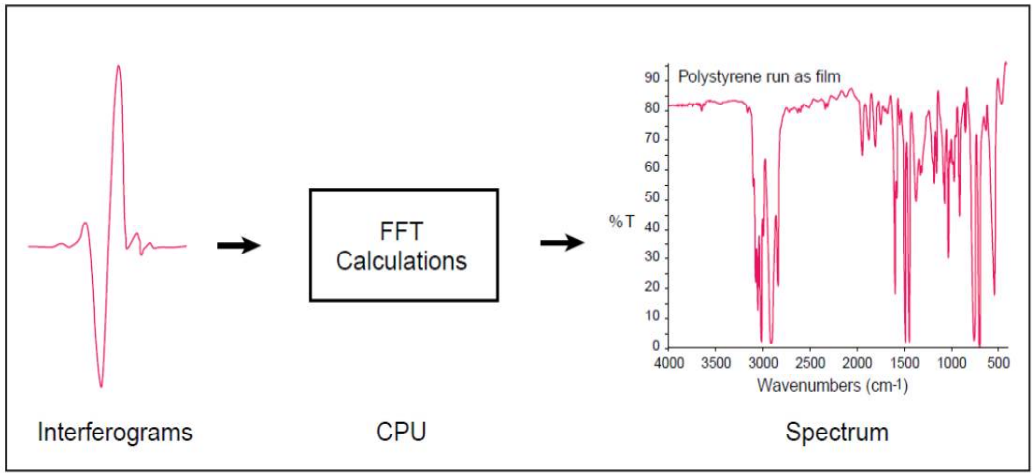

Because there needs to be a relative scale for the absorption intensity, a background spectrum must also be measured. This is normally a measurement with no sample in the beam. This can be compared to the measurement with the sample in the beam to determine the "percent transmittance." This technique results in a spectrum which has all of the instrumental characteristics removed. Thus, all spectral features which are present are strictly due to the sample. A single background measurement can be used for many sample measurements because this spectrum is characteristic of the instrument itself [29].

1.3.11 Advantages of FTIR:

The modern FT-IR spectrometer has three major advantages over a typical dispersive infrared spectrometer. These advantages are the reason FT-IR is now the standard tool, having largely displaced dispersive instruments by the mid 1980's.

A. Multiplex Advantage:

As seen from the operations description above, the interferometer does not separate energy into individual frequencies for measurement. Each point in the interferogram contains information from each wavelength of light being measured. Every stroke of the moving mirror equals one scan of the entire infrared spectrum, and individual scans can be combined to allow signal averaging. In the dispersive instrument, every wavelength across the spectrum must be measured individually as the grating scans. This can be a slow process, and typically only one spectral scan of the sample is made in a dispersive

instrument. The multiplex advantage means many scans can be completed and averaged on an FT-IR in a shorter time than one scan on most dispersive instruments.

B. Throughput Advantage:

The FT-IR instrument does not limit the amount of light reaching the detector using a slit. The Thermo Scientific FT-IR spectrometers also use the fewest number of mirrors necessary, which means less reflective losses occur. Overall, these mean more energy reaches the sample and hence the detector in an FT-IR spectrometer than in a dispersive spectrometer. The higher signal leads to an improved signal-to-noise ratio of the FT-IR. Higher signal-to-noise means that the sensitivity of the instrument for small absorptions will be greater, and details in a sample spectrum will be clearer and more distinguishable. The IR analysis of proteins is a good example – this is almost impossible in a classical dispersive instrument, while it is a fairly routine measurement for FT-IR.

The slit in a dispersive instrument becomes even more of a limitation as the spectral resolution desired increases. To see a narrower range, the slit closes down, choking the amount of light passing the instrument, resulting in poor quality spectra for all except ideal samples. Further, high resolution also implies a very slow scan speed, so it can take long times to collect a high resolution dispersive spectrum. To attain ultra-high resolution, the IR also uses an aperture, but the limitation of the light is not nearly so severe, and the multiplex advantage quickly gains back the loss.

C. Precision Advantage:

An FT-IR spectrometer uses a laser to control the velocity of the moving mirror and to time the collection of data points throughout the mirror stroke. This laser is also used as a reference signal within the instrument. The interferogram of the laser is a constant sine-wave, which provides the reference for both precision and accuracy of the infrared spectrometer. Well-designed FT-IR spectrometers rely exclusively on this reference laser, rather than any external reference sample. In this case, spectra collected with an FT-IR spectrometer can be compared with confidence whether they were collected five minutes or five years apart. This capability is not available on an dispersive infrared system, or any system requiring external calibration standards [30].

1.4 Energy levels of molecules with special reference to biomolecules:

Free atoms do not rotate or vibrate. For an oscillatory or a rotational motion of a pendulum, one end has to be tied or fixed to some point. In molecules such a fixed point is the center of mass. The atoms in a molecule are held together by chemical bonds. The rotational and vibrational energies are usually much smaller than the energies required to break chemical bonds. The rotational energies correspond to the microwave region of electromagnetic radiation ($3x10^{10}$ to $3x10^{12}$ Hz; energy range around 10 to100 J/mol) and the vibrational energies are in the infrared region ($3x10^{12}$ to $3x10^{14}$ Hz; energy range around 10kJ/mol) of the electromagnetic radiation. For rigid rotors (no vibration during rotation) and harmonic oscillators (wherein there are equal displacements of atoms on either side of the center of mass) there are simple formulae characterizing the molecular energy levels. In real life, molecules rotate and vibrate simultaneously and high speed rotations affect vibrations and vice versa.

1.4.1 Rotational Spectra of diatomic molecules:

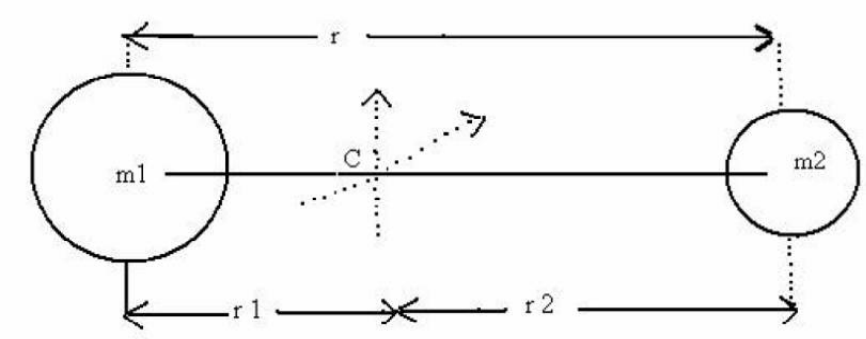

Fig.1.4.1. A rigid diatomic with masses m_1 and m_2 joined by a thin rod of length $r = r_1 + r_2$. The centre of mass is at C.

The two independent rotations of this molecule are with respect to the two axes which pass though C and are perpendicular to the "bond length" r. The rotation with respect to the bond axis is possible only for "classical" objects with large masses. For quantum objects, a "rotation" with respect to the molecular axis does not correspond to any change in the molecule as the new configuration is indistinguishable from the old one.

The center of mass is defined by equating the moments on both segments of the molecular axis.

$m_1r_1 = m_2r_2$ (1)

The moment of inertia is defined by

$I = m_1r_1^2 + m_2r_2^2$ (2)

$= r_1r_2 (m_1 + m_2)$ (3)

Therefore

$$r_1 = \frac{m_2 r}{m_1+m_2} \quad \text{and} \quad r_2 = \frac{m_1 r}{m_1+m_2} \tag{4}$$

Substituting the above equation in (3), we get

$$I = \frac{m_1 m_2 r^2}{m_1 + m_2} = \mu r^2, \quad \mu = \frac{m_1 m_2}{m_1 + m_2} \tag{5}$$

Where μ, the reduced mass is given by

$$\frac{1}{\mu} = \frac{1}{m_1} + \frac{1}{m_2} \tag{6}$$

The rotation of a diatomic is equivalent to a "rotation" of a mass μ at a distance of r from the origin C. The kinetic energy of this rotational motion is $K.E. = L^2/2I$ *where* L is the angular momentum, $I\omega$ where ω is the angular (rotational) velocity in radians/sec. The operator for L^2 is the same as the operator L^2 for the angular momentum of hydrogen atom and the solutions of the operator equations $L^2Y_{lm} = l\ (l + 1)\ Y_{lm}$, where Y_{lm} are the spherical harmonics.

The quantized rotational energy levels for this diatomic are

$$E_J = \frac{h^2}{8\pi^2 I} J(J+1) \tag{7}$$

The energy difference between two rotational levels is usually expressed in cm^{-1}. The wave number corresponding to a given ΔE is given by

$v = \Delta E / hc$, cm^{-1} (8)

The energy levels in cm^{-1} are therefore,

$$E_J = BJ(J+1) \quad where \quad B = \frac{h}{8\pi^2 cI} \tag{9}$$

The rotational energy levels of a diatomic molecule are shown in Fig. 1.4.2.

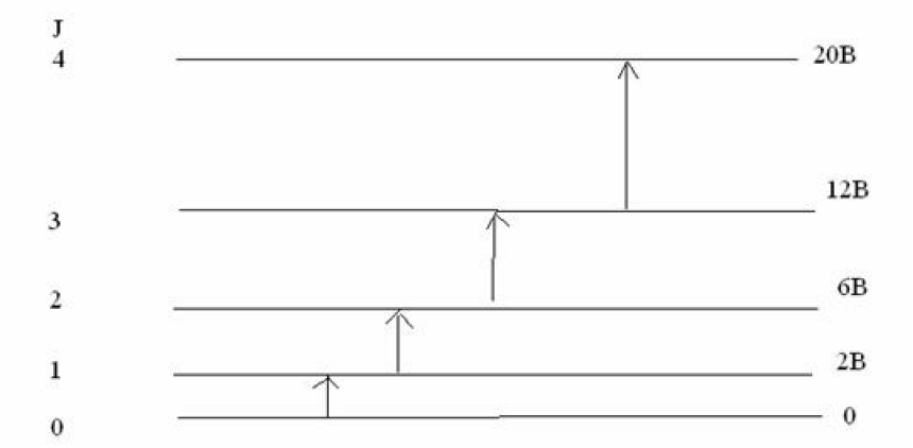

Fig.1.4.2. Rotational energy levels of a rigid diatomic molecule and the allowed transitions.

The selection rule for a rotational transition is,

$$\Delta J = \pm 1 \tag{10}$$

In addition to this requirement, the molecule has to possess a dipole moment. As a dipolar molecule rotates, the rotating dipole constitutes the transition dipole operator μ. Molecules such as HCl and CO will show rotational spectra while H_2, Cl_2 and CO_2 will not. The rotational spectrum will appear as follows

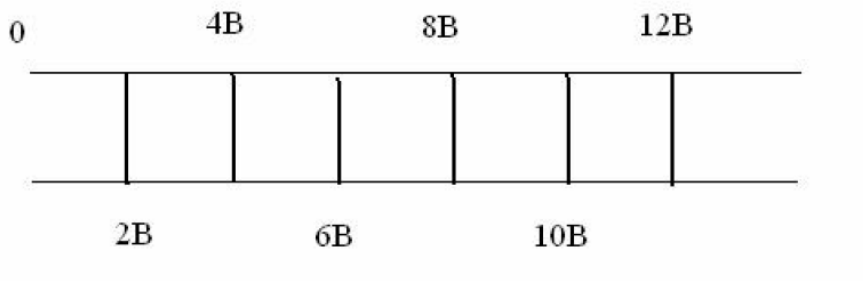

Fig.1.4.3. Rotational spectrum of a rigid diatomic. Values of B are in cm^{-1}. Typical values of B in cm^{-1} are 1.92118 (CO), 10.593 (HCl), 20.956 (HF), $^{1}H_2$ (60.864), $^{2}H_2$ (30.442), 1.9987(N2).

From the value of *B* obtained from the rotational spectra, moments of inertia of molecules *I*, can be calculated. From the value of *I*, bond length can be deduced.

1.4.2 Rotational Spectra of Polyatomic molecules:

Linear molecules such as OCS and HC≡CCl have spectra similar to diatomics. In diatomics as well as linear triatomics, $I_A = I_B$; $I_C = 0$. I_A, I_B and I_C are the three moments of inertia of molecules along three independent axes of rotation. Just as any translation can be decomposed into three independent components along three axes such as x, y and z, any rotation can be decomposed into rotations along three axes A, B, and C. The way to choose these axes is to have the simplest values of I_A, I_B and I_C. Since triatomics are heavier than the constituent diatomics, their moments of inertia are larger and the values of rotational constants, B, are smaller, in the range of 1 cm^{-1}. The value of I_A or I_B determined from the B value gives the total length of the triatomic. To determine the two bond lengths in the linear triatomic, the moment of inertia $I_{A'}$ of an isotope of the triatomic is needed. From two values of I_A and $I_{A'}$, the two bond lengths can be determined.

The rotational spectra of asymmetric molecules for which $I_A \neq I_B \neq I_C$ can be quite complicated. For symmetric tops, two moments of inertia are equal i.e.,

$$I_A = I_B \neq I_C; \qquad I_C \neq 0 \tag{11}$$

In CH_3Cl for example, the main symmetry axis is the C – Cl axis. Two quantum numbers are required to describe the rotational motion with respect to I_A and I_C

respectively. Here *J* represents the total angular momentum of the molecule and *K* the angular momentum with respect to the C – Cl axis of the symmetric top. *J* takes on integer values and *K* cannot be greater than *J* ($m_l \leq l$ for orbital angular momentum). The *(2J + 1)* "degeneracy" is expressed through the *2J + 1* values that *K* can take.

$$K = J, J-1, \ldots\ldots 0, \ldots\ldots, -(J-1), -J \tag{12}$$

The rotational energies of a symmetric top are given by

$$\frac{E_{J,K}}{hc} = BJ(J+1) + (A-B)K^2 \ , \ \ cm^{-1} \tag{13}$$

The moments of intertia are related to *B* and *A* as

$$B = \frac{h}{8\pi^2 I_C c} \qquad and \qquad A = \frac{h}{8\pi^2 I_A c} \tag{14}$$

As the energy depends on K^2, energies for states with + *K* and – *K* are doubly degenerate. Thus there will be *J + 1* levels and *(2J + 1)* states for each values of *J*.

The selection rules for the symmetric top are,

$$\Delta J = \pm 1 \quad and \quad \Delta K = 0 \tag{15}$$

It can be easily shown that

$$\frac{(E_{J+1,K} - E_{J,K})}{hc} = 2BJ(J+1) \tag{16}$$

This implies that the spectrum is independent of the value of K which refers to the rotation about the symmetry axis such as the C - Cl axis. The rotation about this axis does not change the dipole moment. The molecular dipole moment changes during the rotational motion to induce the transition. Rotation along the axis A and B changes the dipole moment and thus induces the transition.

By using rotational or microwave spectroscopy, very accurate values of bond lengths can be obtained. For example, in HCN, the C-H length is 0.106317 ± 0.000005 nm and the CN bond length is 0.115535 ± 0.000006 nm. The principle of the microwave oven

involves heating the molecules of water through high speed rotations induced by microwaves. The glass container containing water however remains cold since it does not contain rotating dipoles.

1.4.3 Vibrations and Rotations of a diatomic:

Simple pendulums or stretched strings exhibit simple harmonic motion about their equilibrium positions. Molecules also exhibit oscillatory motions. A diatomic oscillates about its equilibrium geometry. The quantized vibration energies E_v of a harmonic oscillator are

$$E_v = (v + {}^1/_2)hv \qquad (17)$$

[v = 0, 1, 2, ...]

The vibrational frequency v is related to the force constant k through

$$v = \frac{1}{2\pi}\sqrt{\frac{k}{\mu}}, \quad Hz \qquad (18)$$

The vibrational motion occurs under the action of a binding potential energy. The potential energy (PE) curve for a harmonic oscillator is given in Fig.1.4.4.

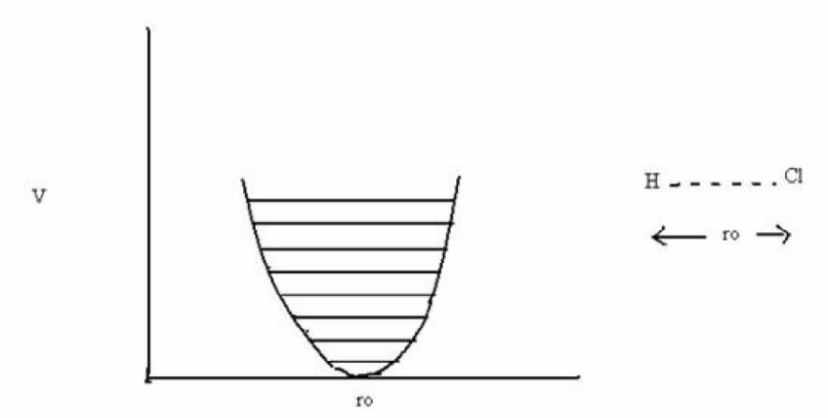

Fig.1.4.4. The potential energy of a harmonic oscillator $V = k(r-r_o)^2$. The force constants k in N/m for a few molecules are, CO (1902), HF (966), HCl (516), HI (314).

On either sides of the equilibrium bond length r_0, the PE rises as a symmetric quadratic function (a parabola). The vibrational wavefunctions can be obtained by solving the Schrodinger equation. The Hamiltonian operator (for energy) now consists of a kinetic energy term and a potential energy term V as shown in Fig. 1.4.4 and the solutions for energy, E_v have already been given in Eq.(17). The selection rules for the harmonic oscillator are:

$$\Delta v = \pm 1 \qquad (19)$$

Several equally spaced lines (spacing hν) corresponding to the transitions 0→1, 1→2, 2→3 and so on are seen. The first transition will be the most intense as the state with ν = 0 is the most populated. In actual diatomics, the potential is anharmonic. A good description of an anharmonic oscillator is given by the Morse potential function.

$$\text{P.E.} = D_{eq}\,[1 - \exp\{a\,(r_o - r\}]^2 \qquad (20)$$

D_{eq} is the depth of the PE curve and r_0 is the bond length. A plot of the Morse curve and the energy levels for the Morse potential are given in Fig. 1.4.5. The formula for the energy levels of this anharmonic oscillator is

$$E_v/hc = e_v = (\nu + ½)\,\nu - (\nu + ½)^2\,\nu\,X_e,\ \text{cm}^{-1} \qquad (21)$$

Here X_e, is called the anharmonicity constant whose value is near 0.01. It can be easily deduced from the above formula that the vibrational energy levels for large ν start bunching together.

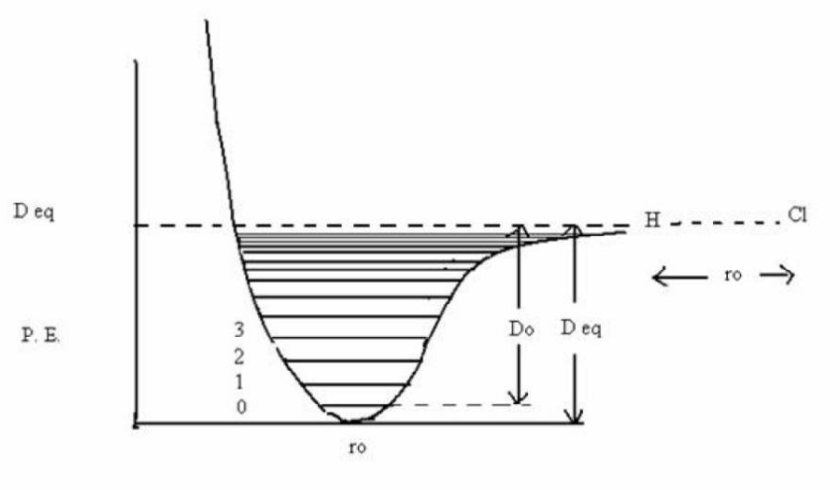

Fig.1.4.5. The Morse potential and the energy levels.

Often, one observes a combined vibrational rotational spectrum. A combined set of vibrational and rotational energy levels of a diatomic is given by

$$E_{total} = BJ\,(J + 1) + (\nu + ½)\,\nu - (\nu + ½)^2\,\nu\,X_e,\ cm^{-1} \qquad (22)$$

The energy level diagram and the spectrum corresponding to the diagram are shown in Fig.1.4.6.

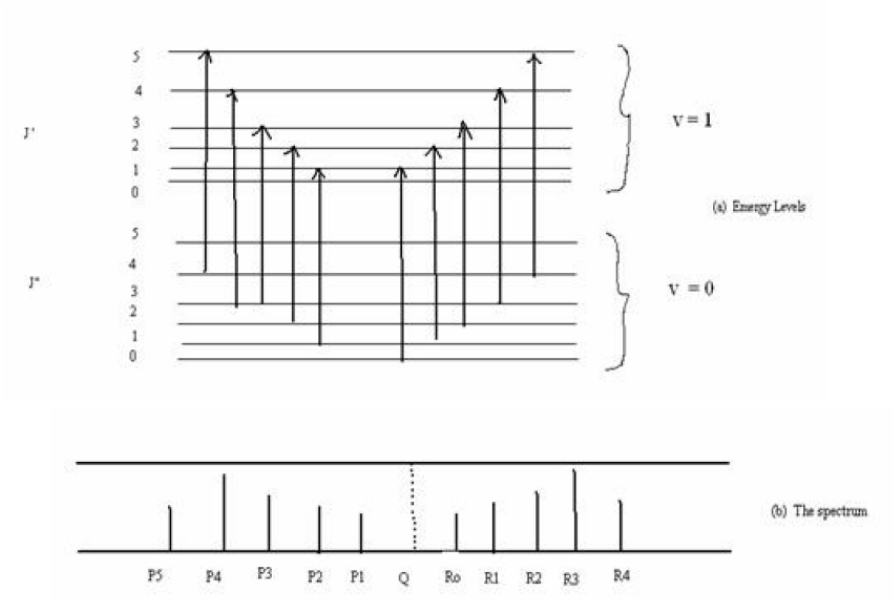

Fig.1.4.6. The vibrational rotational spectrum.

The selection rules are $\Delta\nu = \pm 1, \pm 2, \ldots, \Delta J = \pm 1$. $\Delta J = 1$ corresponds to the R branch on the right at higher frequencies and $\Delta J = J'' - J' = -1$ corresponds to the P branch

on the left. The dashed line Q for which $\Delta J = 0$, is not seen. The difference between R_0 and P_1 is 4B and the difference between adjacent R lines and adjacent P lines is 2B.

1.4.4 Vibrational spectra of Polyatomic molecules:

An atom moving in three dimensions has three degrees of freedom corresponding to the freedom in movement along x, y and z directions. A collection of N unbound atoms will have 3N degrees of freedom. If the N atoms are bound through the formation of a molecule, the 3N degrees of freedom get redistributed into translational, rotational and vibrational modes. Since the molecule can be translated as a unit, there are three translational modes (degrees of freedom). Similarly there are three rotational modes with respect to three independent axis of rotation. The remaining, 3N-6 are the vibrational modes. For a linear molecule, since there are only two rotational modes with respect to the two axes perpendicular to the molecular axis, there are 3N-5 vibrational modes.

If the potential energy functions for all the motions can be assumed to be harmonic, then the 3N-6 modes can be categorized into 3N-6 normal modes. Consider the example of water. There are three atoms and 3N-6 = 3 normal modes. In terms of the potential energy functions for vibrations, there are three functions: one of each corresponding to each O-H bond and one corresponding to the H-O-H bending. In terms of the individual bond vibrations, the vibrational motion can appear quite complex. The total potential energy P.E. may be written as:

$$\text{P.E.} = \tfrac{1}{2} k (r_1 - r_{10})^2 + \tfrac{1}{2} k (r_2 - r_{20})^2 + \tfrac{1}{2} k' (\theta - \theta_0)^2 \qquad (23)$$

Here, r_{10} and r_{20} are the equilibrium bond lengths of the two O-H bonds and θ_0 is the equilibrium bond angle. A normal mode of vibration is defined as a vibration in which all atoms oscillate with the same frequency and pass through their equilibrium positions at the same time. The center of mass is unchanged during a normal mode. The three normal modes of vibration of water are shown in the following figure.

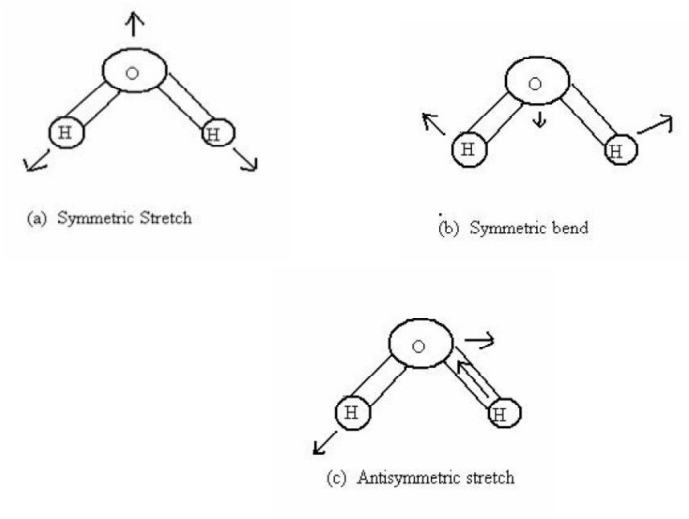

Fig.1.4.7. Normal modes of vibrations of water.

The three normal modes of vibrations of water are the symmetric stretch (ν_1 = 3651.7 cm^{-1}), the antisymmetric stretch (ν_2 = 3755.8 cm^{-1}) and the symmetric bend (ν_3 = 1595.0 cm^{-1}). Bending requires less energy and thus, its frequency is lower. The asymmetric stretch requires greater reorganization than the symmetric stretch and hence a larger frequency. Molecular CO_2 is a linear triatomic and has 3N - 5 = 4 normal modes of vibration. The symmetric stretch (ν_1 = 1330 cm^{-1}) asymmetric stretch (ν_2 = 2349.3 cm^{-1}) and bending (ν_3 = 66.3 cm^{-1}) are shown in Fig 1.4.8. The bending mode is doubly degenerate, owing to the two independent bending modes in two perpendicular planes containing the molecular axis.

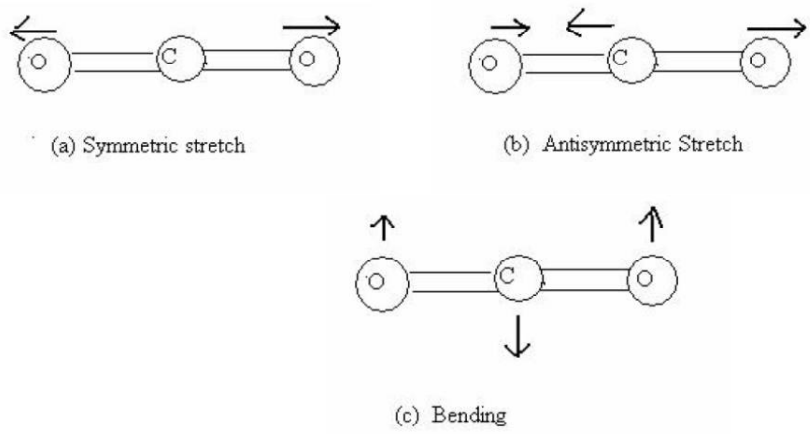

Fig.1.4.8. Normal modes of vibrations of CO_2.

Different molecules can be easily identified by their normal mode frequencies. In addition to these modes, overtones ($2\nu_1$, $3\nu_2$ etc.), combination bonds ($\nu_1 + \nu_2$, $2\nu_1 + \nu_2$, $\nu_1 + \nu_2 + \nu_3$ …), and difference bands ($\nu_1 - \nu_2$, $\nu_1 + \nu_2 - \nu_3$) can be observed. Since a large number of rotational and vibrational levels are closely spaced they provide a rich base for setting up lasers when the upper levels are populated. As in the case of diatomics, rotational lines are richly dispersed in vibrational spectra of polyatomics. The concept of normal modes can be extended to solids and liquids too. Since in a solid, there are a very large number of atoms (of the order of Avogadro number), there are 3N-6 normal modes. These are characterized as phonons, which corresponds to collective motions of atoms in a solid.

1.4.5 Analysis by IR Spectroscopy:

IR spectroscopy has grown into an extremely versatile analytical tool. Most organic and inorganic groups (such as CH_3, -C=C, M-C≡0) have characteristic frequencies and these frequencies provides finger prints, using which the groups in newly synthesized molecules can be identified. Although one cannot "see" molecules, through various spectral methods, but can identify atoms, groups, bond lengths, relative locations (cis/trans, endo/exo) and so on. The IR frequencies of a few common groups are given in the following table.

Group	Approximate frequency	Group	Approximate frequency
C-I	550	S-H	2580
C-Cl	725	$=CH_2$	3030
C=S	1100	C=C	1650
C-O-	1000-1200	C=O	1600-1750
C-N	1000-1200	≡C-H	3300
C-C	1000-1200	$-N=H_2$	3400
C=N-	1600	O-H	3600
-C≡C-	2200		
-C≡N	2250	H- bonds	3200-3570

$-CH_2$	2930(asym stretch), 2860(sym stretch), 1470(deformation)	Aromatic C-H	3060

Table 2. Characteristic frequencies (in cm^{-1}) of some molecular groups.

1.5 Computer Molecular Dynamics Simulation (CMD):

Molecular dynamics (MD) simulation is a computer simulation technique that allows one to predict the time dependent evolution of a system of interacting particles using laws of physics. Studying the dynamic development of a biological system with the consideration of protein flexibility is of vital importance, since many biological phenomena involving proteins are very dynamic processes, which include transport, molecular recognition, enzyme catalysis, and allosteric regulation. The static models produced by NMR, X-ray crystallography, and homology modeling offer valuable insights into macromolecular structure, while MD simulation can provide atomic-level information about protein conformational changes and binding thermodynamics under predefined physiological conditions (e.g., temperature, pressure), allowing for the study of a protein system at a timescale that is not accessible by current experimental approaches [31].

The general workflow of MD simulation service follows these steps: First, a model system is selected, in which missing segments are fixed and the protonation states determined. Then the system is energy minimized and equilibrated by solving Newton's equations of motion until the properties of the system no longer change with time. After equilibration, a production run is performed for an appropriate period of time to output trajectories, which are then analyzed for the properties of interest.

MD simulation method helps to predict the time dependent changes in a protein system, which can contain proteins, DNAs/RNAs, lipids and other small ligands, allowing for the exploration of events of biological and pharmaceutical importance. Specifically, simulation can be performed to characterize protein flexibility, refine experimentally determined structures, evaluate protein-ligand binding, study biocatalysis or even monitor the protein folding process. MD simulation is also particularly useful in computer-aided

drug discovery for the identification of cryptic or allosteric binding sites, the enhancement of traditional virtual-screening methodologies, and the direct prediction of small-molecule binding energies.

1.5.1 Computer Simulation as a Powerful Research Tool:

Experiment plays a central role in science. It is the wealth of experimental results that provides a basis for the understanding of the chemical machinery of life. Experimental techniques, such as X-ray diffraction or nuclear magnetic resonance (NMR), allow determination of the structure and elucidation of the function of large molecules of biological interest. Yet, experiment is possible only in conjunction with models and theories.

Computer simulations have altered the interplay between experiment and theory. The essence of the simulation is the use of the computer to model a physical system. Calculations implied by a mathematical model are carried out by the machine and the results are interpreted in terms of physical properties. Since computer simulation deals with models it may be classified as a theoretical method. On the other hand, physical quantities can (in a sense) be measured on a computer, justifying the term ‘computer experiment’.

The crucial advantage of simulations is the ability to expand the horizon of the complexity that separates ‘solvable’ from ‘unsolvable’. Basic physical theories applicable to biologically important phenomena, such as quantum, classical and statistical mechanics, lead to equations that cannot be solved analytically (exactly), except for a few special cases. The quantum Schrodinger equation for any atom but hydrogen (or any molecule) or the classical Newton’s equations of motion for a system of more than two point masses can be solved only approximately. This is what physicists call the many-body problem.

It is intuitively clear that less accurate approximations become inevitable with growing complexity. More accurate wave function for the hydrogen molecule can be computed than for large molecules such as porphyrins, which occur at the active centres of many important biomolecules. It is also much harder to include explicitly the electrons in the model of a protein, rather than representing the atoms as balls and the bonds as springs. The use of the computer makes less drastic approximations feasible. Thus,

bridging experiment and theory by means of computer simulations makes possible testing and improving models using a more realistic representation of nature. It may also bring new insights into mechanisms and processes that are not directly accessible through experiment.

On the more practical side, computer experiments can be used to discover and design new molecules. Testing properties of a molecule using computer modelling is faster and less expensive than synthesizing and characterizing it in a real experiment. Drug design by computer is commonly used in the pharmaceutical industry [32-35].

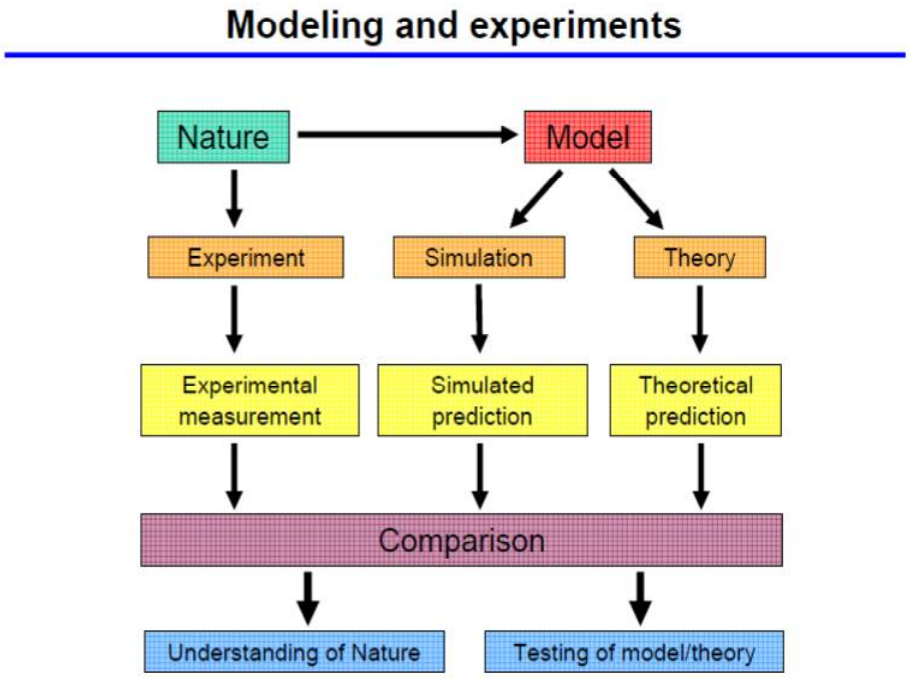

1.6 Factors affecting spectra of biomolecules:

The amount of energy required to stretch a bond depends on the strength of the bond and the masses of the bonded atoms. The stronger the bond, the greater the energy required to stretch it. The frequency of the vibration is inversely proportional to the mass of the atoms, so heavier atoms vibrate at lower frequencies. The value of vibrational frequency of a bond calculated by Hooke's Law is not always equal to their observed value. The force constant is changed with the electronic and steric effects caused by other

groups present in the surroundings. Ultraviolet-visible spectroscopy involves the absorption of ultraviolet/visible light by a molecule causing the promotion of an electron from a ground electronic state to an excited electronic state. Therefore a chromophore may or may not impart colour to a compound depending on whether the chromophore absorbs radiation in the visible or UV region.

There are no standard criteria for the identification of a chromophore because the wavelength and intensity of absorption depend on many factors such as the molecular environment of the chromophore and on the solvent in which the sample is dissolved. Other parameters, such as pH and temperature, also may cause changes in both the intensity and the wavelength of the absorbance maxima. All the compounds having the same functional group will absorb at almost the same wavelength if the other factors such as conjugation, substituents etc are absent [36, 37].

1.6.1 Effects of Conjugation:

When two or more chromophores are conjugated the absorption maxima is shifted to a larger wavelength or shorter frequency. Conjugation increases the energy of the highest occupied molecular orbital and decreases the energy of lowest unoccupied molecular orbital. As a result less energy is required for an electronic transition in a conjugated system than in a non-conjugated system.

1.6.2 Effect of Steric hindrance:

The UV-spectroscopy is very sensitive to the distortion of the chromophores. The position of absorption maximum and its intensity depend on the length and effectiveness of the conjugative system. Electronic conjugation works best when the molecule is planar in configuration. If the presence of an auxochrome prevents the molecule from being planar then it may lead to the red or blue shifts depending upon the nature of distortion.

1.6.3 Effect of solvent:

The absorption spectrum depends on the solvent in which the absorbing substance is dissolved. The choice of solvent can shift peaks to shorter or longer wavelengths. This depends on the nature of the interaction of the particular solvent with the environment of the chromophore in the molecule under study.

1.6.4 Effect of Sample pH:

The pH of the sample solution can also have a significant effect on absorption spectra. The absorption spectra of certain aromatic compounds such as phenols and anilines change on changing the pH of the solution. The acid-base indicators (pH indicators) have their application due to their absorptions in the visible region of the UV-Vis spectrum. A small change in the chemical structure of the indicator molecule can cause a change in the chromophore resulting in significant colour change at different pH values.

1.6.5 Effect of Sample Temperature:

The effect of temperature is less pronounced. However, simple thermal expansion of the solution may be sufficient to change band intensity. Therefore to get more accurate results the spectrum needs to taken at a specified or constant temperature. The following three criteria may be given as general effect of temperature on solution spectra.

1. Band sharpness increases with decreasing temperature.

2. Position of absorption maximum does not move or moves very little towards the longer wavelength side, with decreasing temperature.

3. The total absorption intensity is approximately independent of the temperature.

1.6.6 Effect of sample Concentration:

According to Lambert-Beer law it might be expected that the sample concentration is directly proportional to the intensity of the absorption. But at high concentrations, molecular interactions can take place causing changes to the position and shape of absorption bands. Such effects need to be identified and taken into consideration for quantitative work. The solvent used also affects the fineness of absorption band in UV-spectrum. It has been observed that polar solvents give rise to broad bands, non-polar solvents show more resolution, while completely removing the solvent gives the best resolution. This is due to solvent-solute interaction. If the dielectric constant of the solvent is high, there will be stronger solute-solvent interaction [36].

1.6.7 Effect of Bond Order:

Bond order affects the position of absorption bands. Higher the bond order larger is the band frequency. A C-C triple bond is stronger than a C=C bond, so a C-C triple bond has higher stretching frequency than does a C=C bond. The C-C bonds show stretching vibrations in the region from 1200-800 cm^{-1} but these vibrations are weak and of little value in identifying compounds. Similarly, a C=O bond stretches at a higher frequency than does a C-O bond and a C-N triple bond stretches at a higher frequency than does a C=N bond which in turn stretches at a higher frequency than does a C-N bond.

1.6.8 Resonance and Inductive Electronic Effects:

The discussion about the IR band corresponds to a range of frequency for each stretch is usually assigned as the exact position of the absorption band depends on other structural features of the molecule, such as electron delocalization, the electronic effect of neighbouring substituents, and hydrogen bonding. Important details about the structure of a compound can be revealed by the exact position of the absorption band.

1.6.9 Effect of Hydrogen Bonding:

The presence of hydrogen bonding changes the position and shape of an infrared absorption band. Frequencies of both stretching as well as bending vibrations are changed because of hydrogen bonding. The X-H stretching bands move to lower frequency usually with increased intensity and band widening. The X-H bending vibration usually shifts to higher frequencies. Stronger the hydrogen bonding, greater is the absorption shift from the normal values. The two types of hydrogen bonding (intramolecular and intermolecular) can be differentiated by the use of infrared spectroscopy. Inter-molecular hydrogen bonding involves association of two or more molecules of the same or different compound, and it may results in dimer molecules as in carboxylic acids. Intra-molecular hydrogen bonds are formed when the proton donor and acceptor are present in a single molecule under special conditions that allow the required overlap of orbitals.

The extent of inter-molecular hydrogen bonding depends upon the concentration of the solution and hence the position and the shape of an absorption band also depend upon

the concentration of the solution. The more concentrated the solution, the more likely it is for the OH-containing molecules to form intermolecular hydrogen bonds. It is easier to stretch an O-H bond if it is hydrogen bonded, because the hydrogen is attracted to the oxygen of neighbouring molecule. Therefore, the O-H stretching of a concentrated (hydrogen bonded) solution of an alcohol occurs at about 3550 cm^{-1}, whereas the O-H stretching band of a dilute solution (with little or no hydrogen bonding) appears at 3650 cm^{-1}. Additionally, hydrogen-bonded OH groups also have broader absorption bands whereas the absorption bands of non-hydrogen–bonded OH groups are sharper.

1.6.10 Effect of Fermi Resonance:

Fermi resonance is a phenomenon which was first explained by the Italian physicist Enrico Fermi to account for shifting of the energies and intensities of absorption bands in an infrared spectroscopy. Sometimes, it happens that two different vibrational levels have nearly the same energy. If such vibrations belong to the same species of molecules, then a mutual perturbation of energy may occur, resulting in the shift of one towards lower frequency and the other towards a higher frequency. It is also accompanied by a substantial increase in the intensity of the respective bands.

1.6.11 Effect of Bond angles:

Smaller ring requires the use of more p-character to make the internal C-C bonds for the requisite small angles. This gives more s-character to the C=O sigma bond which causes the strengthening and stiffening of the exo-cyclic double bond. The force constant K is then increased and the absorption frequency increases [37].

References:

[1] Sujata V. Bhat, Biomaterials, Narosa Publishing House, 2002.

[2] Meyers, M. A.; Chen, P. Y.; Lin, A. Y. M.; Seki, Y. "Biological materials: Structure and mechanical properties". Progress in Materials Science, (2008).

[3] Espinosa, H. D.; Rim, J. E.; Barthelat, F.; Buehler, M. J. "Merger of structure and material in nacre and bone-Perspectives on de novo biomimetic materials". Progress in Materials Science, (2009).

[4] Solomon EP, Berg LR, Martin DW, Biology, Cengage Learning. (2004).

[5] Long Island University "The Chemistry of Carbohydrates", (May 29, 2013).

[6] Avenas P ,"Etymology of main polysaccharide names", Springer-Verlag, (2012).

[7] Jenkins DJ, Jenkins AL, Wolever TM, Thompson LH, Rao AV , "Simple and complex carbohydrates", (1986).

[8] Pigman W, Horton D,The Carbohydrates: Chemistry and Biochemistry Vol 1A (2nd ed.). San Diego: Academic Press, (1972).

[9] McNaught, A. D.; Wilkinson, A.,"Lipids". Compendium of Chemical Terminology (2nd ed.), Oxford: Blackwell Scientific Publications, (1997).

[10] Fahy E, Subramaniam S, Murphy RC, Nishijima M, Raetz CR, Shimizu T, Spener F, van Meer G, Wakelam MJ, Dennis EA ,"Update of the LIPID MAPS comprehensive classification system for lipids". Journal of Lipid Research, (2009).

[11] Subramaniam S, Fahy E, Gupta S, Sud M, Byrnes RW, Cotter D, Dinasarapu AR, Maurya MR ,"Bioinformatics and systems biology of the lipidome". Chemical Reviews, (2011).

[12] Mashaghi S, Jadidi T, Koenderink G, Mashaghi A,"Lipid nanotechnology". International Journal of Molecular Sciences, (2013).

[13] Beat Keller, Structural Cell Wall Proteins, Plant Physiol. (1993) 101: 1127-1130.

[14] Andreeva, A, "SCOP2 prototype: a new approach to protein structure mining". Nucleic Acids Res, (2014).

[15] Mertz, E.T., The protein and amino acid needs. In Fish nutrition, edited by J.E. Halver. New York, Academic Press, 1972.

[16] Elson D,"Metabolism of nucleic acids (macromolecular DNA and RNA)". Annu. Rev. Biochem, (1965).

[17] National Institute of Health, "Discovering DNA: Friedrich Miescher and the early years of nucleic acid research", (2007).

[18] Gordy, W. A., Microwave Molecular Spectra in Technique of Organic Chemistry. IX. New York: Interscience, (1970).

[19] Jennings, D.A.; Evenson, K.M; Zink, L.R.; Demuynck, C.; Destombes, J.L.; Lemoine, B; Johns, J.W.C., "High-resolution spectroscopy of HF from 40 to 1100 cm−1: Highly accurate rotational constants". Journal of Molecular Spectroscopy, (1987).

[20] M. Baer, Beyond Born–Oppenheimer: Electronic non-Adiabatic Coupling Terms and Conical Intersections, Wiley and Sons, 2006.

[21] Chang, Raymond, Basic Principles of Spectroscopy. McGraw-Hill, (1971).

[22] Griffiths, P.; de Hasseth, J. A., Fourier Transform Infrared Spectrometry (2nd ed.). Wiley-Blackwell, (2007).

[23] "The Infracord double-beam spectrophotometer". Clinical Science. 16 (2). 1957.

[24] Peter R. Griffiths; James A. De Haseth, Fourier Transform Infrared Spectrometry (2nd ed.). John Wiley & Sons, (2007).

[25] Hariharan, P., Basics of Interferometry, Second Edition. Elsevier, (2007).

[26] Olszak, A.G.; Schmit, J.; Heaton, M.G. "Interferometry: Technology and Applications", 2012.

[27] Griffiths, P.R.; Holmes, C, Handbook of Vibrational Spectroscopy, Vol 1. Chichester: John Wiley and Sons, (2002).

[28] Chamberain, J.; Gibbs, J.E.; Gebbie, H.E. , "The determination of refractive index spectra by fourier spectrometry". Infrared Physics, (1969).

[29] Introduction to Fourier Transform Infrared Spectrometry, Thermo Nicolet Corporation, 2001.

[30] Advantages of a Fourier Transform Infrared Spectrometer, Thermo Fisher Scientific Inc., 2008-2015.

[31] Jarosaw Meller, Molecular Dynamics, Encyclopedia of Life Sciences, (2001).

[32] M. P. Allen and D. J. Tildesley, Computer Simulation of Liquids, Clarendon Press, Oxford, (1987).

[33] A. R. Leach, Molecular Modelling, 2nd edition, Prentice Hall, Harlow, (2001).

[34] D. Frenkel and B. Smit, Understanding Molecular Simulation, Academic Press, San Diego, (2002)

[35] T. Schlick, Molecular Modeling and Simulation, Springer-Verlag, New York, (2002).

[36] Diwan. S. Rawat, D Kumar, Nature of electronic transitions and the factors affecting it, Organic Spectroscopy.

[37] Diwan. S. Rawat, D Kumar, Factors affecting vibrational frequencies and IR Spectroscopy of Hydrocarbons, Organic Spectroscopy.

Chapter 2

Structure and function of bio-molecules

2.1 Structural change of bio-molecule and its detection by FTIR analysis:

Functions of bio-molecules are mostly dependent on their structure and dynamical configuration which are affected by their environment and other physical parameters. Structural and vibrational characteristics of bio-molecules are important in determining bio-molecular functions. Visible region is a small part of a broad spectrum of electromagnetic radiation. On the immediate high energy side of the visible spectrum lies the ultraviolet, and on the low energy side is the infrared. The portion of the infrared region most useful for analysis of organic compounds is not immediately adjacent to the visible spectrum, but is that having a wavelength range from 2,500 to 16,000 nm, with a corresponding frequency range from 1.9×10^{13} to 1.2×10^{14} Hz.

Photon energies associated with this part of the infrared are not large enough to excite electrons, but may induce vibrational excitation of covalently bonded atoms and groups. The covalent bonds in molecules are not rigid sticks or rods, such as found in molecular model kits, but are more like stiff springs that can be stretched and bent. In addition to the facile rotation of groups about single bonds, molecules experience a wide variety of vibrational motions, characteristic of their component atoms. Consequently, virtually all organic compounds will absorb infrared radiation that corresponds in energy to these vibrations. Infrared spectrometers, similar in principle to the UV-Visible spectrometer, permit observer to obtain absorption spectra of compounds that are a unique reflection of their molecular structure.

Infrared spectra may be obtained from samples in all phases (liquid, solid and gaseous). Liquids can be examined by ATR (Attenuated Total Reflectance) which is an accessory of FTIR spectrophotometer to measure surface properties of solid or thin film samples rather than their bulk properties. Generally, ATR has a penetration depth of around 1 or 2 micrometers depending on the sample conditions. The sample must be in direct contact with the ATR crystal. In horizontal ATR (HATR) units, the crystal is a parallel-sided plate, typically about 5 cm by 1 cm, with the upper surface exposed. When

measuring solids by ATR, it is essential to ensure good optical contact between the sample and the crystal. The accessories have devices that clamp the sample to the crystal surface and apply pressure. As with all FT-IR measurements, an infrared background is collected, in this case, from the clean ATR crystal. The crystals are usually cleaned by using a solvent soaked piece of tissue. Typically water, methanol or isopropanol are used to clean ATR crystals. The ATR crystal must be checked for contamination and carry over before sample presentation, this is true for all liquids and solids. Solids may be incorporated in a thin KBr disk, prepared under high pressure [1, 2].

2.1.1 Vibrational Spectroscopy:

A molecule composed of n-atoms has 3n degrees of freedom, six of which are translations and rotations of the molecule itself. This leaves 3n-6 degrees of vibrational freedom (3n-5 if the molecule is linear). Vibrational modes are often given descriptive names, such as stretching, bending, scissoring, rocking and twisting. The exact frequency at which a given vibration occurs is determined by the strengths of the bonds involved and the mass of the component atoms.

In practice, infrared spectra do not normally display separate absorption signals for each of the 3n-6 fundamental vibrational modes of a molecule[3]. The number of observed absorptions may be increased by additive and subtractive interactions leading to combination tones and overtones of the fundamental vibrations, in the same way that acoustic vibrations from a musical instrument interact. Furthermore, the number of observed absorptions may be decreased by molecular symmetry, spectrometer limitations, and spectroscopic selection rules. Some general trends relating to vibrational modes of molecule are-

i) Stretching frequencies are higher than corresponding bending frequencies. (It is easier to bend a bond than to stretch or compress it.)

ii) Bonds to hydrogen have higher stretching frequencies than those to heavier atoms.

iii) Triple bonds have higher stretching frequencies than corresponding double bonds, which in turn have higher frequencies than single bonds. (Except for bonds to hydrogen).

The complexity of infrared spectra in the 1500 to 350 cm^{-1} region makes it difficult to assign all the absorption bands, and because of the unique patterns found there corresponds to some specific functional group or group of atoms, it is often called the fingerprint region. Absorption bands in the 7000 to 1500 cm^{-1} region are usually due to stretching vibrations of diatomic units, and this is sometimes called the group frequency region (functional group region)[4-7]. Fingerprint region is very important in bio-molecular dynamics [8] and it may provide much relevant information about the internal motion of the molecule and is related bio-molecular function in living systems.

2.1.2 Group Frequencies:

Detailed information about the infrared absorptions observed for various bonded atoms and groups is usually presented in tabular form. The following table [9] provides a collection of such data for the most common functional groups. Since most organic compounds have C-H bonds, a useful rule is that absorption in the 2850 to 3000 cm^{-1} is due to sp^3 C-H stretching; whereas, absorption above 3000 cm^{-1} is from sp^2 C-H stretching or sp C-H stretching if it is near 3300 cm^{-1}. Standard abbreviations (str = strong, wk = weak, brd = broad & shp = sharp) are used to describe the absorption bands. Elaborate discussion about various functional groups may be found in standard literatures [10-14].

Functional Group		Characteristic Absorptions(in cm^{-1})
Oxidized Nitrogen Functions	=NOH Oxime O-H (stretch) C=N N-O	 3550-3600 (str) 1665± 15 945± 15
	N-O amine oxide aliphatic aromatic	 960± 20 1250± 50
	N=O nitroso	1550± 50 (str) 1530± 20 (as) & 1350± 30 (s)

	nitro	
Silicon Functions	Si-H silane	2100-2360 cm-1 (str)
	Si-OR	1000-11000 (str & brd)
	Si-CH3	1250± 10 (str & shp)
Sulfur Functions	S-H thiols	2550-2600 (wk & shp)
	S-OR esters	700-900 (str)
	S-S disulfide	500-540 (wk)
	C=S thiocarbonyl	1050-1200 (str)
	S=O sulfoxide sulfone sulfonic acid sulfonyl chloride sulfate	1030-1060 (str) 1325± 25 (as) & 1140± 20 (s) (both str) 1345 (str) 1365± 5 (as) & 1180± 10 (s) (both str) 1350-1450 (str)
Phosphorous Functions	P-H phosphine	2280-2440 (med & shp) 950-1250 (wk) P-H bending
	(O=)PO-H phosphonic acid	2550-2700 (med)
	P-OR esters	900-1050 (str)
	P=O phosphine oxide phosphonate phosphate phosphoramide	1100-1200 (str) 1230-1260 (str) 1100-1200 (str) 1200-1275 (str)

2.2 Structural change of bio-molecule due to radiation damage:

Bio-molecules share a structural complexity that is also reflected in their complex dynamical behaviour. The internal motions in most of the bio-molecules are partly vibrational and partly rotational. The complex motion involves groups of atom undergoing a plethora of continuous or jumplike diffusion. The strategy developed in this research is to combine the results from quantum theory with that of spectroscopy and to compare them with that of the available result. The proposed combined study will provide geometry

of motion and distribution of relaxation times of various parts (within a range of time scales permissible by this study) of bio-molecules along with effect of hydration. This technique can investigate on very small (1 mg) or less amount of specimen in its native/environmental condition. In fact it is superior in the said context over that other technique like inelastic Neutron scattering or XRD and NMR (in some cases) studies. An overall database to be prepared to develop a characterization technique of bio-molecule from this outcome of the present work. The outcome may serve as a new addition to Physics of complex system and related technological applications. Bio-molecules have very low excitation energy (10 meV) and often very small amount of specimens are required. This sort of specimens required very special types of instrument with neutron source having adequate beam flux. That is why it is a less popular technique, however Quasielastic neutron scattering (QENS) [15] may investigate structure and function of bio-molecules elegantly. In another study [16] infrared absorption spectrum of biomolecule of gum acacia was analyzed from measured data of FTIR spectra. The change in characteristics bond vibration detected clearly. The obtained shift of the characteristics frequency caused due to change of molecular structure introduced by polymerization effect.

Combinations of two or more of the simple sugars through glycoside linkages give substances known as polysaccharides. They also are called oligosaccharides if made from two to ten sugar units. The simplest oligosaccharides are disaccharides made of two molecules of simple sugars that can be the same or different. Simple sugars can be joined with 0-glycoside links. Among the more important disaccharides are sucrose, maltose, cellobiose and lactose.

Sucrose and lactose occur widely as the free sugars, lactose in the milk of mammals, and sucrose in fruit and plants (especially in sugar cane and sugar beet). Maltose is the product of enzymatic hydrolysis of starch, and cellobiose is a product of hydrolysis of cellulose.

To fully establish the structure of a disaccharide, one must determine-

(i) The identity of the component monosaccharides;

(ii) The type of ring junction, furanose or pyranose, in each monosaccharide, as it exists in the disaccharide;

(iii) The positions that link one monosaccharide with the other; and

(iv) The anomeric configuration (α or β) of this linkage.

Hydrolysis of disaccharides with enzymes is very helpful in establishing anomeric configurations, because enzymes are highly specific catalysts for hydrolysis of the different types of glycoside linkages.

Sucrose consists of two monosaccharides, glucose and fructose. It is not a reducing sugar, it forms no phenylosazone derivative, and it does not mutarotate. Therefore the anomeric carbons of both glucose and fructose must be linked through an oxygen bridge in sucrose. Thus sucrose is a glycosyl fructoside or, equally, a fructosyl glucoside. Because sucrose is hydrolyzed by enzymes that specifically assist hydrolysis of both α glycosides (such as yeast α-glucosidase) and β-fructosides (such as invertase), it is inferred that the glucose residue is present as an α glucoside and the fructose residue as a β fructoside[17].

The glycosidic bond in sucrose is formed between the reducing ends of both glucose and fructose and not between the reducing end of one and the nonreducing end of the other. Most glycosidic bonds are synthesized in nature from sugars that are activated by a cofactor. The glycosidic bond is formed upon transfer of a sugar molecule from the donor (an activated sugar) to an acceptor molecule (typically another sugar) [18].

In this present work vibrational and rotational characteristic of sucrose molecule along with its characteristic change due to LASER irradiation on it are studied. Both functional group and finger print region are taken into consideration for analyzing the obtained shift in FTIR absorption spectrum of pure sucrose and Laser irradiated sucrose. The objective of this paper is to study the effect of radiation damage on sucrose.

2.2.1 Sample preparation:

The sucrose specimen (S1) was collected in crystal form from Merck (India). Some of these crystals specimen were pressed to get the powder form suitable for analysis. A small portion of the sucrose specimen was taken and irradiated by He-Ne LASER beam (2

mW) for about 45 min. Now the new specimen (S2) was supposed to be partially damaged by LASER radiation.

2.2.2 General procedure:

The developed irradiated sucrose specimen (S2) is supposed to exhibit change in molecular structure over that in S1 due to radiation damage by He-Ne LASER beam. FTIR analysis on pure sucrose specimen was carried out to examine its molecular structure and dynamical information of it. FTIR analysis on specimen S2 was also carried out. Comparing the vibrational and rotational spectrum of the two specimens, effect of radiation damage caused by the irradiation on bio-molecule may be analyzed. The analysis was carried out using FTIR model, IR affinity 1, Shimadzu, Japan, at high resolution (resolution was 0.5 cm^{-1} averaging with 100 scans) using KBr window.

2.3 Analysis of the result:

Fig. 2.3.1 shows the comparison of the FTIR spectra between the developed sucrose specimens within wave number range 380 to 349 cm^{-1}.

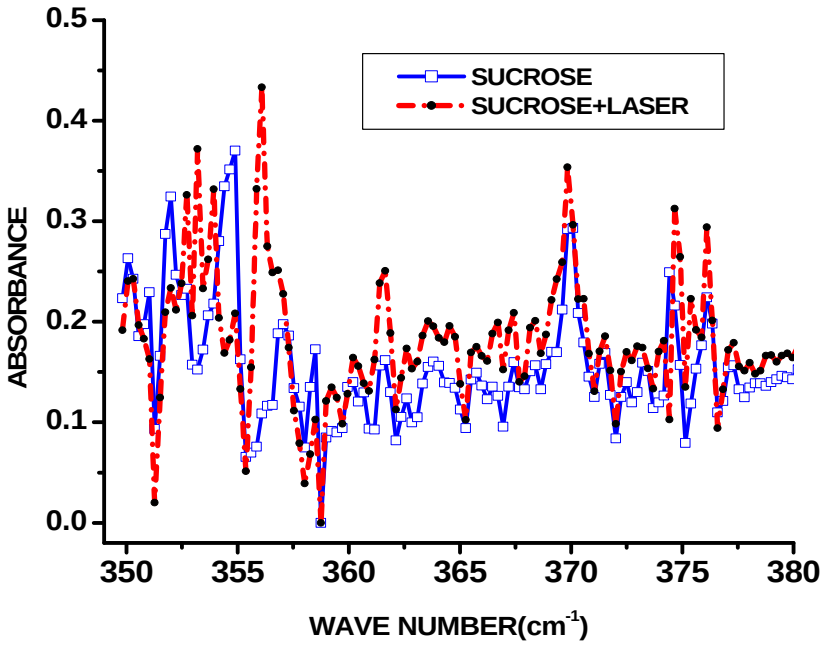

Fig. 2.3.1. FTIR absorption spectrum of specimen S1 and S2 in finger print region at 27 ºC,

Fig. 2.3.2 shows comparison the FTIR spectra of S1 and S2 specimens between wave number 3405 to 3365 cm^{-1}.

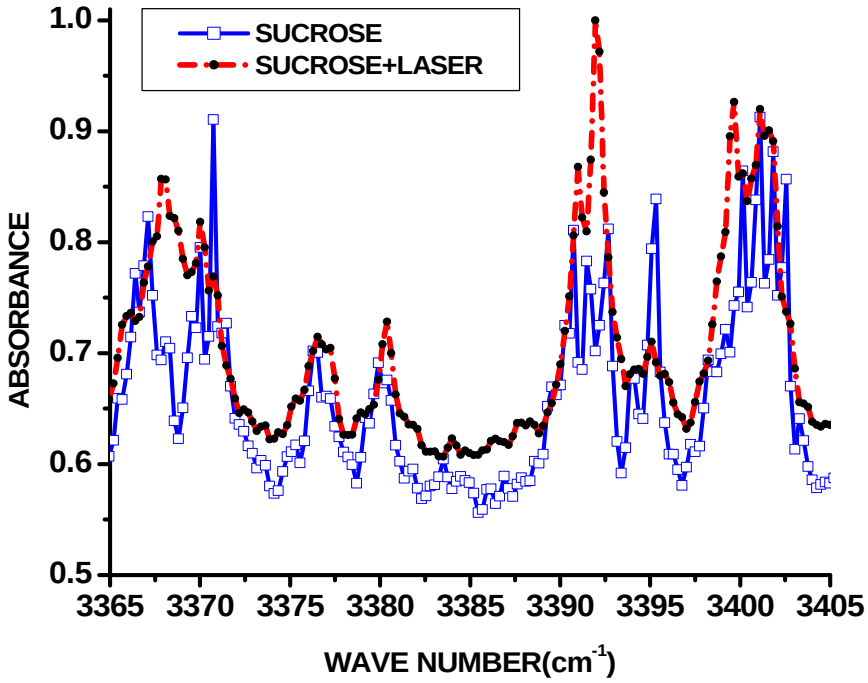

Fig. 2.3.2. FTIR absorption spectrum of specimen S1 and S2 in functional group region at 27 ºC

After analyzing Figs. 2.3.1 and 2.3.2, and entire FTIR spectrum between wave number 4000 to 350 cm^{-1} of both the specimens S1 and S2 (Tables 2.3.1 and 2.3.2). The comparison of peak position and the corresponding absorption intensity between the specimens S1 and S2 were made clearly. Table-2.3.1 shows that the positions of most of the peaks remain same and only the positions of the peaks at wavenumber (cm^{-1}) 419.74, 417.58, 402.39, 400.46, 393.71, 380.45, 373.21, 370.08, 367.43, 360.68, 357.06, 351.03, 350.07, were changed. Whereas from Table-2.3.2 it was found that only the position of the peaks at wave number (cm^{-1})3469.83, 3466.45, 3441.86, 3420.40, 3359.41, 3296.72, remain same and the position of most of the peaks changed. This suggests that irradiation affect vibrational mode more than that of the rotational mode.

Pure Sucrose		Radiation damaged Sucrose	
Peak position(cm^{-1})	**Intensity**	**Peak position(cm^{-1})**	**Intensity**
350.07	0.2630	350.31	0.2428
351.03	0.2292	–	–
352.00	0.3244	352.00	0.2336
352.72	0.2328	352.72	0.3263
354.89	0.3702	354.89	0.2083
357.06	0.1974	356.10	0.4331
358.51	0.1726	358.51	0.1026
360.19	0.1398	360.19	0.1642
360.68	0.1295	–	–
361.64	0.1619	361.64	0.2507
362.61	0.1238	362.61	0.1735
365.74	0.1492	365.74	0.1752
366.46	0.1354	366.43	0.2090
367.43	0.1596	366.70	0.1992
370.08	0.2933	369.84	0.3536
371.53	0.1688	371.53	0.1856
372.49	0.1399	372.49	0.1699
373.21	0.1593	372.97	0.1756
376.11	0.2243	376.11	0.2941
377.31	0.1566	377.31	0.1790
380.45	0.1603	378.04	0.1591
381.89	0.1536	381.89	0.1743
382.86	0.1506	382.86	0.1813
393.71	0.1791	394.43	0.2231
396.84	0.1944	396.84	0.2065
400.46	0.2346	400.22	0.2472
402.39	0.2066	–	–
417.58	0.1841	417.82	0.2010
418.54	0.2114	418.54	0.2290
419.74	0.1877	419.99	0.1990

TABLE 2.3.1. Position of significant peaks and corresponding intensity of different specimens (S1 and S2) between 420 to 350 cm^{-1}.

Pure Sucrose		Radiation damaged Sucrose	
Peak position(cm^{-1})	**Intensity**	**Peak position(cm^{-1})**	**Intensity**
3140.49	0.5080	3222.71	0.5038
3290.94	0.8712	3294.31	0.6814
3296.72	0.7960	3296.72	0.7102
3302.03	0.7487	3302.23	0.7166
3350.73	0.8146	3357.72	0.6463
3359.41	0.7297	3359.41	0.7106
3363.99	0.6428	3366.16	0.7362
3411.97	0.7113	3418.23	0.6203
3420.40	0.6304	3420.40	0.6632
3427.40	0.6309	3425.47	0.6135
3437.04	0.7439	3437.28	0.7069
3441.86	0.5615	3441.86	0.5867
3443.79	0.5690	3445.72	0.5992
3465.01	0.6060	3463.80	0.5563
3466.45	0.7238	3466.45	0.5696
3469.83	0.7748	3469.83	0.5600
3475.62	0.5819	3473.20	0.5319
3592.30	0.5014	3562.41	0.5073

TABLE 2.3.2. Position of significant peaks and corresponding intensity of different specimens (S1 and S2) between 3600 to 3140 cm^{-1}.

The comparison of the FTIR spectra of S1 and S2 specimens between wave number 1080 to 1045 cm^{-1} is shown in Fig. 2.3.3.

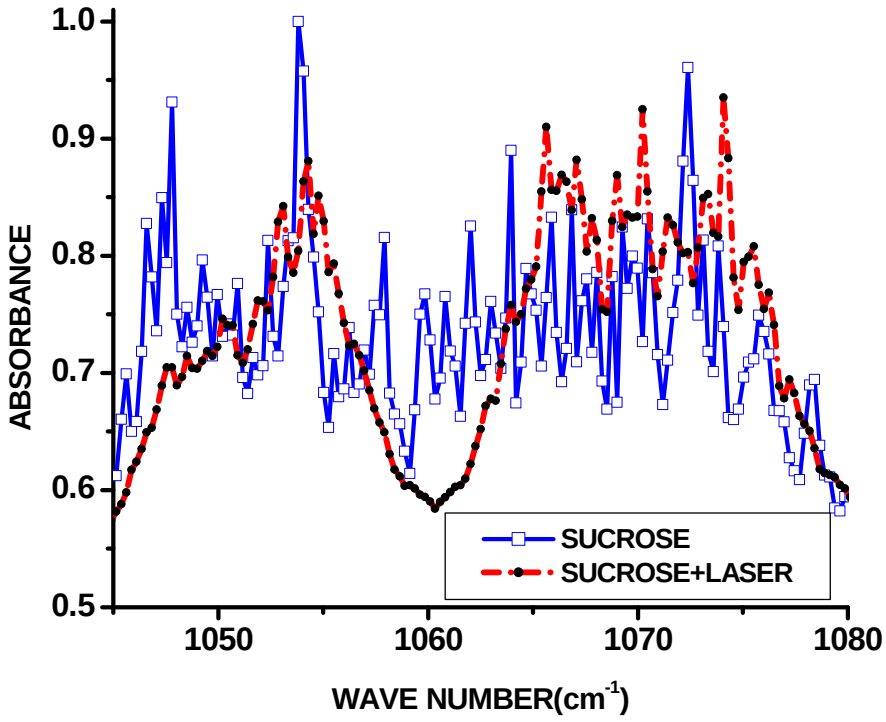

Fig.2.3. 3. Comparison of FTIR absorption spectrum of specimen S1 and S2 at 27 ºC

Temperature dependent vibrational modes of the glycosidic bond [19] in sucrose are found 1200 to 1000 cm^{-1}. Peaks found at wave number (cm^{-1}) 1072.39, 1065.88, 1063.95, 1062.02, 1060.81, 1059.05, 1057.92, 1053.82, 1047.79 for pure sucrose molecule from Fig. 2.3.3 represent the glycosidic bond in sucrose molecule which are absent in the FTIR spectra of irradiated sample. This indicate that during the irradiation most of the glycosidic bond were damaged which cannot be reproduced. But the peaks arise due to -OH bonds are present at wavenumbers [20] ranging from 3600 to 3200 cm^{-1}. These peaks are not absent in the FTIR absorption spectrum of irradiated sucrose but their positions are shifted from that of the pure sucrose specimen.

2.4 Outcome :

The analysis shows that there is some definite change (as mentioned in the previous section and found in Table 2.3.1 and Table 2.3.2) in molecular vibration spectra over its corresponding pure bio-molecule. The laser irradiation on pure sucrose molecule

caused damage, in its molecular structure and its finger print is detectable from FTIR analysis [21]. The glycoside bond of sucrose is affected due to radiation damage.

References:

[1] F. M. Mirabella, Jr., Practical Spectroscopy Series; Internal reflection spectroscopy: Theory and applications, Marcel Dekker, Inc., (1993).

[2] "FT-IR Spectroscopy—Attenuated Total Reflectance (ATR)", Perkin Elmer Life and Analytical Sciences, (2005).

[3] C.N. Banwell and E.M. McCash, Fundamental of Molecular Spectroscopy, Tata McGraw-Hill, edn. 4 (1995).

[4] Allen, H.C.; Cross, P.C., Molecular vib-rotors; the theory and interpretation of high resolution infra-red spectra. New York: Wiley, (1963).

[5] Atkins, P.W.; de Paula, J. , Physical Chemistry (8th ed.). Oxford University Press., (2006).

[6] Hollas, M.J., Modern Spectroscopy (3rd ed.). Wiley, (1996).

[7] Straughan, B.P.; Walker, S., Spectroscopy. 2 (3rd ed.). Chapman and Hall., (1976).

[8] E. Fanchon, E. Geissler, J.-L. Hodeau, J.-R. Regnard and P.A. Timmins, Structure and Dynamics of Biomolecules: Neutron and Synchrotron Radiation for Condensed Matter Studies, Oxford University Press, NY,(2000).

[9] https://www2.chemistry.msu.edu/faculty/reusch/virttxtjml/spectrpy/infrared/infrared.htm

[10] George Socrates, Infrared and Raman Characteristic Group Frequencies: Tables and Charts. John Wiley & Sons, (2004).

[11] Peter Larkin, Infrared and Raman Spectroscopy; Principles and Spectral Interpretation. Elsevier, (2011).

[12] Kazuo Nakamoto, Infrared and Raman Spectra of Inorganic and Coordination Compounds, Applications in Coordination, Organometallic, and Bioinorganic Chemistry. John Wiley & Sons, (2009).

[13] NSRDS-NBS: National Standard Reference Data Series, National Bureau of Standards, U.S. Government Printing Office. June 1972.

[14] Jacox, Marilyn E., "Vibrational and Electronic Energy Levels of Polyatomic Transient Molecules. Supplement B". Journal of Physical and Chemical Reference Data, (2003).

[15] L. Van Hove and K. W. McVoy, Pair distribution functions and scattering phenomena, Nucl. Phys. 33, 468-476 (1962).

[16] A. Dutta and A. Sarkar, Adv. Appl. Sci. Res., 2, 125 (2011).

[17] https://authors.library.caltech.edu/25034/21/BPOCchapter20.pdf

[18] Carme Rovira, HOW DOES NATURE FORM GLYCOSIDIC BONDS? An ab initio molecular dynamics investigation, 2011.

[19] J.A. Seo, H.J. Kwon, H.K. Kim and Y.H. Hwang, Science, 343, 660 (2008).

[20] D.L. Pavia, G.M. Lampman, G.S. Kriz and J.R. Vyvyan, Spectroscopy, Cengage Learning (2007).

[21] Arup Dutta and A. Sarkar, “FTIR Investigation of Structural Change Due to Radiation Damage in Biomolecule”, Asian Journal of Chemistry; Vol. 23, No. 12 (2011), 5584-5586.

Chapter 3

Structural distinction between complex bio-molecules by FTIR technique

3.1 Brief introduction of few complex natural bio-molecules:

All living body contains carbon(C) hydrogen (H), oxygen (O), nitrogen (N), phosphorous (P) and sulfur (S). Of the hundred plus chemical elements, about 31 occur naturally in plants and animals. The elements present in biological material can be divided into three categories:

1. Elements found in bulk form and essential for life: Carbon, hydrogen, oxygen, nitrogen, phosphorus, and sulfur make up about 92% of the dry weight of living things.

2. Elements in trace quantities in most organisms and very likely essential for life, such as calcium, manganese, iron, and iodine.

3. Trace elements that are present in some organisms and may be essential for life, such as arsenic, bromine, molybdenum, and vanadium [1-3].

Biomolecules are molecules that are made by organisms and are essential for performing life functions. They ranged in size and perform specific functions in and among cells. Their function is often determined by their structure. If the structure is disrupted, the biomolecule can no longer function properly. Biomolecules are made of building-block monomers. A monomer is a small molecule that can be combined chemically with other monomers to form larger molecules. Monomers are made up of relatively simple elements. A polymer is a group of monomers linked to form a much larger molecule. “Mono-” means “one,” and “poly-” means many. The process of making a polymer is called polymerization.

When a biomolecule is built, monomers link together via strong covalent bonds. Each time two monomers are linked a water molecule is released. This process is called dehydration synthesis. When a water molecule is added to a polymer, it breaks apart the polymer during a process called hydrolysis.

There are four main types of large biomolecules (called macromolecules): carbohydrates, lipids, proteins, and nucleic acids. As shown in the chart below, they are composed of different types of monomers that link together to form polymers. Lipids are not composed of true polymers because they are smaller, and the monomers are not repeating.

Type of Biomolecule	Monomer	Polymer or Linked – Monomer Compound	Covalent bond name between monomers
Carbohydrate	Monosaccharide	Polysaccharide	Glycosidic bond
Lipid	Fatty acid	Diglyceride, triglyceride, phospholipid	--
Protein	Amino acid	Polypeptide, protein	Peptide bond
Nucleic acid	Nucleotide	DNA, RNA	Phosphodiester bond

Brief introduction of some important complex bio-molecules are given below:

3.1.2 Proteins:

Amino acids are the building blocks of proteins. There are hundreds of types of amino acids, but just twenty of these make up natural proteins. Each amino acid has a common core of a central carbon, an amine group containing nitrogen, a carboxyl group made of carbon and oxygen, and a side chain (labeled R on amino acid diagrams). The side chain is different for each of the twenty amino acids. Some side chains are hydrophobic, while others are hydrophilic, or water-soluble. Some side chains are charged, while others are neutral. The different properties of the side chains give each amino acid different properties. Amino acids are linked together by covalent bonds called peptide bonds. This type of bond only forms between amino acids. The reaction to form a peptide bond is a dehydration synthesis reaction. One hydrogen atom and one hydroxyl group (–OH) are removed from the amino acids to form one water molecule for each peptide bond that is formed. Amino acids are linked together to form a polypeptide chain. Inside

the cell, an organelle called the ribosome is responsible for linking together amino acids to form the polypeptide chain. When a chain contains more than about 50 amino acids arranged in a biologically functional way, it is called a protein. Proteins are essential bio-molecules in all cells. They give a cell structure, communicate information, synthesize molecules, transport molecules, and make up enzymes, molecules that speed up chemical reactions necessary for life.

3.1.2 Nucleic Acids:

Nucleotides are small molecules made of a sugar (monosaccharide), one or more phosphate groups, and a nitrogenous base. The nucleotides ATP (adenosine triphosphate) and GTP (guanosine triphosphate) are important for energy transport within cells. The nitrogenous base of ATP is adenosine, and the phosphate group is a triphosphate (three phosphates linked together). GTP is similar to ATP, with guanosine replacing adenosine as the nitrogenous base. Other nucleotides are enzyme cofactors and signalling molecules. Nucleotides are the building blocks of nucleic acids, including DNA (deoxyribonucleic acid) and RNA (ribonucleic acid). DNA includes four nucleotides— guanine, adenine, thymine, and cytosine. In RNA, uracil replaces thymine as a nucleotide. DNA and RNA are essential for storing and utilizing genetic information. DNA and RNA work together to create proteins. As you can see in the diagram on the left, alternating bonds between sugar and phosphate molecules of adjacent nucleotides link the nucleotides that make up DNA. This forms the sugar-phosphate backbone of a strand of DNA. Two DNA strands typically join together via weak hydrogen bonds between nitrogenous bases. The DNA strands twist around further to form the familiar double helix configuration. In contrast, RNA is typically single stranded and does not form a double helix [4-8].

3.1.3 Gums:

Gums are natural plant exudates that had oozed from site of injury on tree barks or on fruits and hardened upon exposure to air. In general gums may be classified into three major classes, namely, natural gums, chemically modified natural gums and chemically synthesized type synthetic gums. Popular natural gums are arabic, Acacia Catechu, Mangostreen, Karaya , Ghati gum , guar gum , gum tragacanth and some more unidentified gums. Natural exudates gums are produced in response to injury, e.g., Gum

Arabica from *Acacia* species and extractive gums extracted from fruits of some plant e.g. gum Mangostreen from *Garciana Mangostreena* species. Some other exudates gums are, Tragacanth gum from *Asiatic astraglus* species, gum Karaya from *Sterculia* and gum Ghatti from *Anogeissus latifolia*. Natural gums are not plant latex.

Chemical nature of natural gums:

In general natural gums are complex acidic polysaccharides consisting of salts of sugars like L-arabinose, D-galactose, L-rhamnose and D-glucuronic acid complexed with metallic ions like sodium, potassium, calcium and magnesium etc [9]. In fact chemical composition of particular is not unique rather it may vary with geographical location of generic plant. In general these gums have highly branched structures consisting of different monosaccharide units with different possible variations such as degree of branching, length of branches and type of chemical linkages, to give rise a numerous possible chemical structure. Therefore, an almost infinite number of structures are possible. The molecular forces acting between different portion of the polysaccharides molecules and that of solvent are may be of hydrogen bonding, ionic charges, dipole - dipole interactions types. These forces are responsible for the fascinating physical, chemical and adhesive properties of natural gums. The extracted raw gum from their natural sources may contain inorganic and organic impurities like ash, tracer water molecule, heavy metallic ligand, bacteria etc. A purified protected gum may retain its form over thousands of years [10-14].

Rheological Nature

Gum Arabica and **gum Mangostreen** are polyelectrolytes, soluble in water, over a wide range of concentration, below 40% concentration pseudo-plastic characteristics are observed, denoted by a decrease in viscosity. With increasing temperature the relative viscosity and density of Gum Arabica solution decreases in wet-countries.

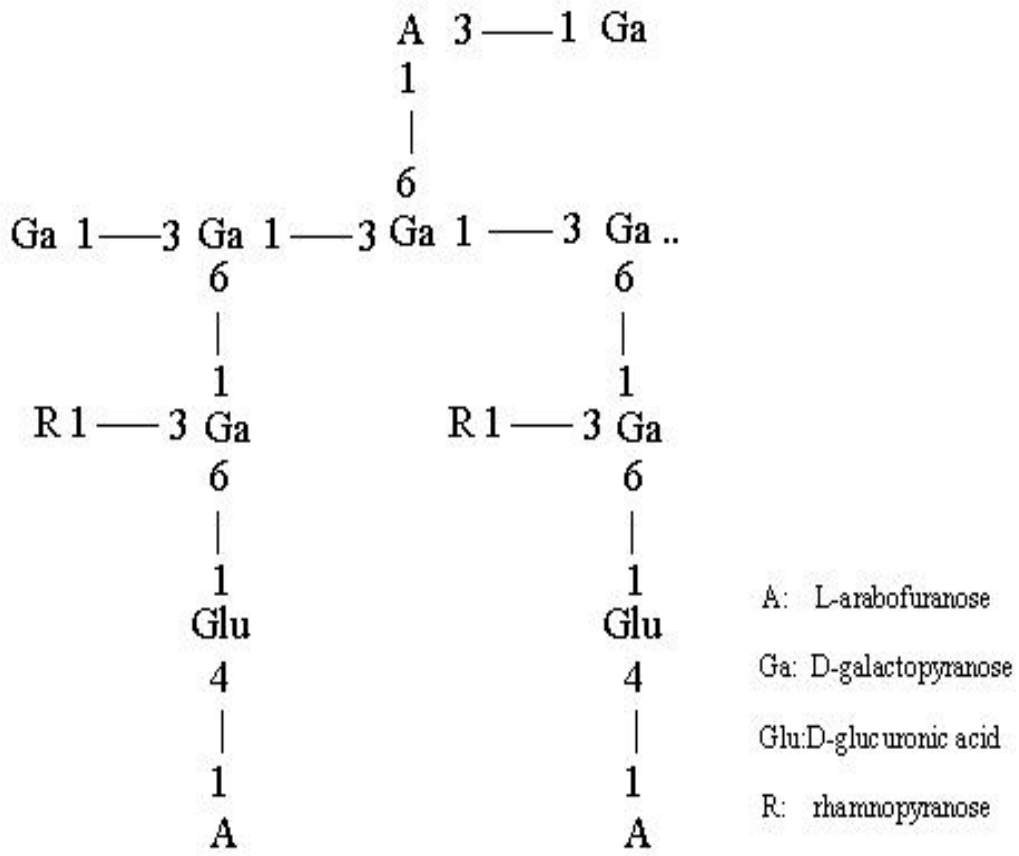

Figure 3.1. The chemical structure of Gum Arabica.

It is an important natural product widely used for medical and other application. The dried solid specimen of the gum is highly stable at room temperature (RT). The chemical composition of this fruit was well analyzed [15, 16]. The fruit shell contains 7 – 13% tannin and the seeds contain 3% oil. The rind contains 5.5% of tannin and a resin as well as a yellow crystalline bitter principle, mangostin ($C_{20}H_{22}O_5$) or mangosim. It was reported [17] that the flesh of the fruit (aril) contains saccharose 10.8%, dextrose 1% and kerrelose 1.2% forming the polysaccharide background.

Gum Karaya is dried exudates of the Stercuila urens tree of Sterculiaceae family. This large and bushy deciduous tree is found in the dry deciduous forest of the Indian Penisula and the sub Himalayan tract in northern India. It is practically acetylated high molecular weight polysaccharide which contains L-rhamnose, D-galacturonic acid and D-glucuronic acid residues.

Gum Ghati is amorphous translucent exudates of the Anogeissus Latifolia tree of the combretaceae family. It can also find in the dry deciduous forest. It is a complex polysaccharide of high molecular weight. It occurs in nature as mixed calcium, Magnesium, Pottasium and Sodium salt. Complete hydrolysis has shown that it is composed of L-Arbinose, D-galactose, D-Mannose, D-xylose and D-glucoronic acid in a molar ratio of 10:6:2:1:2 plus traces less than 1% of 6-Deoxyhexose. Gum Ghati does not dissolve readily in water to give a clear solution rather about 90% of the gum disperses in water with prolong shaking to form a colloidal dispersion. It forms high viscous solutions at concentrations 5% or more and exhibits typical sol-gel behaviour. The viscosity of the solution at particular concentration is intermediate between that of Arabic and Karaya. The normal pH value of the dispersed solution is 4.8 -5.1.

3.1.1 Natural Rubber:

Natural Rubber is an elastic substance obtained from the latex sap of trees, especially those trees which belong to the genera Hevea and Ficus. Technically speaking, natural rubber is an elastomer or an elastic hydrocarbon polymer. Natural rubber is one of the types of rubber that also include vulcanized rubber which is finished into a variety of rubber products. Natural rubber is also known by the names of India rubber, gum elastic, and caoutchouc.

The raw material from which natural rubber is made comes from the sap of rubber trees. The rubber plants are tapped for collecting the rubber latex. For this, an incision is made into the bark of the rubber tree and the latex sap is collected in cups. After collecting the latex sap, the raw natural rubber is refined to convert it into a usable rubber. Initially an acid was added to the latex which used to make the sap set like a jelly. The latex jelly thus obtained was then flattened and rolled into rubber sheets and hung out to dry.

The natural rubber is produced from hundreds of different plant species. However, the most important source is from a tropical tree known as *Hevea brasiliensis*, which is native to the tropical Americas. This tree grows best in areas with an annual rainfall of just under 2000mm and at temperatures of 21-28 degrees. Due to these features and the preferred altitude of the tree around 600 meters, the prime growing area is around 10

degrees on either side of the equator. However it is also cultivated further north in China, Mexico, and Guatemala [18-21].

3.2 Structure and dynamics of bio-molecules from other study:

The structure, association and dynamics of biomolecules is important for its function. A biomolecule must adopt a defined three-dimensional (3D) structure to be active. A specific arrangement of biomolecules (or subunits) may be necessary to form a functional complex. One static 3D structure may not be sufficient for conformational changes and transitions can be necessary for the function of biomolecules. Most experimental methods to study the structure and dynamics of biomolecules have either a high spatial or a high time time resolution. The most important experimental methods apart from FTIR are NMR spectroscopy, X-ray crystallography, Dynamic light scattering, Raman spectroscopy etc [22-24].

3.2.1 NMR spectroscopy:

Nuclear magnetic resonance (NMR) is a spectroscopic technique that detects the energy absorbed by changes in the nuclear spin state. The application of NMR spectroscopy to the study of proteins and nucleic acids has provided unique information on the dynamics and chemical kinetics of these systems. One important feature of NMR is that it provides information, at the atomic level, on the dynamics of proteins and nucleic acids over an exceptionally wide range of time scales, ranging from seconds to pico-seconds. In addition, NMR can also provide atomic level structural information of proteins and nucleic acids in solution i.e. there is no need to crystallize the sample for NMR studies. Thus NMR provides a method of obtaining structural information if the molecule cannot be crystallized or there is some question regarding a structure obtained by X-ray crystallography. Lastly, it is relatively easy to study protein-ligand interactions under physiological conditions by simply adding ligand to the NMR sample of the unliganded protein.

Although NMR is a powerful technique, it does have its limitations. First, almost all experiments require that the observed NMR absorption peaks are assigned to a

particular atom in the protein. Although resonance assignment methods are well characterized, they do require considerable time for data acquisition and analysis. Secondly, the size of the protein or nucleic acid that can be studied by NMR is limited. Assemblies with rotational correlation time of greater than 25 ns (corresponding to a protein with a molecular weight of 60 kDa) may be difficult to study at the detailed atomic level. However, more limited NMR studies can be performed on much larger proteins and biological assemblies. Generally, it is necessary to label larger proteins with ^{13}C, ^{15}N, and perhaps ^{2}H, to successfully apply NMR techniques to such large systems. Labeling of this type is most easily accomplished biosynthetically in either E. coli or in tissue culture (at a much higher expense). Lastly, due to the small energy difference between the ground and excited state of the nuclear spins, NMR is a particularly insensitive technique. Protein concentrations on the order of 0.5 to 1 mM are typical, thus a single 0.4 ml NMR sample of a 20 kDa protein would require between 4 and 8 mg of protein. Fortunately, the techniques are not destructive and the sample can be used for other purposes [25-31].

3.2.2 X-ray crystallography:

X-ray crystallography is the study of crystal structures through X-ray diffraction techniques. When an X-ray beam bombards a crystalline lattice in a given orientation, the beam is scattered in a definite manner characterized by the atomic structure of the lattice. This phenomenon, known as X-ray diffraction, occurs when the wavelength of X-rays and the interatomic distances in the lattice have the same order of magnitude. Modern X-ray crystallography provides the most powerful and accurate method for determining single-crystal structures. Through X-ray crystallography the chemical structure of thousands of organic, inorganic, organometallic, and biological compounds are determined.

X-ray crystallography is an experimental technique that exploits the fact that X-rays are diffracted by crystals. It is not an imaging technique. X-rays have the proper wavelength (in the Angstrom range, ~10^{-8} cm) to be scattered by the electron cloud of an atom of comparable size. Based on the diffraction pattern obtained from X-ray scattering off the periodic assembly of molecules or atoms in the crystal, the electron density can be reconstructed. Additional phase information must be extracted either from the diffraction data or from supplementing diffraction experiments to complete the reconstruction (the phase problem in crystallography). A model is then progressively built into the

experimental electron density, refined against the data and the result is a quite accurate molecular structure.

The knowledge of accurate molecular structures is a prerequisite for rational drug design and for structure based functional studies to aid the development of effective therapeutic agents and drugs. Crystallography can reliably provide the answer to many structure related questions, from global folds to atomic details of bonding. In contrast to NMR (which is a spectroscopic method), no size limitation exists for the molecule or complex to be studied. The price for the high accuracy of crystallographic structures is that a good crystal must be found, and that limited information about the molecule's dynamic behavior in the solution is available from one single diffraction experiment. In the core regions of the molecules, X-ray and NMR structures agree very well, and enzymes maintain their activity even crystal, which often requires the design of non-reactive substrates to study enzyme mechanisms. X-ray crystallography is probably the most important technique to determine the structure of any molecule (from small molecule to large assemblies of biological macromolecules) at atomic resolution [32-34].

3.2.3 Dynamic light scattering:

Dynamic light scattering (DLS), sometimes referred to as Quasi-Elastic Light Scattering(QELS), is a non-invasive, well-established technique for measuring the size and size distribution of molecules and particles typically in the submicron region, and with the latest technology lower than 1nm.

Typical applications of DLS are the characterization of particles, emulsions or molecules, which have been dispersed or dissolved in a liquid. The Brownian motion of particles or molecules in suspension causes laser light to be scattered at different intensities. Analysis of these intensity fluctuations yields the velocity of the Brownian motion and hence the particle size using the Stokes-Einstein relationship [35-37].

DLS offers the following advantages:

i) Accurate, reliable and repeatable particle size analysis in one or two minutes.

ii) Measurement in the native environment of the material.

iii) High concentration, turbid samples can be measured directly.

iv) Measurement is fully automated.

v) Low volume requirement (as little as 2µl).

3.2.3 Raman spectroscopy:

Raman spectroscopy is a form of vibrational spectroscopy, much like infrared (IR) spectroscopy. However, whereas IR bands arise from a change in the dipole moment of a molecule due to an interaction of light with the molecule, Raman bands arise from a change in the polarizability of the molecule due to the same interaction. This means that these observed bands (corresponding to specific energy transitions) arise from specific molecular vibrations. When the energies of these transitions are plotted as a spectrum, they can be used to identify the molecule as they provide a "molecular fingerprint" of the molecule being observed. Certain vibrations that are allowed in Raman are forbidden in IR, whereas other vibrations may be observed by both techniques although at significantly different intensities thus these techniques can be thought of as complementary [38-41].

3.3 Structural distinction between black and grey human hair: A FTIR Investigation:

Hair is an important biomaterial primarily composed of structural protein, notably keratin. Each strand of hair is made up of the medulla, cortex, and cuticle. The cortex contains melanin, which colors the fiber based on the number, distribution and types of melanin granules. Hair color is the pigmentation of hair follicles due to two types of melanin: eumelanin and pheomelanin. Greying of human hair, in most of the cases, is a natural consequence due to some characteristics changes of molecular structure in it.

FTIR spectroscopy [42] is a measurement of variation intensity of the absorption of IR radiation by a sample with wavelength of IR radiation. The polypeptide and protein

repeat units give rise to nine characteristic IR absorption bands, namely, amide A, B, and I-VII. Of these, the amide I and II bands are the two most prominent vibrational bands of the protein backbone. The most sensitive spectral region to the protein secondary structural components is the amide I band (1700-1600 cm^{-1}), which is due almost entirely to the C=O stretch vibrations of the peptide linkages (approximately 80%). The frequencies of the amide I band components are found to be correlated closely to the each secondary structural element of the proteins. The amide II band, in contrast, derives mainly from inplane NH bending (40-60% of the potential energy) and from the CN stretching vibration (18-40%), showing much less protein conformational sensitivity than its amide I counterpart. Other amide vibrational bands are very complex depending on the details of the force field, the nature of side chains and hydrogen bonding, which therefore are of little practical use in the protein conformational studies [43].

3.3.1 Sample preparation for FTIR analysis:

Black and grey hair of same person was collected. These two types of hair were cut into very small pieces by sharp edges separately. KBr pellets were formed by mixing the small pieces of hairs with KBr. The experimental specimens were developed in adequate pressure by hydraulic press at environmental condition.

3.3.2 Experiments:

FTIR analyses on black and grey hair (specimens collected from same person) were carried out to examine their molecular structure and dynamical information. The analysis was carried out using FTIR model, IR affinity1, Shimadzu, Japan, at high resolution (resolution was 0.5 cm^{-1}) using KBr window.

3.3.3 Results and discussions:

Figure 3.3.1 and Figure 3.3.2 show the comparison of the FTIR spectrum of black and grey hair between wave number 2355 to 2370 cm^{-1} and 1075 to 1275 cm^{-1} respectively. Figure 3.3.3 shows the comparison of the FTIR spectrum of black and grey hair between wave number 1540 to 1560 cm^{-1} and Figure 3.3.4 shows the comparison of the FTIR spectrum of previous samples between wave number 520 to 532 cm^{-1}.

These bands assured the information for the nucleic acid conformation. The change in molecular vibration as indicated in Figure 3.3.1 is mainly for the tertiary amine salt (NH+). Figure 3.3.2 shows that the structural change occurs in RNA while the structure of DNA remains unchanged. Some peaks are shifted in the amide I and amide II region due to C=O stretching, C-N stretching and N-H bending as shown in Figure 3.3.3. Some rotational energy level also altered according to Figure 3.3.4. The spectrum of nucleic acids (DNA and RNA) formed by its constituent bases have characteristic bands in the range of 1800-1500 cm^{-1}. The results are correlated with change in protein structure in the human hair and not merely due to melanin content.

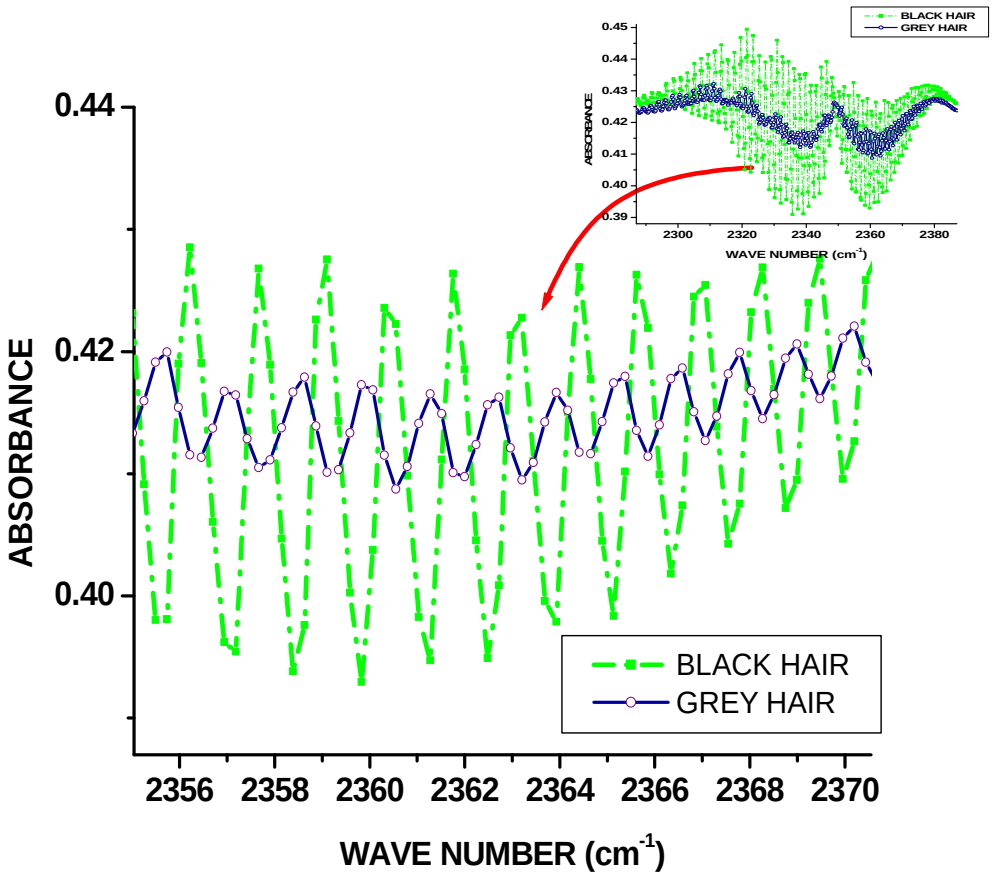

Figure.3.3.1. FTIR absorption spectrum of black and grey human hair in between 2355 to 2370 cm^{-1} at 30ºC.

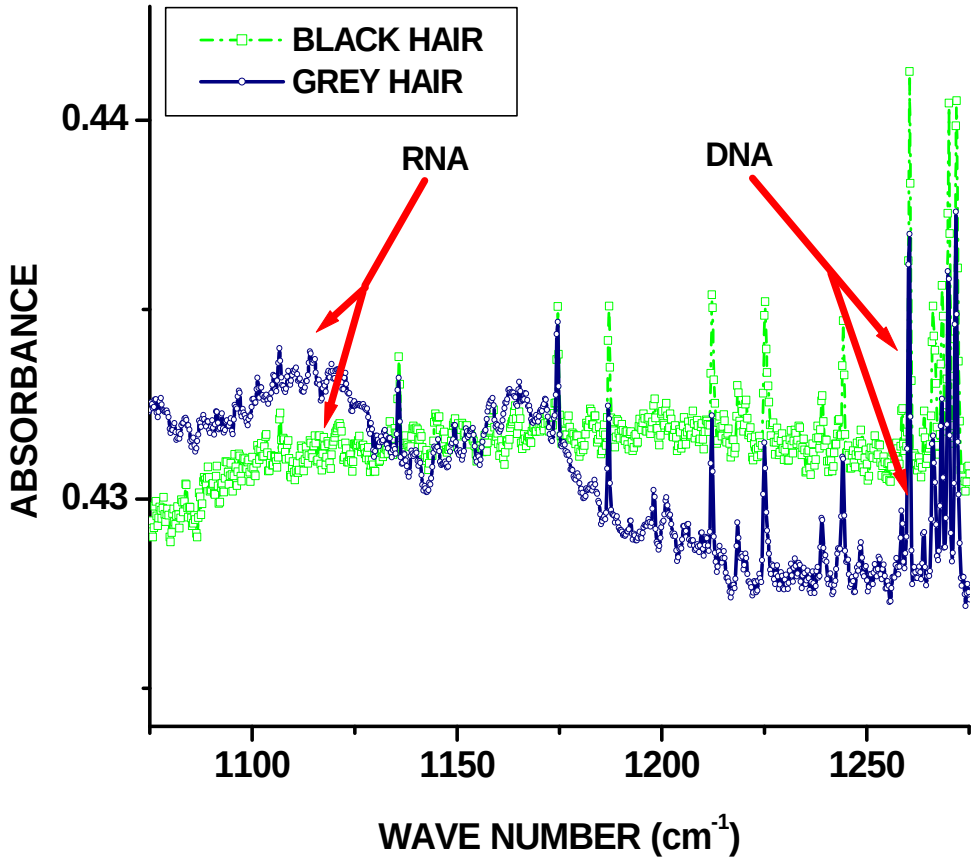

Figure.3.3.2. FTIR absorption spectrum of black and grey human hair in Amide III region at 30ºC.

The bands at 1500-1250 cm^{-1} are transcribed for vibration combination between base and the relevant carbohydrate, at 1250-1000 cm^{-1} are associated with carbohydrate-phosphate vibrations.

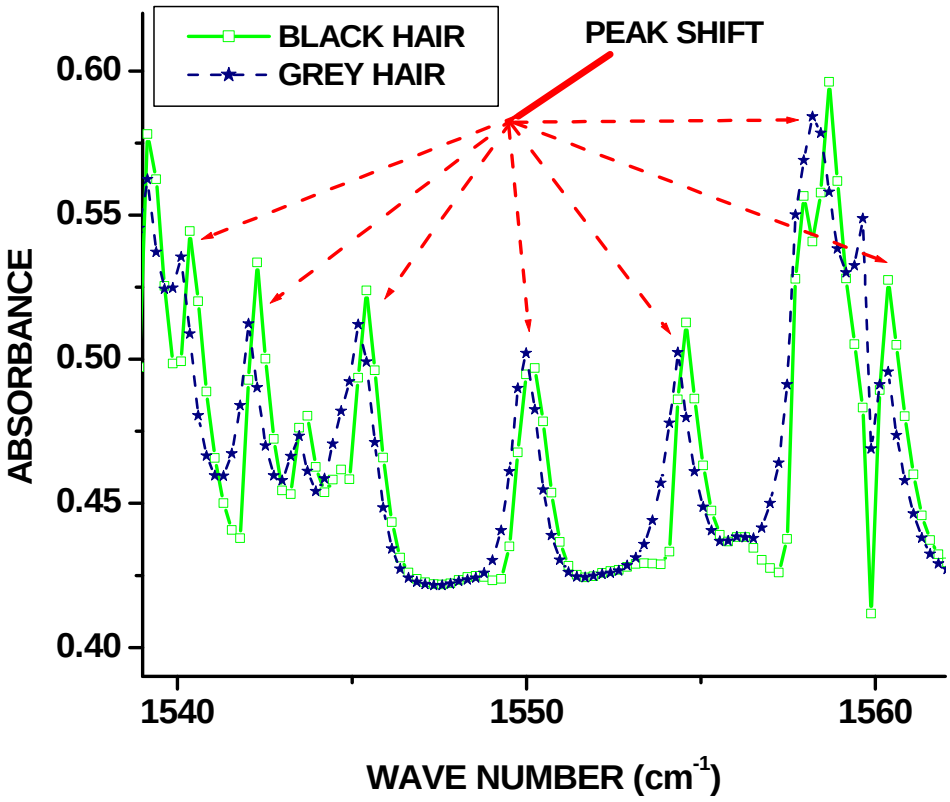

Figure.3.3.3. FTIR absorption spectrum of black and grey human hair in Amide II region at 30ºC.

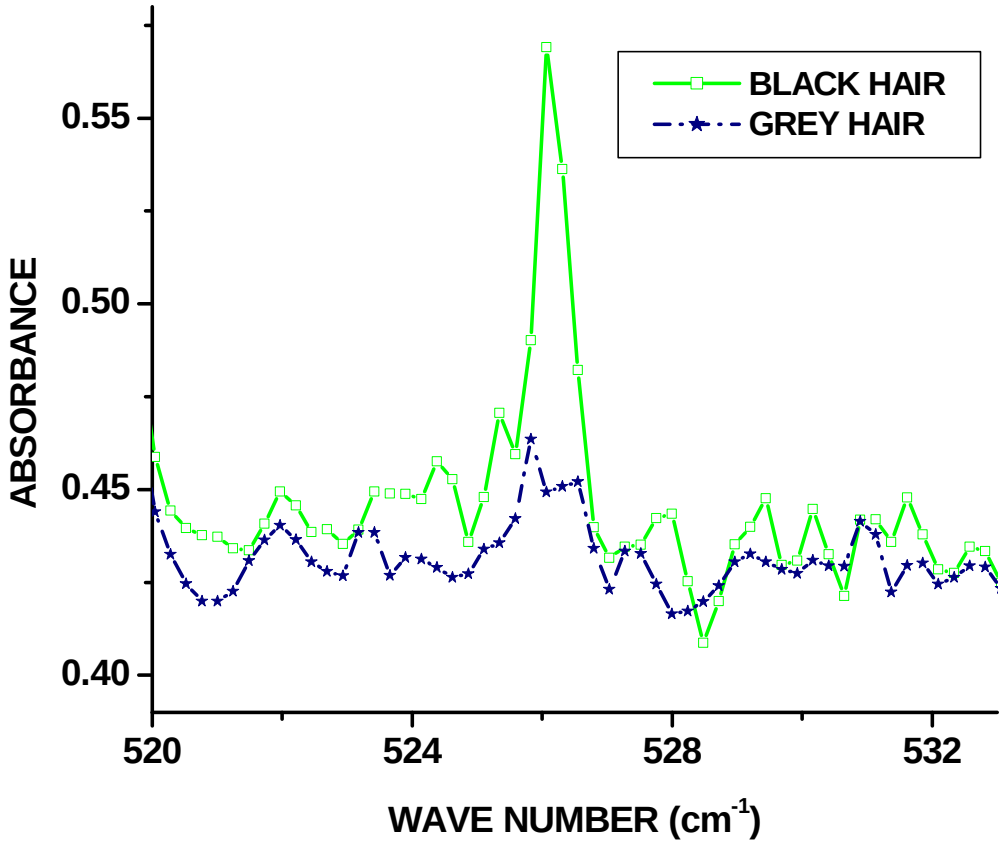

Figure.3.3.4. FTIR absorption spectrum of black and grey human hair in finger print region at 30ºC.

3.3.4 Impressions:

The distinction in molecular vibration due to the tertiary amine salt (NH+) in black and grey hair is clearly visible. This study [44] also confirms the structural change occurred in RNA while the structure of DNA remains unchanged in the two types of human hair. Some peaks are found to be shifted in the amide I and amide II region due to C=O stretching, C-N stretching and N-H bending in types of specimens. The overall results give a good account of change in molecular structure in the black and grey hair.

References:

[1] Boyer, R., Centrifugation in biochemical research. In Modern Experimental Biochemistry, 3rd ed., San Francisco: Benjamin/Cummings, 2000.

[2] Bullock, C., The Archaea—a biochemical perspective. Biochem. Mol. Biol. Educ., 2000.

[3] Cohn, M., Biochemistry in the United States in the first half of the twentieth century. Biochem. Mol. Biol. Educ., 2002.

[4] BIOMOLECULES, 2013-2014 Accelerate Learning Nucleic acid.

[5] Dahm, R , "Discovering DNA: Friedrich Miescher and the early years of nucleic acid research". Human Genetics, (2008).

[6] Elson D, "Metabolism of nucleic acids (macromolecular DNA and RNA)". Annu. Rev. Biochem, (1965).

[7] Hardinger, Steven. Chemistry 14C: Structure of Organic Molecules: Course Thinkbook. Plymouth, 2011.

[8] Hardinger, Steven. Chemistry 14C: Organic Molecular Structures and Interactions: Lecture Supplements. Plymouth, MI: Hayden,McNeil Publishing, 2008.

[9]. R. A. L. Jones, Soft Condensed Matter, Ch. 8, Oxford Univ. Press Inc., New York (2002).

[10]. B. Jirgensons, Natural Organic Macromolecules, Pergamon Press, (1962).

[11]. Meer, Handbook of Water Soluble gums & resins, McGraw Hill, (1980).

[12]. G.O. Aspinall and T.M. Wood, J.Chem.Soc. London (1965).

[13]. G. O. Aspinall et al, Carbohydrate Res.7 (1968).

[14]. D. Barton and W.O. Olis (eds.), Comprehensive organic chemistry, the systhesis and reaction of organic compound in biological compounds, Oxford, Pergamon Press, U.K., Vol. 5 (1969).

[15] H. Asai, F. Tosa and M. A. Ianakat, Iinuma Phytochemistry 39 (4) (1995) 943.

[16] K. M. Nadkami and A. K. Nadkarmi, in Indian Material Media- with Ayurvedic, Unani-Tibbi-Siddha Allopathic, Homeopathic, Naturopathic and Home Remedies, vol. 1, Popular Prokashan. Pvt Ltd., Bombay India, (1999) pp.142-149.

[17]. H. M. Burkill, in The Useful Plants of West Tropical Africa, ed. 2, vol. 2, Families E-1, Royal Botani Gardens. Kew, (1994).

[18] Heinz-Hermann Greve "Rubber, 2. Natural" in Ullmann's Encyclopedia of Industrial Chemistry, Wiley-VCH, Weinheim, 2000.

[19] Hosler, D.; Burkett, S. L.; Tarkanian, M. J., "Prehistoric polymers: Rubber processing in ancient Mesoamerica". Science, (1999).

[20] Koyama, Tanetoshi; Steinbüchel, Alexander, "Biosynthesis of Natural Rubber and Other Natural Polyisoprenoids". Polyisoprenoids. Biopolymers. 2. Wiley-Blackwell, (2011).

[21] Paterson-Jones, J.C.; Gilliland, M.G.; Van Staden, J., "The Biosynthesis of Natural Rubber". Journal of Plant Physiology, (1990).

[22] Alder, B. J.; Wainwright, T. E., "Studies in Molecular Dynamics. I. General Method". J. Chem. Phys, (1959).

[23].Schlick, T., "Pursuing Laplace's Vision on Modern Computers". In J. P. Mesirov, K. Schulten and D. W. Sumners. Mathematical Applications to Biomolecular Structure and Dynamics, IMA Volumes in Mathematics and Its Applications. 82. New York: Springer-Verlag, (1996).

[24] Molecular Simulations: Applications to biomolecular interactions and conformational flexibility, Martin Zacharias International University Bremen School of Engineering and Science.

[25] Paudler, William, Nuclear Magnetic Resonance. Boston: Allyn and Bacon Chemistry Series, (1974).

[26] "Background and Theory Page of Nuclear Magnetic Resonance Facility". Mark Wainwright Analytical Centre - University of Southern Wales Sydney. 9 December 2011.

[27] Shah, N; Sattar, A; Benanti, M; Hollander, S; Cheuck, L , "Magnetic resonance spectroscopy as an imaging tool for cancer: a review of the literature". The Journal of the American Osteopathic Association, (2006).

[28] Johnson Jr., C. S. , "Diffusion ordered nuclear magnetic resonance spectroscopy: principles and applications". Progress in Nuclear Magnetic Resonance Spectroscopy, (1999).

[29] James Keeler. "Chapter 2: NMR and energy levels" (reprinted at University of Cambridge). Understanding NMR Spectroscopy. University of California, Irvine. Retrieved 2007-05-11.

[30] Pople, J.A.; Bernstein, H. J.; Schneider, W. G., "The Analysis of Nuclear Magnetic Resonanace Spectra". Can J. Chem, (1957).

[31] Wemmer, David , "Chapter 5: Structure and Dynamics by NMR". In Bloomfield, Victor A.; Crothers, Donald M.; Tinoco, Ignacio. Nucleic acids: Structures, Properties, and Functions. Sausalito, California: University Science Books, (2000).

[32] Shafranovskii I I & Belov N V , Paul Ewald, ed. "E. S. Fedorov", 50 Years of X-Ray Diffraction. Springer, (1962).

[33] Andre Guinier , X-ray Crystallographic Technology. London: Hilger and Watts LTD., (1952).

[34] Pauling L , "The Principles Determining the Structure of Complex Ionic Crystals". J. Am. Chem. Soc., (1929).

[35] Berne, B.J.; Pecora, R. Dynamic Light Scattering. Courier Dover Publications (2000).

[36] Pecora., R., "Doppler Shifts in Light Scattering from Pure Liquids and Polymer Solutions". The Journal of Chemical Physics, (1964).

[37] Frisken, Barbara J., "Revisiting the Method of Cumulants for the Analysis of Dynamic Light-Scattering Data", Applied Optics, (2001).

[38] Schrader, B. Infrared and Raman Spectroscopy; Schrader, B. ed., VCH Publishers Inc.: New York, 1995.

[39] Myers, A.B., Mathies, R.A. Biological Applications of Raman Spectroscopy: Volume 2: Resonance Raman Spectra of Polyenes and Aromatics, Spiro, T.G. ed., John Wiley and Sons: New York, 1987.

[40] Kerker, M., Wang, D.-S., Chew, H., Siiman, O., Bumm, L.A. Surface Enhanced Raman Scattering, Chang, R.K., Furtak, Plenum Press: New York, 1982.

[41] Morris, M.D. Applied Laser Spectroscopy; Andrews, D.L. ed., VCH Publishers Inc.: New York, 1992.

[42] H. Fabin and W. Mäntele, in Handbook of Vibrational Spectroscopy, edited by J. M. Chalmers and P.R.Griffiths, John Wiley & Sons, 1999, pp. 3399-3425.

[43] Jilie KONG and Shaoning YU, Acta Biochimica et Biophysica Sinica, 39(8): 549–559(2007).

[44] Arup Dutta and A. Sarkar, “Structural distinction between black and grey human hair: A FTIR Investigation” Proceeding of International Conference on Recent Trends in Applied Physics and Material Science 2013, AIP Conf. Proc. 1536, 1250-1251 (2013).

Chapter 4

Solvation effect on molecular spectra of some specific bio-molecules

4.1 Brief introduction of solvation effect:

In molecular biology it is attempted to obtain an understanding of biological function in terms of structure, interactions, and processes at the molecular or even atomic level. Experimental techniques, such as X-ray crystallography and NMR spectroscopy, are routinely used to provide an atomic picture of the structure and mobility of biomolecules, for example proteins and DNA fragments. More flexible molecules, such as lipids and sugars, are less accessible to structure determination by these methods. Information with respect to dynamics is even more difficult to obtain; only spectroscopic measuring techniques yield such information, but only for special groups of atoms, not for all atoms in a biomolecule. Generally, energetic information cannot be measured at the atomic level. Because of the limitations of experimental measuring techniques, the characterization of a biomolecular system at the atomic level in terms of structure, mobility, dynamics, and energetic is incomplete. These four types of information are listed in the order of decreasing knowledge about them. This incomplete molecular picture makes it difficult to establish the link between molecular structure, mobility, dynamics, and interactions on the one hand and biological function on the other. An alternative way to study biomolecular systems at the atomic level is simulation on a computer. It involves three basic choices.

1. A biomolecular system generally has too many degrees of freedom (electronic, atomic) to be simulated. However, the ones that are essential to a proper representation of the quantity or phenomenon one is interested in must be explicitly present in the molecular model.

2. An interaction function for these degrees of freedom must be defined, which contains the average effect of the degrees of freedom that have been omitted in the molecular model.

3. The motion of the molecular system is governed by equations of motion. Depending on the type of degrees of freedom in the model (quantum-mechanical,

classical, or stochastic), this can be Schrodinger's, Newton's or Lagrange's, or Langevin's equation of motion. The length of the simulation must be sufficiently long to allow for an adequate sampling of essential degrees of freedom.

Whether a biomolecular system can be usefully simulated depends on three factors:

1. The time scale of the quantity or process of interest,

2. The required accuracy of the simulated property or process,

3. The available computing power.

Solvent molecules play different roles with respect to protein properties one is interested in, for example:

1. The structure and stability of a folded protein depends on the type of solvent. In aqueous solution a protein tends to minimize it s a polar surface area (hydrophobic effect).

2. Individual water molecules play a structural role in folded proteins, e.g. the four internally bound water molecules in bovine pancreatic trypsin inhibitor (BPTI).

3. Polar solvents exert a dielectric screening effect on interactions between protein charges.

4. The viscosity of the solvent will influence the dynamics of the protein atoms and may thereby influence the kinetics of processes [1].

Solvation Effects on Molecules and Biomolecules provides a comprehensive overview of state-of-the-art molecular modeling methodologies which are most relevant to handling solvation properties of molecules and biomolecules. By outlining the essential theoretical framework and technical details, together with practical applications, Solvation Effects on molecules and biomolecules serves as an essential guide in the promotion of interactions between theoretical and experimental groups. Solvation effects on molecules and biomolecules thus forms a powerful resource for students, researchers and is also an excellent companion for research professionals engaged in computational chemistry, material science, nanotechnology, physics, drug design, and molecular biochemistry[2].

4.2 Effect of solvation on molecular spectra:

The electronic absorption and emission spectra of organic molecules are usually modified in solvation processes. The intensity, frequency or the shape of the absorption and/or fluorescence spectra support modifications when the spectrally active molecules pass from the gaseous phase to the liquid phase. The modifications induced by a solvent in the electronic spectra of molecules can offer information on the local electric field acting on the spectrally active molecule [3-13]. Attempts to evidence some empirical relations between the spectral characteristics and the microscopic or macroscopic parameters of the solutions were made in the first stage of research on the intermolecular interactions. Then, the interactions in the condensed phase were theoretically described in some kinetic and cell models [5, 10, 14, 15]. Very large category of interactions act in solutions, so, the verification of the existent theories is made only in some restrictive situations, neglecting a series of contributions to the spectral shifts. For example, in the theories of simple liquids, the specific interactions are neglected and consequently, when act in solutions they are described by empirical terms [16, 17]. These terms must be proportional with parameters characterizing the atomic groups' ability in achieving hydrogen bonds, such as the electro negativity, electronic charge near the proton from – NH or – OH groups, the degree of delocalization of the molecular electronic charge, or spectral signals such as wave numbers in FTIR spectra, or chemical shifts measured in NMR spectra.

Computational methods [18] are used to decide which the terms are giving a dominant contribution to the total spectral shift. So, in relations of the type [15, 19]:

$$\Delta\tilde{\upsilon} = C_1.f(\varepsilon) + C_2.f(n) + C_3.\alpha + C_4.\beta \qquad (1)$$

The universal interactions are described by the first two terms and the specific interactions of the donor or acceptor types are described by the last two terms. The last two terms in (1) describe specific interactions of the type donor or acceptor of protons or electrons between the solvent and solute molecules. The contribution of each type of interactions is given by the value of the regression coefficients C_j, j = 1, 2, 3, 4. The interactions described by terms with small regression coefficients are finally neglected.

Study of the effect of solvents on the electronic absorption and fluorescence spectra of a variety of molecules (e.g. anthraquinone derivatives, azo compounds, azo disperse red dyes [20] forms an important subject for research in least years because can play a significant role in the photophysics of the excited states [21]. Some electro-optical parameters of the solute molecules can be estimated by spectral means, especially when the solute molecules are active both in absorption and in fluorescence electronic spectra. In solutions, the solvent environment determines important changes in the electro-optical properties of the spectrally active molecule compared to those in its gaseous phase. Several reports are now available on the correlation of UV absorption frequencies with the solvent parameters [22–26].

Theories regarding the solvent action on the electronic spectra developed in the last time [27, 28] permit to estimate the electro-optical parameters, such as dipole electric moments or polarizabilities for the spectrally active molecules using the spectral shifts as indicators of the strength of the internal interactions and some macroscopic parameters of the solvents such as electric permittivity and refractive indices. When the microscopic parameters in the ground electronic state are known by experiments or computations, the corresponding values in the excited electronic spectra can be evaluated.

The solvatochromism is one of the few methods that permit to estimate the local field of forces in the interior of liquids, indirectly, by the energy of the intermolecular interactions.

The existent theories on the intermolecular interactions in liquids express the supply of some types of interactions by different functions of solvent parameters, neglecting the presence of the possible specific interactions. Some theories take into consideration only the long range interactions, neglecting the supply of the specific interactions to the total shift measured into a given solvent. Usually, the supply of the specific interactions is expressed by semi-empirical terms dependent on the local distribution of the electronic charges in the interacting molecules [16, 17].

In Bakhshiev theory [10], the supply of the long range interactions to the total spectral shift $\Delta\tilde{\upsilon} = \tilde{\upsilon} - \tilde{\upsilon}_0$ measured in electronic spectra of the solute (spectrally active molecule) is expressed by relations of the type:

$$\tilde{\upsilon}_{max} = \tilde{\upsilon}_{max,0} + C_1 f(\varepsilon) + C_2 f(n) \quad (2)$$

In relation (2) $\tilde{\upsilon}_{max}$ (cm^{-1}) is the wavenumber in the maximum of the electronic absorption band, expressed in cm^{-1} in a given solvent, $\tilde{\upsilon}_{max,0}$ has the significance of the wavenumber in the maximum of the same electronic absorption band recorded for the vaporous state of the solute, $f(\varepsilon) = \frac{\varepsilon-1}{\varepsilon+2}$ and $f(n) = \frac{n^2-1}{n^2+2}$ (where $\varepsilon = n^2$) are solvent functions depending of electric permittivity and refractive index, respectively. The second and the third terms in relation (2) express the contributions of the orientation and dispersive-induction polarization interactions, respectively. One can admit that $C_1 f(\varepsilon)$ expresses the spectral shift corresponding to the orientation interactions, and $C_2 f(n)$ is due to the dispersive-inductive-orientation forces. There are a great number of studies in which the different types of interactions are evidenced for diverse molecular structures [29-36].

If the contribution $\Delta\tilde{\upsilon}_{sp}$ of specific interactions to the total spectral shift is added to the function (2), one obtains relation (3):

$$\tilde{\upsilon}_{max} = \tilde{\upsilon}_{max,0} + C_1 f(\varepsilon) + C_2 f(n) + \Delta\tilde{\upsilon}_{sp} \quad (3)$$

And can obtain relation (4) in which the energies of interactions are expressed in fractions [30].

$$1 = \frac{C_1 f(\varepsilon)}{\Delta\tilde{\upsilon}} + \frac{C_2 f(n)}{\Delta\tilde{\upsilon}} + \frac{\Delta\tilde{\upsilon}_{sp}}{\Delta\tilde{\upsilon}} \quad (4)$$

Only the universal interactions, described by the first two terms have theoretical correspondents in Bakhshiev theory, the contribution of the specific interactions is described in (4) by an empirically introduced term [36-38]. This term can contain parameters proportional to the local charge density in the local molecular zones in which specific interactions arise. Specific interactions are usually localized in a zone of the molecule in which atoms of different electronegativity are bonded covalently and consequently, a pronounced local separation of charges becomes possible [39, 40], or estimation of some mechanical properties of solutions when additional techniques are used [41].

Different types of intermolecular interactions in solutions were evidenced by solvatochromism studies. The separation of the universal and specific interactions permits to estimate the strength of each type of interactions acting in a given solution.

When relations of the type (3), or more complicated dependences, are verified for spectral data, an important role plays the aberrant data elimination, due to the fact that these data could significantly modify the values of the regression coefficients C_1 or C_2 (for a given number of known data regarding the wavenumber in the maximum of the electronic bands and the solvent parameters) [42]. In the case of azobenzene derivatives the elimination of the aberrant data permitted us to evaluate the coefficients depending on the polarizabilities in the ground and excited state or on the dipole moments in the electronic states participating to the electron transition responsible for the absorption band appearance. A good estimation of the coefficients C_1 and C_2 offer the possibility to evaluate the electro-optical molecular parameters in the excited electronic states, when the corresponding parameters in the ground state are computed by quantum-chemical procedures. The higher the numbers of the experimental data, the more precisely the regression coefficients are determined. The importance of a precise determination of the regression coefficients is due to their utilization in estimation of some electro-optical parameters such as electric permittivity or dipole moment in the molecular excited states [29, 31, 43-45].

The kinetics of chemical reactions can be characterized on the basis of spectral data in different solvents [46, 47]. This is a systematic and comprehensive study of solvent effects on the electronic (absorption and fluorescence) spectra. It is directed to describe some applications giving information about the liquid structure, including the internal forces in liquid state and also allowing estimation the molecular electro-optical parameters in the electronic excited states of the spectrally active molecules.

4.2.1 Effects of solvent on UV-VIS absorption spectra of materials:

When absorption spectra of required material are recorded in solvents of different polarity, it is found that the positions, intensities and shapes of the absorption bands are usually modified. Usually, the spectral shifts are attributed to specific solute-solute and solute-solvent interaction in form of hydrogen bonding or bulk solvent properties. Apart

from these interactions, there are several other factors that may influence the spectra such as acid-base chemistry or charge transfer interactions.

The magnitude of the spectral shifts in various solvents (with different polarities) mainly depends on the strength of the intermolecular hydrogen bond(s) between the substituent groups of the spectrally active molecule and the – OH or – NH groups of the solvent molecules and whether the intramolecular hydrogen bonds are present or not. For the molecular systems without intramolecular hydrogen bond, the spectral shifts are sensitive to the solvent polarity. Thus, in many molecules the bands (π-π^*) are shifted bathochromically when the solvent polarity increases. These changes were attributed to hydrogen-bonding interaction between the solute molecule and the solvent molecule. On the other hand, the spectral shifts in the molecular systems with intramolecular hydrogen bonds are very small. In the absence of the intermolecular hydrogen bonds in all the intramolecular hydrogen bonded systems, the solvent shifts are well interpreted by the solvent polarity function.

An exception is polyene dye for which the solvent effect shows inverted solvatochromism [48, 49] that is, the change from positive to negative solvatochromism with increasing solvent polarity. This phenomenon is ascribed to a solvent-induced change in the ground-state structure from a less dipolar polyene-like structure to a strongly dipolar one.

Solvatochromatic effect has been used to determine the magnitude of the solute-solvent interactions such as the polarizability /dipolarity parameter, π^*, of the solvent, as well as giving information about hydrogen bond donor (HBD), α and/or acceptor (HBA), β ability of the solvent. It is well known that the bands due to local transitions are solvent insensitive, whereas the charge transfer bands are sensitive to environmental changes [50].

Solvent effects may be attributed to hydrogen bonding which assists electron migration in the molecules [51], to the stabilization of preferred resonance structures due to their electric permittivity or electron donor character [52, 53], to dipole-dipole interaction and the change in the dipole moment during the solute transition on the solvent effect.

The monitoring the absorption and fluorescence properties in different solvents of the PPO-block-PpPE - poly(propylene-oxide)-poly(p-phenylene-ethynylene) block copolymers [54] can permits to establish the aggregation tendency of these compounds.

A. Theory of Solvent Effects That Uses a Stokes Shift:

The solvatochromic shift shows the relationship of the absorption/emission spectra and the polarity of the solvent and gives information on the electronic excited states of the molecule. The Stokes shifts ($\tilde{\upsilon}_a - \tilde{\upsilon}_f$) are based on a linear correlation between the wave numbers of the absorption and fluorescence maxima and a solvent polarity function which involves both dielectric permittivity, ε and refractive index, n of the medium [55-57].

4.2.2 Specific solvent effects on UV-VIS absorption spectra:

To understand the behavior of a solvent involved in a process, it is important to understand the solute-solvent interactions from liquids. The effects of the solvent dipolarity/polarizability (non-specific solvent interactions) and hydrogen bonding (specific solvent interactions) on the electronic absorption spectra are interpreted using the linear solvation energy relationship. In recent decades, the Kamlet–Taft approaches [58] have been applied to separate the influence of non-specific interactions, from specific interactions. Specific solvent–solute interactions (hydrogen bonding) are expressed by the solvent acidity, α or SA, and the solvent basicity, β or SB which can be evaluated by multilinear regression analysis. The non-specific interactions are expressed by Catalan's SP parameter (solvent polarizability) as well as by the π^* or SPP parameter (both of which represent a combination of the solvent dipolarity and polarizability).

4.2.3 Solvent effect on fluorescence spectra:

Fluorescence band maxima are largely red shifted when the solvent polarity increases, compared to absorption band under the same condition. This fact indicates an increase in dipole moment of excited state compared to ground state. Generally, the polarity of a solvent will influence the emission spectra of fluorophores by changes in quantum yields and spectral shifts [59]. Normally, a fluorescent probe is weakly fluorescent in hydrophilic environment (or in more polar solvents) but strongly fluorescent

in hydrophobic environment [59-61]. Very interesting is the opposite behavior of the some fluorophores (with strongly fluorescence in protic solvents whereas they show weak fluorescence in aprotic solvents) such as acridine [62], pyrene-3-carboxaldehide and 7-methoxy-4- methylcoumarins [63, 64].

4.3 Change in molecular spectra of Gum Agar under the solvent H_2O and D_2O:

Agar is an important biomaterial consists of a mixture of agarose and agaropectin. Agarose is a linear polymer, of molecular weight about 120,000. An agarose is a polysaccharide polymer material, generally extracted from seaweed. Agarose is a linear polymer made up of the repeating unit of agarobiose, which is a disaccharide made up of D-galactose and 3, 6-anhydro-L-galactopyranose. Agarose is frequently used in molecular biology for the separation of large molecules, especially DNA, by electrophoresis. On the other hand agaropectin is a heterogeneous mixture of smaller molecules that occur in lesser amounts. Their structures are similar but slightly branched and sulfated, and they may have methyl and pyruvic acid ketal substituents. Gum Agar has a poor gel formation ability compared to that with agarose alone. Agar is insoluble in cold water but dissolves to give random coils in boiling water.

FTIR spectroscopy is a measurement of variation intensity of the absorption of IR radiation by a specimen with wavelength of IR radiation [65]. This work [66] makes an attempt to detect structural change in Gum Agar samples at different polymerized state with H_2O and D_2O by FTIR spectroscopy.

There are some proteins of alike structure are present in agar. The amide I and II bands are the two most prominent vibrational bands of the protein backbone. The frequencies of the amide I band components are found to be correlated closely to the each secondary structural element of the proteins. The amide II band, in contrast, derives mainly from in plane N-H bending (40-60% of the potential energy) and from the CN stretching vibration (18-40%), showing much less protein conformational sensitivity than

its amide I counterpart. Other amide vibrational bands are very complex depending on the details of the force field, the nature of side chains and hydrogen bonding, which therefore are of little practical use in the protein conformational studies [67]. N-H bending, N-H stretching, CN stretching vibrations are found in Agar spectrum. The overall results give a good account of change in molecular structure in the Gum Agar specimens.

4.3.1 Sample preparation:

The Gum Agar powder specimen (S1) was collected from Merk (India) and was subjected to a sol gel process along with (i) sterile water and (ii) D_2O. In both the polysaccharide host chain can form more complex higher polymers over that of its normal powdered form. D_2O exchange can occur leading to replacement of -OH group by -OD. The sol specimens are extracted at initial state, 30, 60 and 120 minutes after that. The experimental specimens S2- S5 (sol specimens of D_2O) were developed with subsequent adequate drying of the sols at environmental condition.

4.3.2 Experiments:

The developed Gum Agar specimens are supposed to exhibit change in molecular structure over that in S1 due prolongation of sol gel process. FTIR analysis on pure Gum Agar and specimens S2 to S5 were carried out to examine its molecular structure and dynamical information. The analysis was carried out using FTIR model, IR affinity1, Shimadzu, Japan, at high resolution (resolution was 0.5 cm^{-1}) using KBr window. The sol specimens of Gum Agar with H_2O and D_2O collected at 0, 30, 60 and 120 minutes after sol initiation and were also analyzed by ATR using ZnSe window at 0.5 cm^{-1} resolution.

4.4 Comparison of the results:

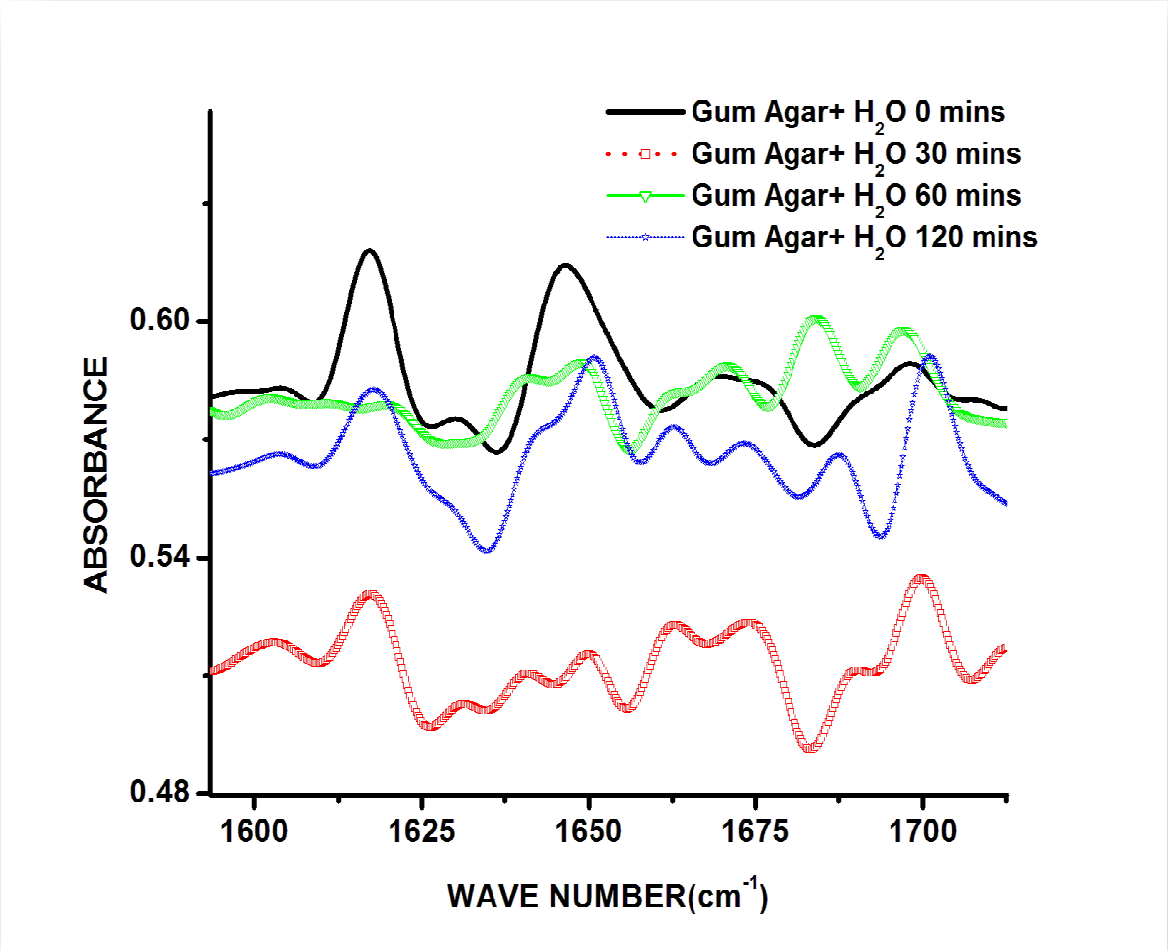

Figure.4.4.1. ATR absorption spectrum of different Gum Agar specimens in between 1595 to 1710 cm^{-1} at 25ºC.

Fig. 4.4.1 shows the comparison of the ATR spectrum of different Gum Agar sol specimens between wave number 1595 to 1710 cm^{-1}. Peaks around the wave number 1615, 1650, 1680 and 1700 cm^{-1} of different specimens are shifted. These peak shifts give a clear picture for change in molecular structure in the bio-molecule due to polymerization.

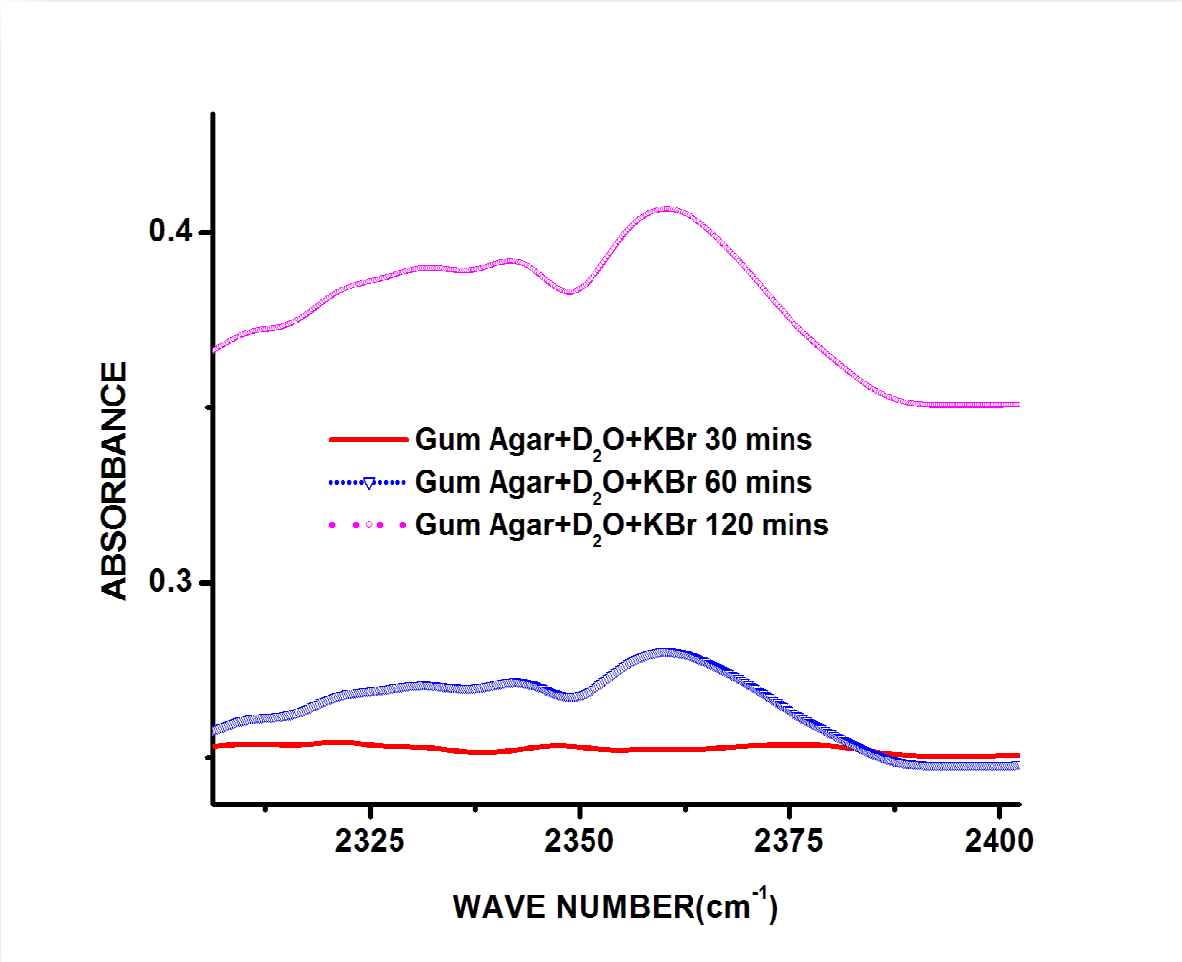

Figure.4.4.2. FTIR absorption spectrum of different Gum Agar specimens in between 2315 to 2400 cm^{-1}at 25ºC.

In Fig. 4.4.2 FTIR spectrum (between wave number 2315 to 2400 cm^{-1}) of Gum Agar specimens (sol specimens of D_2O) developed by adequate drying of the sols at environmental condition are compared. From this D_2O peaks are clearly observed around the wave number 2365 cm^{-1} for the specimens collected 60 and 120 minutes after initial state but is absent for the specimen collected 30 minutes after initial state.

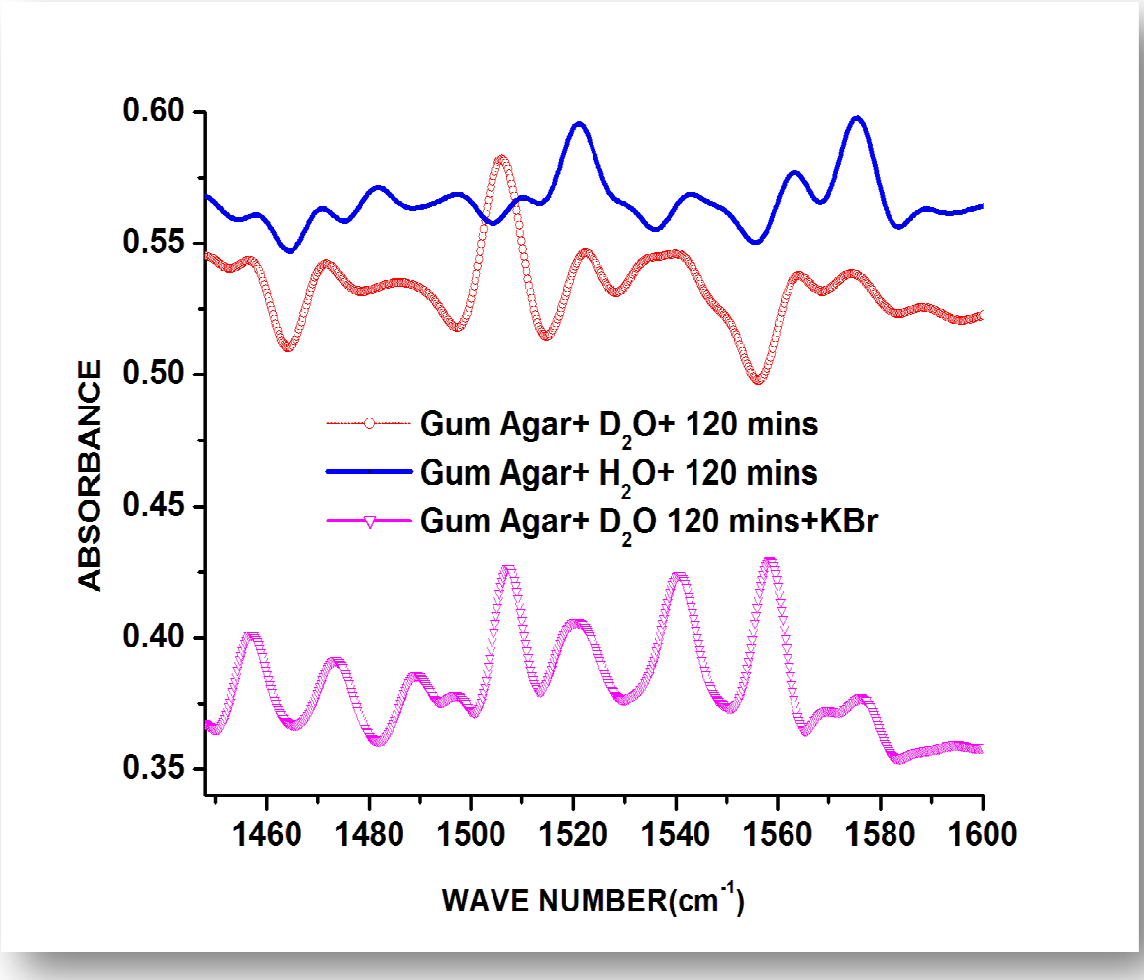

Figure.4.4.3. FTIR and ATR absorption spectrum of different Gum Agar specimens in N-H bend region (between 1450 to 1600 cm^{-1}) at 25ºC.

Both the FTIR and ATR spectrum are compared in Fig. 4.4.3 and Fig.4.4.4 as the solid samples of Gum Agar were used besides the liquid specimens. Comparison of N-H bending of different specimens is shown in Fig. 4.4.3 between wave number 1450 to 1600 cm^{-1}. Peaks arising from N-H bending around the wave number 1525 and 1580 cm^{-1} disappear due D_2O exchange.

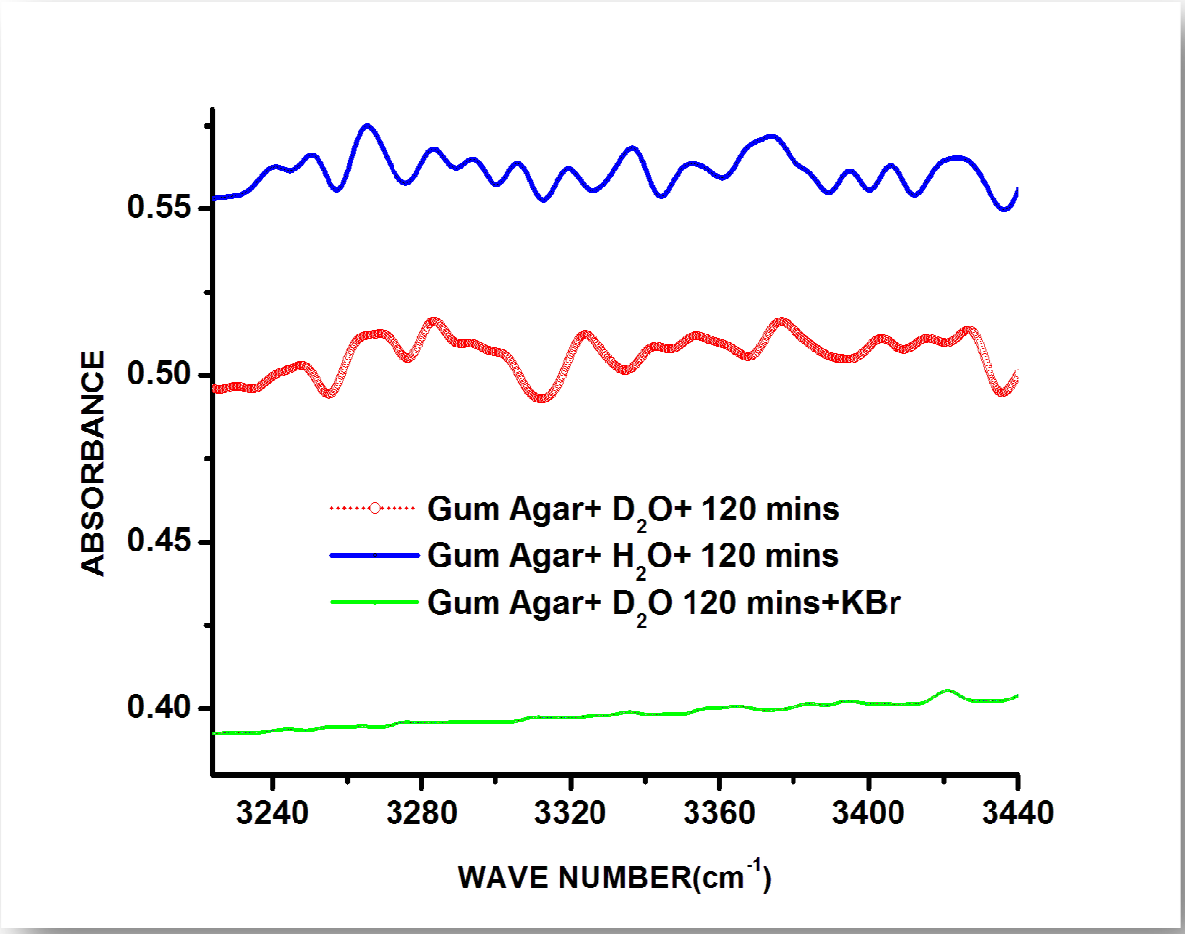

Figure.4.4.4. FTIR and ATR absorption spectrum of different Gum Agar specimens in N-H stretch region (between 3225 to 3440 cm^{-1}) at 25ºC.

Fig. 4.4.4 shows the comparison of the spectrum of different Gum Agar specimens between wave number 3225 to 3440 cm^{-1} in N-H stretching region. The N-H peaks are often very broad and weak without any distinct coupling to be caused by chemical exchange of the NH proton or by a property of nitrogen atoms called quadrupolar broadening. The hydrogens of amino group will exchange with D_2O, causing the peaks to disappear (around the wave number 3270, 3360, 3400 cm^{-1}) [68].

$$-N-H + D_2O = -N-D + DOH \quad (1)$$

Fig. 4.4.3 and Fig.4.4 4 indicate that some N-H peaks are absent from the spectra due to D_2O exchange as shown in Eq. (1).

4.5 Effect of polymerization on bio-molecules:

In another work [69] gum Arabica powder specimen (S1) was collected from Merck (India) and was subjected to a sol–gel process along with pure water so that the polysaccharide host chain can form more complex higher polymers over that in normal powder form. The sol specimens are extracted at initial state, 30, 60 and 120 minutes after that. The experimental specimens (S2, S3, S4 and S5 respectively) were developed by adequate drying of the sols at environmental condition.

FTIR analysis on pure gum Arabica was carried out to examine its molecular structure and dynamical information. The analysis was carried out using FTIR Model, IR Affinity 1, Shimadzu, Japan, at high resolution using KBr window.

4.5.1 Results and discussions:

Figure 4.5.1 shows the FTIR spectrum gum Arabica specimen between wave number 350 to 4000 cm^{-1}. Broad peaks are obtained in the IR spectrum of gum Arabica at 3365.2 cm^{-1} (O-H stretching of carbohydrates), 2939.1 cm^{-1} (CH_2 asymmetric stretching), 1379.3cm^{-1} (CH, CH_2 and OH in-plane bending in carbohydrates), 1042.9 cm^{-1} (C-O stretching region as complex bands, resulting from C-O and C-O-C stretching vibrations), 704.8 cm^{-1}, 641.7 cm^{-1} and 603 cm^{-1} (pyranose rings)It shows the distinctive absorption in finger print region at 603 , 641.7 and 704.8 cm^{-1}. The three frequencies represent the characteristics of bond stretching vibration of the bio-molecule.

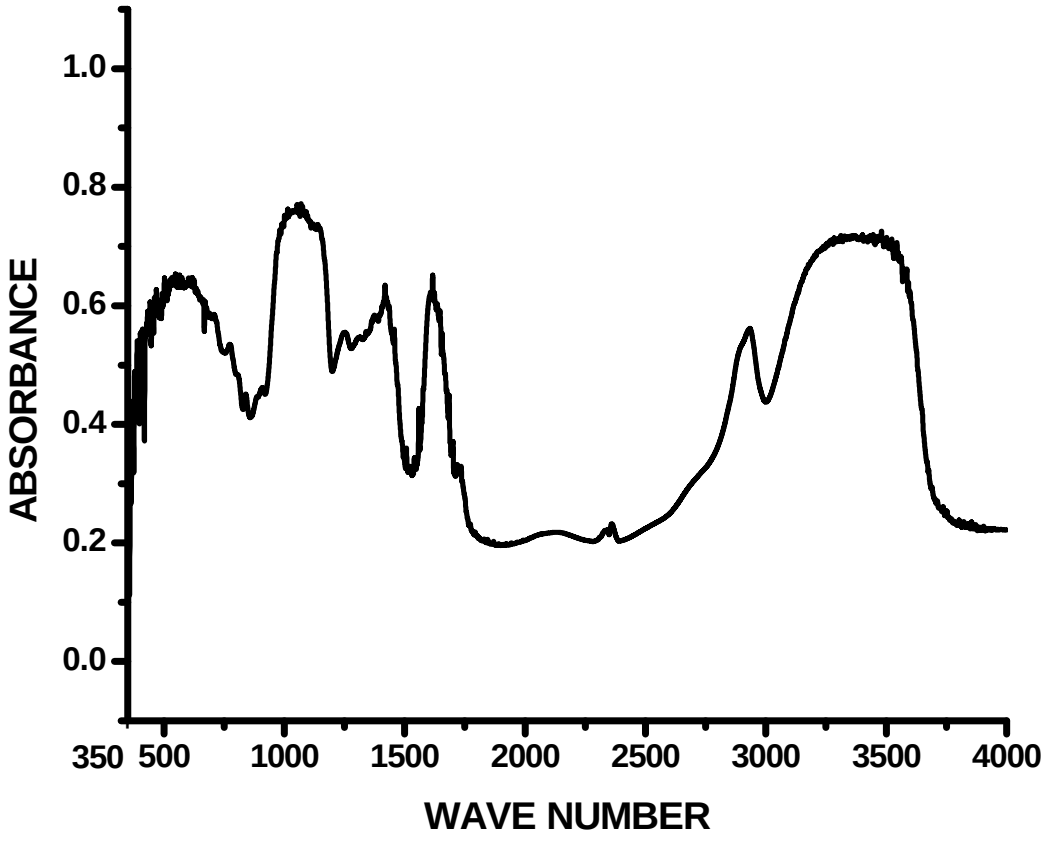

Figure.4.5.1. FTIR spectrum of gum Arabica specimen (between wave number 350 to 4000 cm^{-1}).

Figure 4.5.2 and Figure.4.5.3 show the comparison of the FTIR spectrum of different gum Arabica specimens between wave number 600 to 607 cm^{-1} and 638 to 645 cm^{-1} respectively. Figure 4.5.2 shows that the characteristics vibration at 603cm^{-1} decrease while passing from S1 to S5 whereas Figure.4.5.3 represents the same corresponding to absorption peak at 641.7 cm^{-1}.

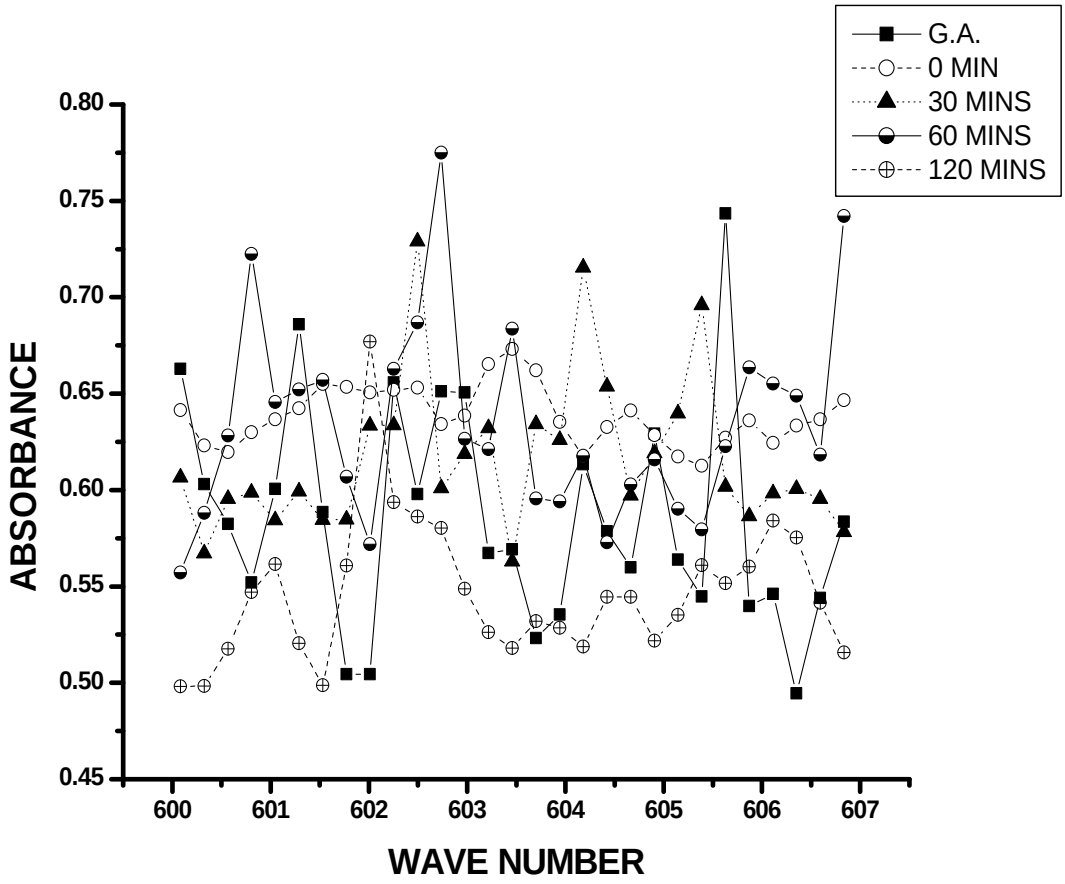

Figure.4.5.2. FTIR spectrum of gum Arabica specimen(between wave number 600 to 607 cm^{-1}).

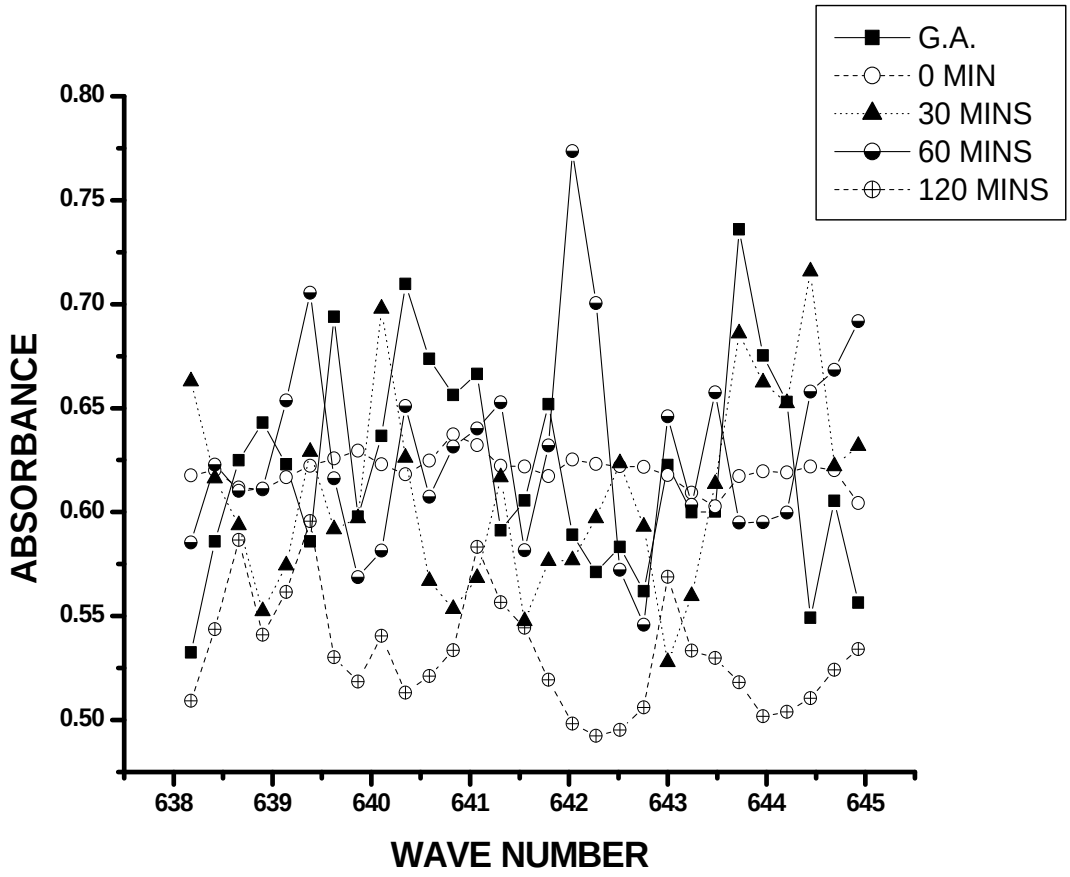

Figure.4.5.3. FTIR spectrum of gum Arabica specimen (between wave number 638 to 645 cm^{-1}).

TABLE 4.5.1. Comparison of the FTIR spectrum peak for S1 – S5 around wavenumber 704.8 cm^{-1}

Wave Number	G.A. (Absorbance)	0 Min (Absorbance)	30 Mins (Absorbance)	60 Mins (Absorbance)	120 Mins (Absorbance)
704.47749	0.59586	0.5822	0.66863	0.59402	0.50622
704.71858	0.6251	0.58692	0.65667	0.64203	0.51766
704.95967	0.61138	0.58325	0.72432	0.66985	0.51106
705.20077	0.81885	0.58042	0.66517	0.64703	0.50187
705.44186	0.59711	0.58188	0.59367	0.75077	0.4769

Table 4.5.1 summarizes the mentioned change in absorption frequency at 704.8 cm^{-1}. The overall results give a clear picture for change in molecular structure in the bio-molecule due to polymerization.

4.6 Impression:

The change in molecular structure, of the constituent biomolecules of Gum Agar, due polymerization is detected from analysis of FTIR and ATR spectra. The distinction in molecular vibration due to the D_2O exchange is also clearly visible. IR absorbance of D_2O exchanged dried Agar specimens show an increase in peak height with increase of sol-gel time. Due to D_2O exchange -NH bending and stretching peaks disappeared from the spectra. This study also confirms that rehydration occur only for the NH bending but structural change occurred in NH stretching are permanent and no rehydration takes place. Also the change in molecular structure, of the constituent bio-molecules of gum Arabica, due polymerization is directly determined from analysis of FTIR spectrum in finger print region. This novel technique may be applied to bio-molecular analysis.

References:

[1] W. F. van Gunsteren, F. J. Luque, D. Timms, A. E. Torda, MOLECULAR MECHANICS IN BIOLOGYF: from Structure to Function, Taking Account of Solvation, Annu. Rev. Biophys. Biomol. Struct. 1994.23:847 63.

[2] Solvation Effects on Molecules and Biomolecules: Computational Methods and Applications, edited by S. Canuto, 2008.

[3] N. Bayliss, “The effect of the electrostatic polarization of the solvent on electronic absorption spectra in solution”, J. Chem. Phys., 18, 1950, pp. 292-297.

[4] Y. Ooshika, “Absorption spectra of dyes in solution”, J. Phys. Soc. Jpn., 9, 1954, pp. 594-602.

[5] E. Mc. Rae, “Theory of solvent effects on molecular electronic spectra. Frequency shifts”, J. Phys. Chem., 61, 1957, pp. 562-572.

[6] E. Lippert, „Dipolmoment und elektronstrukturen von angeregten molekülen“, Z. Naturforsch., 10 A, 1955, pp. 541-545.

[7] N.G. Bakhshiev, “Universal intermolecular interactions and their effect on the position of the electronic spectra of molecules in two component solutions” Opt. Spectrosk., 13, 1962, pp. 24-29.

[8] M. E. Baur, and M. Nicol, “Solvent stark effect and spectral shifts”, J. Chem. Phys., 44, 1966, pp. 3337-3344.

[9] M. Nicol, J. Swain, Yin-Yan Shun, R. Merin, and R.H.H. Chen, “Solvent stark effect and spectral shifts. II.”, J. Chem. Phys., 48, 1968, pp. 3587-3597.

[10] N. G. Bakhshiev. Spektroskopija mezhmolekuljarnyh vzaimodestvii. Izd. Nauka, Leningrad, 1972.

[11] S. Nagakura, M. Kojima, I. Marujama, J. Mol. Structure, 13, 174, 1974.

[12] V. Macovei, Revue Roumaine de Chimie, 21, 1137, 1976.

[13] C. Reichardt, Solvent and Solvent Effects in Organic Chemistry, 3-Rd Edition, Wiley, VCH,Verlach, GmbH& Co.KGaA, Weinheim, 2004.

[14] T. Abe, “Theory of solvent effects on molecular electronic spectra. Frequency shifts”, Bull. Chem. Soc. Jpn., 30, 1965, pp. 1314-1318.

[15] T. Abe “The dipole moment and polarizability in the n–π* excited state of acetone from spectral solvent shifts”, Bull. Chem. Soc. Jpn., 39, 1966, pp. 936-939.

[16] D.O. Dorohoi, “Electronic spectroscopy of N-ylids”, J. Mol. Struct., 704, 2004, pp. 31-43.

[17] D.O. Dorohoi, “Electric dipole moments of the spectrally active molecules estimated from the solvent influence on the electronic spectra” , J. Mol. Struct., 792, 2006, pp. 86-92.

[18] G. Henrion, A. Henrion, and R. Henrion, Biespiele Zur Datenanalyse Mit BASIC Programmen VEB D.V.W., Berlin, 1988.

[19] E. Rusu, D.O.Dorohoi, and A. Airinei, "Solvatochromic effects in the absorption spectra of some azobenzene compounds", J. Mol. Struct., 887, 2008, pp. 216-219.

[20] A. Airinei, M. Homocianu, and D.O. Dorohoi, "Changes induced by solvent polarity in electronic absorption spectra of some azo disperse dyes", J. Mol. Liq., 157, 2010, pp. 13-17.

[21] P. Suppan, and N. Ghoneim, "Solvatochromism" Royal Society of Chemistry, Cambridge, 1997.

[22] N.V. Valenti, G.S. Ušumli, M. Radojkovi, Velikovi, and M. Miši- Vukovi, "Solvent effects on electronic absorption spectra of 3-N-(4-substituted phenyl)-5- carboxy uracils", J. Serb. Chem. Soc, 64, 1999, pp. 149–154.

[23] J.B. Nikoli, G.S. Ušumli, and V.V. Krsti, "Solvent effects on electronic absorption spectra of cyclohex-1-enylcarboxylic and 2- methylcyclohex-1-enylcarboxylic acids", J. Serb. Chem. Soc., 65, 2000, pp. 353–359.

[24] D.Ž. Mijin, G.S. Ušumli, and N.V. Valenti, "Synthesis and investigation of solvent effects on the ultraviolet absorption spectra of 5-substituted-4-methyl-3-cyano-6-hydroxy-2-pyridones", J. Serb. Chem. Soc., 66, 2001, pp. 507–516.

[25] G.S. Ušumli, A.A. Kshad, and D.Ž. Mijin, "Synthesis and investigation of solvent effects on the ultraviolet absorption spectra of 1,3-bis-substituted-5,5-dimethylhydantoins", J. Serb. Chem. Soc., 68, 2003, pp. 699–706.

[26] K. Suganya, and S. Kabilan, "Substituent and solvent effects on electronic absorption spectra of some N-(substitutedphenyl) benzene sulphoamides", Spectrochim. Acta, Part A, 60, 2004, pp. 1225–1228.

[27] G. Bourhill, J.L. Brédas, L.T. Cheng, S.R. Marder, F. Meyers, J.W. Perry, and B.G. Tiemann, "Experimental demonstration of the dependence of the first hyperpolarizability of donor-acceptorsubstituted polyenes on the ground-state polarization and bond length alternation", J. Am. Chem. Soc., 116, 1994, pp. 2619– 2620.

[28] M. Blanchard-Desce, V. Alain, P.V. Bedworth, S.R. Marder, A. Fort, C. Runser, M. Barzoukas, S. Lebus, and R. Wortmann, Large quadratic hyperpolarizabilities with donor-

acceptor polyenes exhibiting optimum bond length alternation: Correlation between structure and hyperpolarizability“, Chem. Eur. J,. 3, 1997, pp. 1091– 1104.

[29] D.O. Dorohoi, and M. Dimitriu, “Dispersive intermolecular interactions in non-polar solvents”, Rev. Chimie Buc., 58, 2007, pp. 1060.

[30] M. Dimitriu, D.G. Dimitriu, and D.O. Dorohoi, “Supply to the spectral shifts of each type of interactions in binary solvents”, Optoelectron. Adv. Mat.-Rapid Commun., 2, 2008 pp. 867-870.

[31] I.R. Tigoianu, and D.O.,Dorohoi A. Airinei, “Solvent influence on the electronic absorption spectra of anthracene”, Revista de Chimie, 60, 2009, pp. 42-44.

[32] D.O. Dorohoi, A. Airinei, and M. Dimitriu, “Intermolecular interactions in solutions of some amino-nitro-benzene derivatives, studied by spectral means”, Spectrochim. Acta Part A, 73, 2009, pp. 257-262.

[33] A. Airinei, E. Rusu, and D.O. Dorohoi, “Solvent influence on the electronic absorption spectra of some azoaromatic compounds”, Spectroscopy Lett., 34, 2001, pp. 65-74.

[34] E. Rusu, D.O. Dorohoi, and A. Airinei, “Solvatochromic effects in the absorption spectra of some azobenzene compounds”, J. Molec. Struct., 887, 2008, pp. 216-219.

[35] C. Nadejde, D.E. Creanga, I. Humelncu, E. Filip, and D.O. Dorohoi, “Study on the intermolecular interactions in rifampicin ternary solutions-calculation of microscopic parameters of rimfampicin molecule”, J. Mol. Liq., 150, 2009, pp. 51-55.

[36] D.O. Dorohoi, and H. Partenie, “The spectroscopy of the cycloimmonium ylides, J. Molec. Struct. 293, 1993, pp. 129-132.

[37] D.O. Dorohoi, D.H. Partenie, L.M. Chiran, and C. Anton, “About the electronic absorption-spectra (eas) and the electronic diffusion spectra (eds) of some pyridazinium-ylids”, Journal de Chimie Physique et de Physico-Chimie Biologique, 91, 1994, pp. 419-431.

[38] C. Gheorghies, L.V. Gheorghies, and D.O. Dorohoi, “Solvent influence on some complexes realized by hydrogen bonds”, J. Molec. Struct., 887, 2008, pp. 122-217.

[39] L.M. Ailioaie, E. Filip, and D.O. Dorohoi, „Intermolecular interactions in water ethanol mixtures studied by ultrasound technique, Revista de Chimie, 59, 2008, pp. 733-738.

[40] D. Dorohoi, M. Avadanei, and M. Postolache, „Characterization of the solvation spheres of some dipolar spectrally active molecules in binary solvents”, Optoelectron. Adv. Mat.-Rapid Communic., 2, 2008, pp. 511-515.

[41] S. Oancea, and D. Dorohoi , “Determinarea compresibilitatii solutiilor binare din masuratori ale vitezei ultrasunetelor”, Rev. Chim. Buc., 56, 2005, pp. 371-374.

[42] D.O. Dorohoi, “About the multiple linear regressions applied in studying the solvatochromic effects”, Spectrochim. Acta Part A, 75, 2010, pp. 1030.

[43] D.O. Dorohoi, “Electric dipole moments of the spectrally active molecules estimated from the solvent influence on the electronic spectra”, J. Molec. Struct., 792, 2006, pp. 86-92,

[44] M. Toma, I.A. Rusu, S. Filoti, and Dorohoi D.O., “Electric dipole moments in the excited states determined by means of the spectral methods”, J. Optoelectron. Adv. Mat., 5, 2006, pp. 1951-1955.

[45] M. Dimitriu, L.M. Ivan, and D.O. Dorohoi, “Electro-optical parameters of some benzene derivatives obtained by molecular orbital calculations”, Revista de Chimie, 59, 2008, pp. 216-219.

[46] D.O. Dorohoi, M. Cotlet, and I. Mangalagiu, „Spectral kinetics of 3 + 3 dipolar thermal dimerization in some carbanion monosubstituted 3-(p-halo-phenyl)-pyridazinium ylid solutions”, Int. J. Chem. Kinetics, 34, 2002, pp. 613-619.

[47] V. Melnig, I. Humelnicu, and D.O. Dorohoi, “Thermal dimerization kinetics of 3-(p-bromophenyl)-pyridazinium benzoyl methylid in solutions”, Int. J. Chem. Kinetics., 40, 2008, pp. 230-239.

[48] A.V. Kulinich, N.A. Derevyanko, and A.A. Ishchenko, “Synthesis, structure, and solvatochromism of merocyanine dyes based on barbituric acid”, Russ. J. Gen. Chem. (Engl. Trans.), 76, 2006, pp. 1441–1457.

[49] B.W. Domagalska, K.A. Wilk, and R. Zielinski, “Spectroscopic and electrochemical properties of new amphiphilic donor–acceptor conjugated polyenes”, J. Photochem. Photobiol. A Chem. 184, 2006, pp. 193–203.

[50] O.E. Sherif, “Effect of solvents on the electronic absorption spectra of some substituted diarylformazans”, Monatshefte ftir Chemie, 128, 1997, pp. 981-990.

[51] S. Nagakura, and H. Baba, “Dipole moments and near ultraviolet absorption of some monosubstituted benzenes — The effect of solvents and hydrogen bonding”, J. Am. Chem. Soc., 74, 1952, pp. 5693-5698.

[52] L.G.S. Brooker, G.H. Keyes, R.H. Sprague, R.H. VanDyke, E. VanLare, G. VanZandt, F.L. White, H.W.J. Cressman, and S.G. Dent Jr., “Color and constitution. X.1 Absorption of the merocyanines2”, J. Am. Chem. Soc., 73, 1951, pp. 5332-5350.

[53] H.E. Ungnada, “The effect of solvents on the absorption spectra of aromatic compounds”, J. Am. Chem. Soc., 75, 1953, pp. 432-434.

[54] A.M.B. Block, and S. Hecht, “Poly(propylene oxide)−poly(phenylene ethynylene) block and graft copolymers”, Macromolecules, 41, 2008, pp. 3219-3227.

[55] A. Kawski “On the estimation of excited-state dipole moments from solvatochromic shifts of absorption and fluorescence spectra”, Z. Naturforsch., 57a, 2002, pp. 255–262.

[56] B. Koutek, “Dipole moments in excited state”, Collect. Czech Chem. Commun., 43, 1978, pp. 2368-2386.

[57] N. Mataga, Y. Kaifu, and M. Koizumi, “Solvent effects upon fluorescence spectra and the dipole moments of excited molecules”, Bull. Chem. Soc. Jpn., 29, 1956, pp. 465-470.

[58] M.J. Kamlet, J.L.M. Abboud, M.H. Abraham, and R.W. Taft, “Linear solvation energy relationships. 23. A comprehensive collection of the solvatochromic parameters,

π*, α and β, and some methods for simplifying the generalized solvatochromic equation" J. Org. Chem., 48, 1983, pp. 2877–2887.

[59] Lakowicz J.R., "Principles of fluorescence spectroscopy", 3rd.ed, Ed. Springer, University of Maryland School of Medicine Baltimore, Maryland, USA, 2006, pp. 1-954.

[60] D. Citterio, K. Minamihashi, Y. Kuniyoshi, H. Hisamoto, S. Sasaki, and K. Suzuki, "Optical determination of low-level water concentrations in organic solvents using fluorescent acridinyl dyes and dye-immobilized polymer membranes", Anal. Chem., 73, 2001, pp. 5339–5345

[61] J. Nakanishi, T. Nakajima, M. Sato, T. Ozawa, K. Tohda, and Y. Umezawa, "Imaging of conformational changes of proteins with a new environment-sensitive fluorescent probe designed for site-specific labeling of recombinant proteins in live cells", Anal. Chem., 73, 2001, pp. 2920–2928.

[62] A. Kellmann, "Intersystem crossing and internal conversion quantum yields of acridine in polar and nonpolar solvents", J. Phys. Chem., 81, 1977, pp. 1195–1198.

[63] J.S.S. de Melo, R.S. Becker, and A.L. Macanita, "Photophysical behavior of coumarins as a function of substitution and solvent: Experimental evidence for the existence of a lowest lying 1(n, π*) State", J. Phys. Chem., 98, 1994, pp. 6054–6058.

[64] S. Uchiyama, K. Takehira, T. Yoshihara, S. Tobita, and T. Ohwada, "Environment-sensitive fluorophore emitting in protic environments", Org. Lett., 8, 2006, pp. 5869–5872.

[65] H. Fabin and W. Mäntele, Handbook of Vibrational Spectroscopy, edited by J. M. Chalmers and P.R.Griffiths, John Wiley & Sons, 1999, pp. 3399-3425.

[66] Arup Dutta and A. Sarkar, "Vibrational Spectrum of Gum Agar in Pure and D_2O Exchange state by FTIR Analysis", Proceedings of AMRP-2013, International Journal Of Engineering Research and Technology (IJERT).

[67] Fourier Transform Infrared Spectroscopic Analysis of Protein Secondary Structures Biochimica et Biophysica Sinica, 39(8): 2007, pp. 549 559.

[68] D.L. Pavia, G.M. Lampman, G.S. Kriz and J.R. Vyvyan, Spectroscopy, Cengage Learning, 2007.

[69] Arup Dutta and A. Sarkar, “FTIR Investigation of Structural Change in Bio-molecule”, Advances in Applied Science Research, 2011, 2 (1): 125-128.

Chapter 5

Mapping of molecular energy levels

5.1 Principle underlying molecular energy level mapping:

In recent years, there has been great progress in the development of suitable techniques for mapping of molecular energy level. Molecular spectroscopy is especially well suited to this task. A wide variety of recently developed laser-based spectroscopic detection schemes are not only highly sensitive but also space and time specific. The laboratory application of sophisticated sampling and observation techniques has yielded a wealth of vibrational and electronic spectral data for molecular energy level mapping [1].

The most crucial and basic element in any structural analysis algorithm is to introduce a metric to measure similarity or dissimilarity between two atomic configurations. Many options are available, with different levels of complexity and generality, starting from the commonly used root mean square distance. In order to deal with symmetry operations or condensed phase structures, several frameworks have been developed [2, 3–15], that assign a unique vector of order parameters to each molecular or crystalline configuration.

When a molecule absorbs light, it gains energy and reaches a state called an excited state. With visible or ultraviolet (UV) light, the electrons in the molecule are excited and with infrared (IR) light, the molecular vibration is excited. When a molecule absorbs microwave, its molecular rotation is excited. The precise geometrical structures of molecules can be determined by molecular spectroscopy and gas electron diffraction.

In molecular spectroscopy, we obtain the energies of discrete levels of a molecule by taking advantage of the absorption and emission of light observed in molecules. To determine the geometrical structure of a molecule, we mainly look for the energy level associated with its rotational motion, so that we can calculate the moment of inertia for the molecule. Once we have the moment of inertia, we can determine the distances between the atoms that compose the molecule, or the internuclear distances. We can also determine the molecular structure of a molecule at its electronic ground state or its electronically

excited state by observing the rotational structure of its absorption and emission spectra of the electronic transition in the visible and ultraviolet regions. An alternative to these spectroscopic methods is the electron diffraction method. When molecules are in the gas phase, their geometrical structures have been determined though rotational structures observed in the molecular spectroscopic method as well as through electron diffraction images obtained by the electron diffraction method [16]..

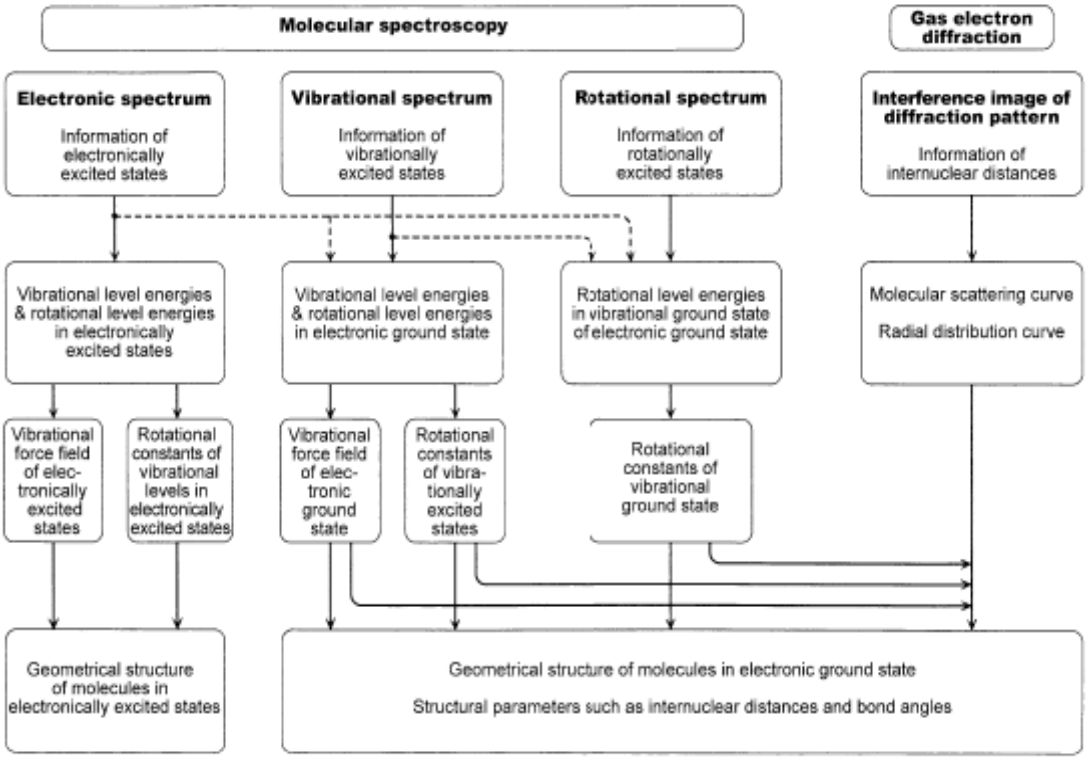

Flow chart for determination of structures of molecule

If an atom, ion, or molecule is at the lowest possible energy level, it and its electrons are said to be in the ground state. If it is at a higher energy level, it is said to be excited, or any electrons that have higher energy than the ground state are excited. If more than one quantum mechanical state is at the same energy, the energy levels are called degenerate energy levels. Energy can be stored either as potential energy or kinetic energy, in a variety of ways including translational energy (small amounts of energy stored as

kinetic energy), rotational energy (kinetic energy associated with the rotational motion of molecules), vibrational energy (the oscillatory motion of atoms or groups of atoms within a molecule), electronic energy (energy stored as potential energy in excited electronic configurations). All except the Translational energy are quantized.

$$E_{molecule} = E_{rotational} + E_{vibrational} + E_{electronic}$$

5.1.1 Molecular models :

Electron densities show the locations of electrons. Large values of the density will first reveal atomic positions (the X-ray diffraction experiment) and then chemical bonds, while smaller values will indicate overall molecular size. Unlike conventional structure models, electron densities assume no prior knowledge about bonding and, therefore, can be used to elucidate bonding. Electron densities allow description of the bonding in transition states where there can be no (direct) information from experiment.

The electrostatic potential is the energy of interaction of a point positive charge with the nuclei and electrons of a molecule. Negative electrostatic potentials indicate areas that are prone to electrophilic attack. A sufficiently small value of the electron density provides overall molecular size and shape. The electrostatic potential can then be mapped onto the electron density by using color to represent the value of the potential. The resulting model simultaneously displays molecular size and shape and electrostatic potential value [17]. The polarization potential provides the energy due to electronic reorganization of the molecule as a result of its interaction with a point positive charge. The sum of the electrostatic and polarization potentials provides a better account of the energy of interaction of a point positive charge than available from the electrostatic potential alone [18- 24].

Molecular orbital descriptions offer quantitative information about molecular charge distributions. Solutions of the approximate quantum mechanical equations of electron motion, are made up of sums and differences of atomic solutions (atomic orbitals), just like molecules are made up of combinations of atoms. Molecular orbitals for very simple molecules may often be interpreted in terms of familiar chemical bonds [17].

For closed-shell molecules (in which all electrons are paired), the spin density is zero everywhere. For open-shell molecules (in which one or more electrons are unpaired), the spin density indicates the distribution of unpaired electrons. Spin density is an obvious indicator of reactivity of radicals (in which there is a single unpaired electron). Bonds will be made to centers for which the spin density is greatest. A more important application of the local ionization potential is as an alternative to the electrostatic potential as a graphical indicator of electrophilic reactivity. This is in terms of a property map rather than as an isosurface.

5.1.2 Property Maps:

Additional information (a "property") may be added to any isosurface by using color to represent the value of the property. Colors at one end of the visible spectrum could represent "small" property values and at the other end, "large" property values. This gives rise to a model which actually conveys four dimensions of information. Most commonly, a property is mapped onto the size surface. This depicts overall molecular size and shape and, therefore, demarks surface regions "visible" to an incoming reagent. There are situations where a property is more clearly visible when mapped instead onto a bond surface.

5.1.3 Electrostatic Potential Map:

The most commonly employed and most important property map is the electrostatic potential map. This gives the electrostatic potential at locations on a particular surface, most commonly a surface of electron density corresponding to overall molecular size (a size surface). An electrostatic potential map conveys information about the distribution of charge in a molecule. It also gives information about delocalization of charge. Electrostatic potential maps may also be employed to characterize transition states in chemical reactions.

5.1.4 Molecular Orbital Maps:

Molecular orbitals may also be mapped onto electron density surfaces. Maps of "key" molecular orbitals may also lead to informative models. The most popular and (to date) most important of these is the so-called "LUMO map", in which the lowest-unoccupied molecular orbital (the LUMO) is mapped onto a size surface. LUMO map shows which regions of a molecule are most electron deficient, and hence most subject to nucleophilic attack.

5.1.5 Local Ionization Potential Map:

Mapping the local ionization potential onto a size surface reveals those regions from which electrons are most easily ionized. Such a representation is referred to as a local ionization potential map. Local ionization potential maps provide an alternative to electrostatic potential maps for revealing sites which may be particularly susceptible to electrophilic attack.

5.1.6 Spin Density Map:

The spin density of a radical indicates where its unpaired electron resides. This in turn allows qualitative assessment of radical stability. A radical in which the unpaired electron is localized onto a single center is likely to be more labile than a radical in which the unpaired electron is delocalized over several centers. An even more useful indicator of radical stability and radical reactivity is provided by a so-called spin density map. Like the other property maps this measures the value of the property on an electron density surface corresponding to overall molecular size [18- 24].

5.2 FTIR results towards energy level mapping:

In an n-atom non linear molecule there are 3n-6 possible vibrational modes. The vibration includes bond bending and bond stretching. The energy difference between vibrational states corresponds to the energy level of IR Radiation. Normally two major region in the IR spectrum of a molecule are the functional group region between 7000 cm^{-1} to 1500 cm^{-1} it includes the X-H stretching region and finger print region between1500 cm^{-1} to 350 cm^{-1} . The later region is very important in bio-molecular dynamics and it may provide much relevant information about the internal motion of the molecule and is related bio-molecular function in living systems [25]. The objectives of the FTIR spectroscopic study are (i) to recognize the most reliable absorption frequencies for a particular functional group of a bio-molecule (ii) to use the group frequencies to distinguish the spectra of the sample (iii) to understand the factor which complicate (e.g. overtone and combinational bands, Fermi resonance and most important for a bio-molecule – hydrogen bonded system) IR spectra and be able to recognize the effect that these have on the spectra. The proposed plan is however to be spanned over ultraviolet-visible spectroscopy (UV-VIS) and IR range. The objective is to get an idea of the ground rotational state (i.e. non rotating molecule) by considering the difference between various allowed rotational energy levels of different specimens of bio-molecules of gum Arabica.

In this present work [26] vibrational and rotational characteristic of Gum Arabica molecule along with its characteristics change due to deuterium exchange are studied. Studies of bio-molecules and protein conformation in solution-phase under hydrogen/deuterium exchange have been found to be important [27-29] and well documented [30, 31]. The Gum Arabica [32, 33] is a bio-molecule with polysaccharide in nature. The said study is confined in IR region of spectrum recorded by FTIR technique. The FTIR technique of analysis of bio-molecule is popular and gained considerable success [34-36] in this field. Rotational energy level and rotational constant are extracted from various series in the recorded IR spectrum on Gum Arabica specimens. The results obtained may be correlated with the dynamical and structural characteristic of the bio-molecule.

5.2.1 Elementary theory of molecular spectra:

Rotational energy of a molecule is quantized. So they have some particular value of angular momentum [37, 38]. For a rigid diatomic molecule the reduced mass μ may be written as

$$\mu = \frac{m_1 m_2}{m_1 + m_2} \quad (1)$$

The absorbed rotational energy levels of a rigid diatomic molecule is given by the expression

$$E_J = \frac{h^2}{8\pi^2 I} J\,(J+1) \quad (2)$$

[Where J = 0, 1, 2, 3…; h = Plank's constant; I = Moment of inertia; J = Rotational quantum number].

The difference between the energy levels is significant to analyze the rotational energy levels. The corresponding transition frequency is $\nu = \Delta E/h$ or wave number is $\bar{\nu} = \Delta E/hc$ Energy of j th excited state may be expressed in terms of wave number as

$$\varepsilon_J = \frac{E_J}{hc} = \frac{h^2}{8\pi^2 Ic} J\,(J+1)\ \text{cm}^{-1} \quad (3)$$

$$\varepsilon_J = BJ\,(J+1)\ \text{cm}^{-1} \quad (4)$$

B is the rotational constant given by,

$$B = \frac{h}{8\pi^2 I_B c} \quad (5)$$

(Where c = velocity of light; I_B = moment of inertia)

From Eq. 4 we see that for J = 0, $\varepsilon_J = 0$ which implies that the molecule is not rotating. For J = 1, $\varepsilon_J = 2B$ i.e. a rotating molecule in its lowest angular momentum. The incident IR radiation which is absorbed for the transition J = 0 state (ground rotational state) to J = 1 is

$$\varepsilon_{J=1} - \varepsilon_{J=0} = 2B - 0 = 2B\ \text{cm}^{-1} \quad (6)$$

$\bar{\nu}_{J=0\rightarrow J=1} = 2B$

$\bar{\nu}_{J=1\rightarrow J=2} = 4B$

$\ldots\ldots\ldots\ldots = 6B$

In general to raise the molecule from the state J to state J+1 we would have

$$\bar{\nu}_{J\rightarrow J+1} = B(J+1)(J+2) - BJ(J+1)$$

$$= 2B(J+1) \quad (7)$$

The quantum selection rule for rigid diatomic rotator is given by

$$\Delta J = \pm 1 \quad (8)$$

All other transitions but in which J changes by unity are spectroscopic forbidden. Using Eq. 5 one can write

$$I = \frac{h}{8\pi^2 Bc} \quad (9)$$

With the knowledge of reduced mass the bond length may be estimated from the relation

$$r^2 = \frac{I}{\mu} \quad (10)$$

While centrifugal rotational constant (D) is taken into consideration energy of j th excited state may be expressed as

$$\varepsilon_J = \frac{E_J}{hc} = BJ\,(J+1) - DJ^2\,(J+1)^2\ cm^{-1} \quad (11)$$

The centrifugal rotational constant (D) is given by

$$D = \frac{h^3}{32\pi^4 I^2 r^2 kc}\ cm^{-1} \quad (12)$$

Which is a positive quantity. Assuming that the force field is simple harmonic all other small constant dependent upon the geometry of the molecule are neglected.

From the defining equations of B and D it may be shown directly that

$$D = \frac{16B^3\pi^2\mu c^2}{k} = \frac{4B^3}{\bar{\omega}^2} \text{ cm}^{-1} \quad (13)$$

The analytical expression for the transitions may be written as

$$\varepsilon_{J+1} - \varepsilon_J = \bar{\nu}_J = B\,[(J+1)(J+2) - J(J+1)] - D[(J+1)^2(J+2)^2 - J^2(J+1)^2]$$

$$= 2B\,(J+1) - 4D\,(J+1)^3 \text{ cm}^{-1} \quad (14)$$

5.2.2 Materials and Methods:

I. Sample Preparation.

The high purity grade Gum Arabica powder specimen (S1) was collected from Merck (India) and was subjected to a sol–gel process along with pure water so that the polysaccharide host chain can form more complex higher polymers over that in normal powder form. The sol specimen (S2) is extracted after 120 minutes. The same sol-gel process was applied along with D_2O so that the polysaccharide host chain can form in the previous manner and hydrogen is replaced by deuterium from –OH bond. This sol specimen (S3) is also extracted after 120 minutes. The experimental solid specimens S2 and S3 were developed by adequate drying of the sols at environmental condition.

II. Experiments.

The developed Gum Arabica specimens (S2- S3) are supposed to exhibit change in molecular structure over that in S1 due prolongation or polymerization effect on corresponding monomer by sol gel process. Beside this frequency shift may also be observed due to deuterium exchange in the presence of D_2O for the specimen S3. FTIR analysis on Gum Arabica specimens (S1, S2, and S3) were carried out at room temperature (25°C) to examine their molecular spectrum and dynamical information. From the recorded FTIR spectrum of various samples the difference of rotational energy level

was estimated to have a complete dynamical picture of the bio-molecule. The analysis was carried out using FTIR Model, IR Affinity 1 (Shimadzu, Japan,) at high resolution using KBr window.

5.2.3 Results and discussion:

Figure 5.2.1 shows the comparison of the FTIR spectra among the developed Gum Arabica specimens S2 and S3 between wave number 3493 cm^{-1} to 3505 cm^{-1}. Frequency shift is obtained around the O-H stretching region at wave numbers ranging from 3200 cm^{-1} to 3600 cm^{-1}.

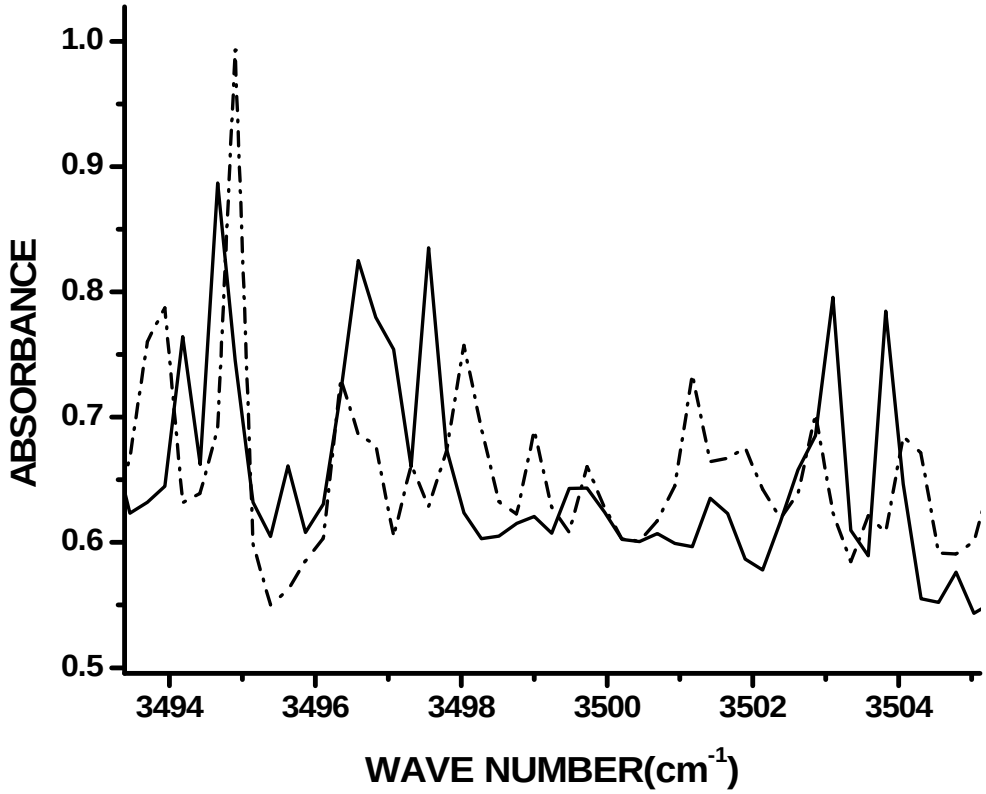

Figure 5.2.1. FTIR absorption spectra of (i) Gum Arabica specimen S2 is indicated by solid line and (ii) Gum Arabica specimen S3 is indicated by dash-dot line.

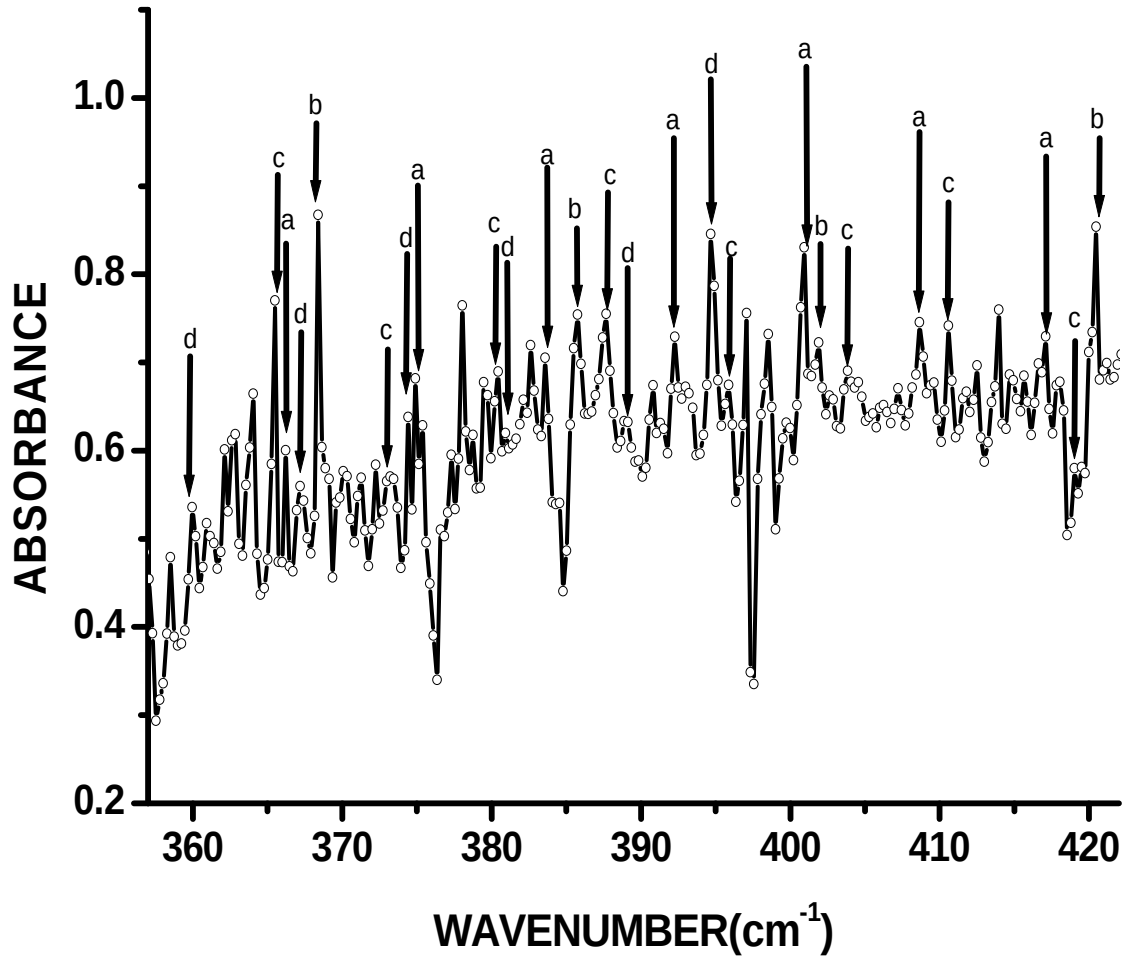

Figure 5.2.2. FTIR absorption spectrum of pure Gum Arabica powder (S1)

It shows the FTIR spectra of Gum Arabica powder (specimen S1) between wave number 355 cm^{-1} to 420 cm^{-1}. Different arrows indicate the peaks obtained from various bonds. In this figure peaks found from different bonds are marked as a, b, c, and d.

The tables containing peaks of absorption spectra for the different specimens of Gum Arabica were prepared using experimental FTIR spectrum. The energy difference of transition between the successive energy levels in the finger print region is integral multiple of 2B cm^{-1}. Thus the peaks satisfy the mention criterion is chosen for preparing peak tables. Analysis shows that there may be four different series in the recorded FTIR

spectrum from which each of the peak table can be extracted. The marked in the graph of the corresponding specimens were found to form the mentioned series. Sometimes departure from the mentioned empirical rule are also found and they may be due coupling with other effect. It is difficult to identify the bonds for which the peaks arise in the FTIR spectrum as Gum Arabica has a complex molecular structure. Details knowledge of the structure and dynamics of the system can lead to have a verification of the obtained value of the rotational constant. The estimated value of rotational constant (2B) of the first transition or close to the average value of the transition which was observed from the peak tables of the each series of each specimen are chosen due to the mentioned limitation. In this way one may have a map of quantum energy levels of Gum Arabica molecule from the measured. FTIR spectra of the specimen below however a direct knowledge of ground or lower energy state at RT requires FTIR spectra below the wave number 350 cm^{-1} .

Analysis from series 'a' of the FTIR spectrum					Analysis from series 'c' of the FTIR spectrum				
J	$\bar{\nu}_{theo}$	$\bar{\nu}_{expt}$	$\Delta\bar{\nu}_{expt}$	B_{expt}	J	$\bar{\nu}_{theo}$	$\bar{\nu}_{expt}$	$\Delta\bar{\nu}_{expt}$	B_{expt}
41	366.22	366.22			46	365.50	365.50		
			8.68	4.34				7.71	3.86
42	374.90	374.90			47	373.21	373.21		
			8.68	4.34				7.24	3.62
43	383.58	383.58			48	380.92	380.45		
			8.68	4.34				7.23	3.62
44	392.26	392.26			49	388.63	387.68		
			8.68	4.34				8.13	4.06
45	400.94	400.94			50	396.34	395.87		
			7.71	3.86				7.96	3.98
46	409.62	408.65			51	404.05	403.83		
			8.45	4.22				6.93	3.46
47	418.30	417.10			52	411.76	410.76		
								8.26	4.13
					53	419.47	419.02		

Analysis from series 'b' of the FTIR spectrum					Analysis from series 'd' of the FTIR spectrum				
J	$\bar{\nu}_{theo}$	$\bar{\nu}_{expt}$	$\Delta\bar{\nu}_{expt}$	B_{expt}	J	$\bar{\nu}_{theo}$	$\bar{\nu}_{expt}$	$\Delta\bar{\nu}_{expt}$	B_{expt}
20	368.39	368.39			49	359.95	359.95		
			17.36	8.68				7.24	3.62
21	385.75	385.75			50	367.19	367.19		
			16.15	8.08				7.23	3.62
22	403.11	401.90			51	374.43	374.42		
			18.57	9.28				6.50	3.25
23	420.47	420.47			52	381.67	380.92		
								7.96	3.98
					53	388.91	388.88		
								5.79	2.90
					54	396.15	394.67		

Table 5.2.1. Rotational spectrum of Gum Arabica powder (S1) ($\bar{\nu}_{theo}, \bar{\nu}_{expt}, \Delta\bar{\nu}_{expt}$ and B_{expt} are in cm^{-1})

The Table 5.2.1 was obtained from IR spectrum shown in Fig. 5.2.2.Using the average of the different transitions of series 'a', 'b', 'c', 'd' the values of 2B that we get are 8.48, 17.36, 7.64, 6.94 respectively. In this case we take the values of first transition that we observed from peak table as their values do not differ much from the average values. The estimated values of rotational constants 2B and energy difference between ground state to first excited state ($\varepsilon_{J=0\rightarrow1}$) for the four mention series are , 2B = 8.68 cm^{-1} and $\Delta\varepsilon = 1.7242\times10^{-15}$ erg., 2B = 17.36 cm^{-1} ,$\Delta\varepsilon = 3.4485\times10^{-15}$ erg., 2B = 7.71 cm^{-1} and $\Delta\varepsilon = 1.5315\times10^{-15}$ erg., 2B = 7.24 cm^{-1} and $\Delta\varepsilon = 1.4382\times10^{-15}$ erg. For series 'a', 'b', 'c' and 'd' respectively.

Fig. 5.2.3 shows of the FTIR spectra of Gum Arabica specimen (S2) between wave number 355 cm^{-1} to 425 cm^{-1}. Different arrows indicate the peaks obtained from various bonds. In this figure peaks found from different bonds are marked as a, b, c, d.

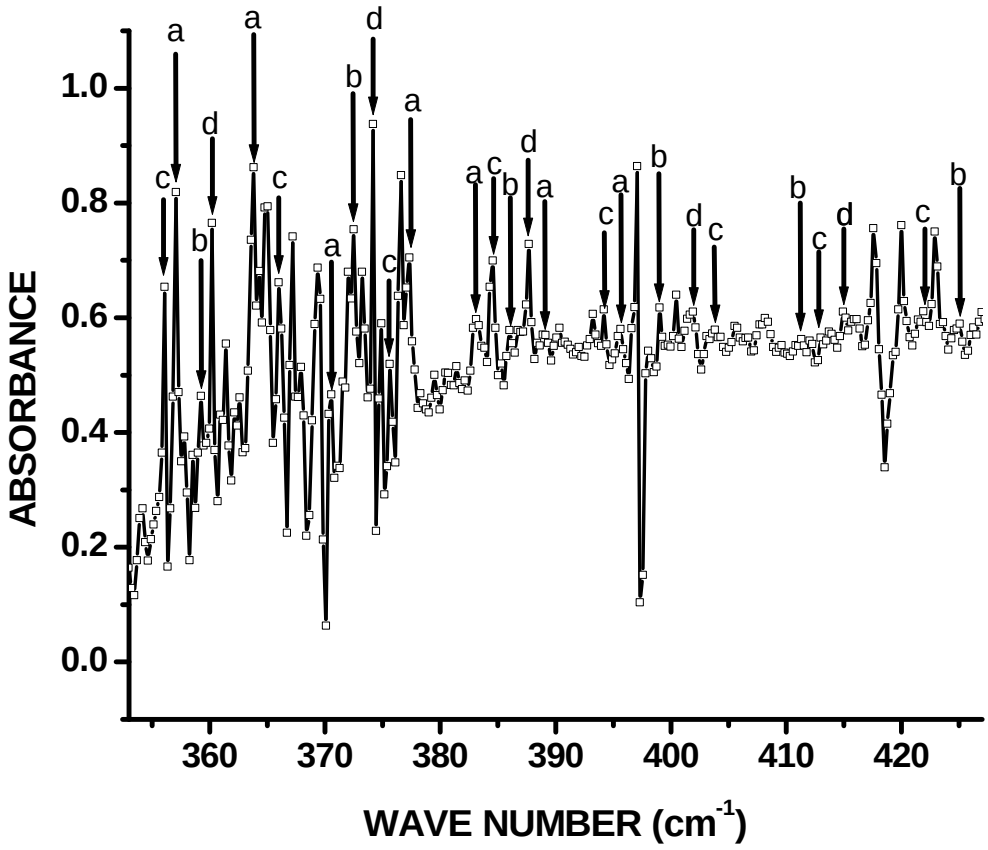

Figure 5.2.3. FTIR absorption spectrum of Gum Arabica specimen S2. It shows the FTIR spectra of Gum Arabica powder (specimen S2) between wave number 355 cm^{-1} to 430 cm^{-1}. Different arrows indicate the peaks obtained from various bonds. In this figure peaks found from different bonds are marked as a, b, c, and d.

Analysis from series 'a' of the FTIR spectrum					Analysis from series 'c' of the FTIR spectrum				
J	$\bar{\nu}_{theo}$	$\bar{\nu}_{expt}$	$\Delta\bar{\nu}_{expt}$	B_{expt}	J	$\bar{\nu}_{theo}$	$\bar{\nu}_{expt}$	$\Delta\bar{\nu}_{expt}$	B_{expt}
52	357.06	357.06			35	356.10	356.10		
			6.75	3.86				9.88	4.94
53	363.81	363.81			36	365.98	365.98		
			6.75	3.62				9.64	4.82
54	370.56	370.56			37	375.86	375.62		
			6.75	3.62				8.93	4.46
55	377.31	377.31			38	385.74	384.55		

			5.79	4.06				9.64	4.82
56	384.06	383.10			39	395.62	394.19		
			5.79	3.98				9.64	4.82
57	390.81	388.89			40	405.50	403.83		
			6.75	3.46				9.16	4.58
58	397.56	395.64			41	415.38	412.99		
								8.92	4.46
					42	425.26	421.91		
Analysis from series 'b' of the FTIR spectrum					Analysis from series 'd' of the FTIR spectrum				
J	$\bar{\nu}_{theo}$	$\bar{\nu}_{expt}$	$\Delta\bar{\nu}_{expt}$	B_{expt}	J	$\bar{\nu}_{theo}$	$\bar{\nu}_{expt}$	$\Delta\bar{\nu}_{expt}$	B_{expt}
27	359.95	359.23			25	360.19	360.19		
			13.26	6.63				13.99	7.00
28	372.97	372.49			26	374.18	374.18		
			13.50	6.75				13.50	6.75
29	385.99	385.99			27	388.17	387.68		
			13.02	6.51				14.22	7.11
30	399.01	399.01			28	402.16	401.90		
			12.30	6.15				13.02	6.51
31	412.03	411.31			29	416.15	414.92		
			13.74	6.87				12.06	6.03
32	425.05	425.05			30	430.14	426.98		

Table 5.2.2: Rotational spectrum of Gum Arabica specimen S2 ($\bar{\nu}_{theo}, \bar{\nu}_{expt}, \Delta\bar{\nu}_{expt}$ and B_{expt} are in cm^{-1})

The above table was obtained from IR spectrum shown in Figure 5.2.3. Using the average of the different transitions of series 'a', 'b', 'c', 'd' the values of 2B that we get are 6.43, 13.16, 9.40, 13.36 respectively. In this case we take the values of first transition that we observed from peak table as their values do not differ much from the average values. The estimated values of rotational constants 2B and energy difference between ground state to first excited state ($\varepsilon_{J=0\rightarrow1}$) for the four mention series are , 2B = 6.75 cm^{-1} and $\Delta\varepsilon = 1.3409\times10^{-15}$ erg., 2B = 13.26 cm^{-1} ,$\Delta\varepsilon = 2.6340\times10^{-15}$ erg., 2B = 9.88 cm^{-1} and $\Delta\varepsilon = 1.9626\times10^{-15}$ erg., 2B = 13.99 cm^{-1} and $\Delta\varepsilon = 2.7790\times10^{-15}$ erg. For series 'a', 'b', 'c' and'd' respectively.

Figure 5.2.4 shows of the FTIR spectra of Gum Arabica specimen (S3) between wave number 355 cm^{-1} to 400 cm^{-1}. Different arrows indicate the peaks obtained from various bonds. In this figure peaks found from different bonds are marked as a, b, c, d.

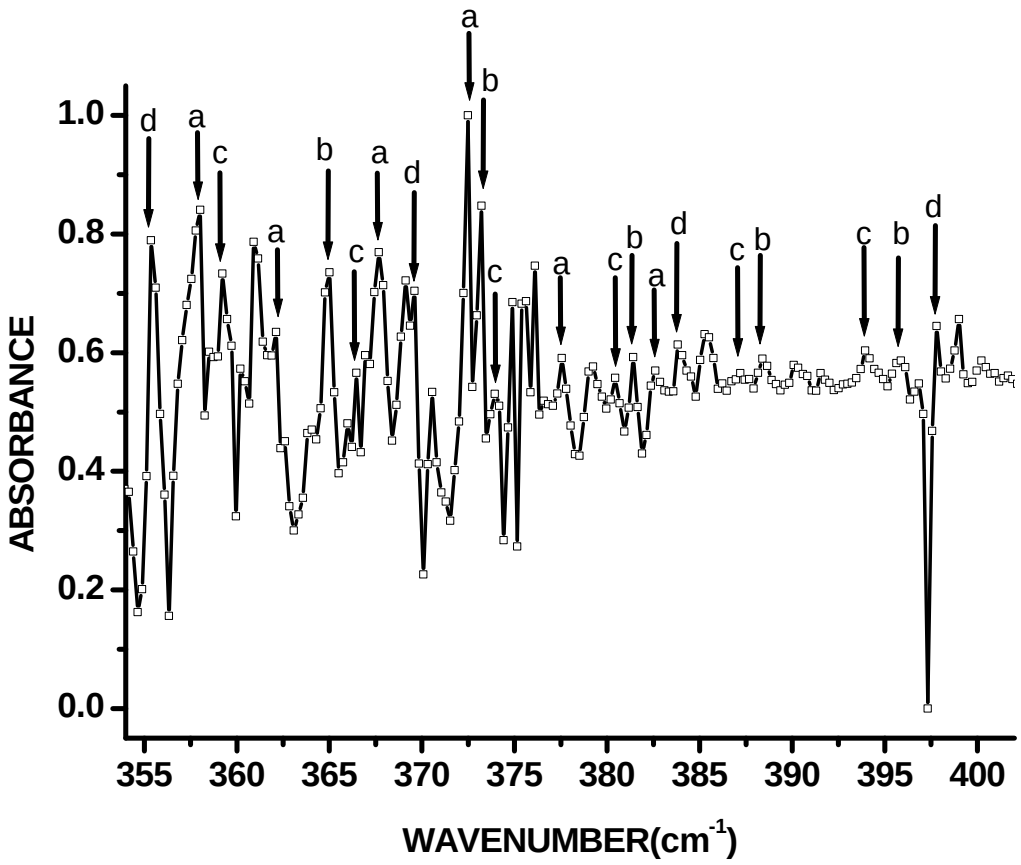

Figure 5.2.4. FTIR absorption spectrum of Gum Arabica specimen S3

Analysis from series 'a' of the FTIR spectrum					Analysis from series 'c' of the FTIR spectrum				
J	$\bar{\nu}_{theo}$	$\bar{\nu}_{expt}$	$\Delta\bar{\nu}_{expt}$	B_{expt}	J	$\bar{\nu}_{theo}$	$\bar{\nu}_{expt}$	$\Delta\bar{\nu}_{expt}$	B_{expt}
73	358.03	358.03			49	359.23	359.23		
			4.09	2.04				7.23	3.62
74	362.85	362.12			50	366.46	366.46		
			5.55	2.78				7.48	3.74
75	367.67	367.67			51	373.69	373.94		
			4.82	2.41				6.51	3.26
76	372.49	372.49			52	380.92	380.45		
			5.06	2.54				6.75	3.38
77	377.31	377.55			53	388.15	387.20		
			5.07	2.54				6.75	3.38
78	382.13	382.62			54	395.38	393.95		
			2.65	1.32					
79	386.95	385.27							
Analysis from series 'b' of the FTIR spectrum					Analysis from series 'd' of the FTIR spectrum				
J	$\bar{\nu}_{theo}$	$\bar{\nu}_{expt}$	$\Delta\bar{\nu}_{expt}$	B_{expt}	J	$\bar{\nu}_{theo}$	$\bar{\nu}_{expt}$	$\Delta\bar{\nu}_{expt}$	B_{expt}
44	365.02	365.02			24	355.37	355.37		
			8.19	4.10				14.23	7.12
45	373.21	373.21			25	369.60	369.60		
			8.20	4.10				14.22	7.11
46	381.40	381.41			26	383.83	383.82		
			6.99	3.50				13.99	7.00
47	389.59	388.40			27	398.06	397.81		
			7.48	3.74					
48	397.78	395.88							

Table 5.2.3. Rotational spectrum of Gum Arabica specimen S3 ($\bar{\nu}_{theo}, \bar{\nu}_{expt}, \Delta\bar{\nu}_{expt}$ and B_{expt} are in cm^{-1})

The table 5.2.3 was obtained from IR spectrum shown in Figure 4. Using the average of the different transitions of series 'a', 'b', 'c', 'd' the values of 2B that we get are 4.92, 7.72, 6.94, 14.15 respectively. For the series 'b', 'c', 'd' we take the values of first transition that we observed from peak table as their values do not differ much from

the average values. For series 'a' we neglect the transition between J=78 to J=79 and as the average value of 2B for this series differs an amount of .83 cm^{-1}, we consider the transition between J=75 to J=76. The estimated values of rotational constants 2B and energy difference between ground state to first excited state ($\varepsilon_{J=0\rightarrow 1}$) for the four mention series are , 2B = 4.82 cm^{-1} and $\Delta\varepsilon=9.5747\times10^{-16}$ erg., 2B = 8.19 cm^{-1} ,$\Delta\varepsilon=1.6269\times10^{-15}$ erg., 2B = 7.23 cm^{-1} and $\Delta\varepsilon=1.4362\times10^{-15}$ erg., 2B = 14.23 cm^{-1} and $\Delta\varepsilon=2.8267\times10^{-15}$ erg. For series 'a', 'b', 'c' and 'd' respectively.

Specimen S1		Specimen S2		Specimen S3	
Rotational constant(B) (cm^{-1})	Moment of inertia (I) of the rotational Group (gm cm^2)	Rotational constant(B) (cm^{-1})	Moment of inertia (I) of the rotational Group (gm cm^2)	Rotational constant(B) (cm^{-1})	Moment of inertia (I) of the rotational Group (gm cm^2)
3.62	7.73271×10^{-40}	3.38	8.28178×10^{-40}	2.41	11.61510×10^{-40}
3.86	7.25192×10^{-40}	4.94	5.66648×10^{-40}	3.62	7.73271×10^{-40}
4.34	6.44986×10^{-40}	6.63	4.22208×10^{-40}	4.10	6.82741×10^{-40}
8.68	3.22493×10^{-40}	7.00	3.99891×10^{-40}	7.12	3.93152×10^{-40}

Table 5.2.4. Comparison of rotational constant and moment of inertia of rotational Group among different Gum Arabica specimens

The contents of Table 5.2.4 compare that rotational constant and estimated moment of inertia of the corresponding rotation group in the experimental bio-molecule and their modified version due to deuterium exchange. However the analysis may be complicated for the higher order rotational energy due to the rotational-vibrational coupling. The moment of inertias are calculated using equation (9) and the estimated values of the corresponding rotational constant as given in Table 5.2.4.

5.3 Outcome:

The change in molecular structure, of the constituent bio-molecules of Gum Arabica, due deuterium exchange is directly determined from analysis of FTIR spectrum

in functional group region. This novel technique may be applied to bio-molecular analysis. The values of rotational constant are consistent with the results those are obtained from the peak table of the different specimens as rotational constant is inversely proportional to the moment of inertia of the system.

References:

[1] Marilyn E. Jacox, Vibrational and Electronic Energy Levels of Polyatomic Transient Molecules, J.Phys. Chem. Vol. 19, No. 6, 1990.

[2] Rupp M, Tkatchenko A, Müller KR, von Lilienfeld OA (2012) Fast and accurate modeling of molecular atomization energies with machine learning. Phys Rev Lett 108(5):058301.

[3] Pietrucci F, Andreoni W (2011) Graph theory meets ab initio molecular dynamics: atomic structures and transformations at the nanoscale. Phys Rev Lett 107(8):85504.

[4] Szlachta WJ, Bartók AP, Csányi G (2014) Accuracy and transferability of Gaussian approximation potential models for tungsten. Phys Rev B Condens Matter Mater Phys 90(10):104108.

[5] Lopez-Bezanilla A, Von Lilienfeld OA (2014) Modeling electronic quantum transport with machine learning. Phys Rev B Condens Matter Mater Phys 89(23):235411.

[6] Pilania G, Wang C, Jiang X, Rajasekaran S, Ramprasad R (2013) Accelerating materials property predictions using machine learning. Sci Rep 3:2810.

[7] Bartók AP, Gillan MJ, Manby FR, Csányi G (2013) Machine-learning approach for one- and two-body corrections to density functional theory: applications to molecular and condensed water. Phys Rev B Condens Matter Mater Phys 88(5):054104.

[8] Rupp M, Proschak E, Schneider G (2007) Kernel approach to molecular similarity based on iterative graph similarity. J Chem Inf Model 47(6):2280–2286.

[9] Hirn M, Poilvert N, Mallat S (2015) Quantum energy regression using scattering transforms.

[10] Montavon G, Rupp M, Gobre V, Vazquez-Mayagoitia A, Hansen K, Tkatchenko A et al (2013) Machine learning of molecular electronic properties in chemical compound space. New J Phys 15(9):95003.

[11] Snyder JC, Rupp M, Hansen K, Müller KR, Burke K (2012) Finding density functionals with machine learning. Phys Rev Lett 108(25):253002.

[12] Ghasemi SA, Hofstetter A, Saha S, Goedecker S (2015) Interatomic potentials for ionic systems with density functional accuracy based on charge densities obtained by a neural network. Phys Rev B 92(4):045131.

[13] Von Lilienfeld OA (2013) First principles view on chemical compound space: gaining rigorous atomistic control of molecular properties. Int J Quantum Chem 113(12):1676–1689.

[14] Hansen K, Biegler F, Ramakrishnan R, Pronobis W, Von Lilienfeld OA, Müller KR et al (2015) Machine learning predictions of molecular properties: accurate many-body potentials and nonlocality in chemical space. J Phys Chem Lett 6(12):2326–2331.

[15] Zhu L, Amsler M, Fuhrer T, Schaefer B, Faraji S, Rostami S et al (2016) A fingerprint based metric for measuring similarities of crystalline structures. J Chem Phys 144(3):034203.

[16] K. Yamanouchi, Quantum Mechanics of Molecular Structures, Springer-Verlag Berlin Heidelberg 2012.

[17] Warren J. Hehre, Alan J. Shusterman, Molecular Modeling in Undergraduate Chemistry Education.

[18] R.B. Woodward and R.Hoffmann, The Conservation of Orbital Symmetry, Verlag-Chemie, Weinhein, 1970.

[19] P. Politzer and J.S. Murray, Reviews in Computational Chemistry, vol. 2, K.B. Lipkowitz and D.B. Boyd, eds., VCH Publishers, New York, 1991.

[20] G. Náray-Szabó and G.G. Ferenczy, Chem. Rev., 95, 829 (1995).

[21] M.M. Francl, J. Chem. Phys., 89, 428 (1985).

[22] P. Sjoberg, J.S. Murray, T. Brinck and P. Politzer, Can. J. Chem. , 68, 1440 (1990).

[23] J.S. Murray and P. Politzer, in Theoretical Organic Chemistry. Theoretical and Computational Chemistry, vol. 5, C. Párkányi, ed., Elsevier, Amsterdam, p. 189, 1998.

[24] P. Politzer, J.S. Murray and M.C. Concha, Int. J. Quantum Chem., 88, 19 (2002).

[25] Structure and Dynamics of Biomolecules: Neutron and Synchrotron Radiation for Condensed Matter studies. eds. E. Fanchon et al, Oxford University Press, NY, Ch 8-10. 2000.

[26] Arup Dutta and Aloke Kumar Sarkar , "FTIR Investigation of Rotational Spectra and Structural Change due to Deuterium Exchange in Bio-Molecule", Journal of Biomimetics, Biomaterials and Biomedical Engineering; Vol. 26, pp 73-83, 2016.

[27] Helen S. Beeston, James R. Ault, Steven D. Pringle, Jeffery M. Brown and Alison E.Ashcroft, Proteomics, 2015, pp. 2842–2850.

[28] Khadijeh Rajabi, Alison E. Ashcroft and Sheena E. Radford, Methods, Volume 89, 2015, pp. 13–21.

[29] Iversen R, Mysling S, Hnida K, Jørgensen TJ, Sollid LM., Proc Natl Acad Sci U S A., 11(2014) 46-51.

[30] Joseph P Salisbury, Qian Liu and Jeffrey N Agar, BMC Bioinformatics, 15 (2014).

[31] Tivadar Orban, Beata Jastrzebska, and Krzysztof Palczewski, Curr Opin Cell Biol., 2014 pp. 32–43.

[32] H. Mallick and A. Sarkar, Bull. Mater. Sci. 23 (2000) 319.

[33] S. S. Pradhan and A. Sarkar, Materials Science and Engineering C 29 (2009) 1790–1793.

[34] Robert Lindner, UdoHeintz and AndreasWinkler, Frontiers in Molecular Bioscience, Review, 2015.

[35] Min Zhou and Carol V Robinson, Current Opinion in Structural Biology 2014, 28:122–130.

[36] Yechiel Shai, Biochimica et Biophysica Acta, Volume 1828, 10 (2013) 2306–2313.

[37] Donald L. Pavia, Gary M. Lampman, George S. Kriz, James R. Vyvyan, Spectroscopy, Cengage Learning, 2007.

[38] Colin N. Banwell, Elaine M. McCash, Fundamentals of molecular spectroscopy. Tata McGraw Hill Education Private Limited, 2010.

OVER ALL CONCLUSION

Bio-molecules show some beautiful characteristics that cannot be found in simpler systems. The goal of this work is to describe the physics of biological systems, to find new technique that characterize biological entities. The gum Arabica is a bio-molecule with polysaccharide in nature. Vibrational characteristics of gum Arabica along with its change due to in growing polymerization effect are studied. Gum Agar is another important biomaterial consists of a mixture of agarose and agaropectin. Gum Agarose is a linear polymer, of molecular weight about 120,000. Gum Agar has found to be a poor gel formation ability compared to that with agarose alone. Agar is insoluble in cold water but dissolves to give random coils in boiling water. The change in molecular structure, of the constituent biomolecules of Gum Agar, due polymerization is also detected from analysis of FTIR and ATR spectra. The distinction in molecular vibration due to the D_2O exchange is also clearly visible. IR absorbance of D_2O exchanged dried Agar specimens show an increase in peak height with increase of sol-gel time. Due to D_2O exchange -NH bending and stretching peaks disappeared from the spectra. Further it has been found that rehydration occurs only for the –NH bending but structural change occurred in -NH stretching are permanent and no rehydration takes place. The laser irradiation on pure sucrose molecule caused partial damage, in its molecular structure and its finger print has been detected from FTIR analysis. The glycoside bond of sucrose is affected due to radiation damage. Changes occur in molecular vibration spectra over its corresponding pure bio-molecule. In another studythe distinction in molecular vibration take place due to the tertiary amine salt (NH^+) in black and grey hair(structural protein). The structural change occurred in RNA while the structure of DNA remains unchanged in the two types of human hair. Some peaks are found to be shifted in the amide I and amide II region due to C=O stretching, C-N stretching and N-H bending in types of specimens. Studies on rotational energy level and rotational constant are carried out and extracted from various series in the recorded IR spectrum on Gum Arabica specimens (both pure and D_2O exchanged state). The values of rotational constant are in well agreement with the results those are obtained from the analysis of peak table of the different specimens as rotational constant is inversely proportional to the moment of inertia of the system. This novel technique may be applied to bio-molecular analysis. A map of quantum energy levels of the bio-molecule has been extracted from this research scheme. The overall results obtained are good and encouraging.